International Journal of Modern Physics B
Vol. 20, No. 28 (2006) 1–70

World Scientific
www.worldscientific.com

ADSORPTION OF POLYATOMICS: THEORETICAL APPROACHES IN MODEL SYSTEMS AND APPLICATIONS

JOSÉ L. RICCARDO*, FEDERICO J. ROMÁ† and ANTONIO J. RAMIREZ-PASTOR‡

Departamento de Física,
Laboratorio de Ciencias de Superficies y Medios Porosos,
Universidad Nacional de San Luis, CONICET, Chacabuco 917
San Luis, 5700, Argentina
**jlr@unsl.edu.ar*
†*froma@unsl.edu.ar*
‡*antorami@unsl.edu.ar*

Received 14 September 2006

The adsorption of polyatomics on one- and two-dimensional lattices is studied by combining theoretical modeling, Monte-Carlo (MC), simulations and their correspondence with experimental results. In one dimension, the rigorous statistical thermodynamics of interacting chains has been presented. With respect to two-dimensional adsorption, six different models to study non-interacting adsorbates have been discussed: (i) an extension to two dimensions of the exact thermodynamic functions obtained in one dimension; (ii) the Flory–Huggins's approximation and its modification to address linear adsorbates; (iii) the well-known Guggenheim–DiMarzio approximation; (iv) the fourth one is a new description of adsorption phenomena, based on Haldane's fractional statistics; (v) the fifth so-called Occupation Balance, based on the expansion of the reciprocal of the fugacity; and (vi) a simple semi-empirical model obtained by combining exact one-dimensional calculations and Guggenheim–DiMarzio approach. In addition, the statistical thermodynamics of interacting polyatomics has been developed on a generalization in the spirit of the Bragg–Williams and the quasi-chemical approximations. Comparison with MC simulations and experimental adsorption isotherms are used to test the accuracy and reliability of the proposed models. Finally, applications to heterogeneous systems and multilayer adsorption are discussed.

Keywords: Adsorption; multisite occupancy; lattice-gas models; chain adsorption.

1. Introduction

This review is concerned with the theoretical description of thermodynamic equilibrium of adlayers with the polyatomic components.

Adsorption is a relevant elementary phenomenon in interface and surface science with significant impact in technological applications. From the simplest case of atoms or small molecules adsorbed on perfectly defined surfaces, such as Ar and N_2 on graphite,[1] or small adsorbates like O_2, CO, CO_2 and oligomers[2–5] in

molecular carbon or zeolites, polymer films,[6,7] the problem of elucidating the adsorption configurations, heats, entropy, phase behavior, and ordering has challenged experimentalist and theoreticians for decades.

It is known that various characteristics of the gas-solid system are important in determining the equilibrium of the interface, namely, the surface atoms lattice, the geometrical disorder, chemical heterogeneities, the polar-nonpolar character of the atom-surface interaction and the size and internal degrees of freedom of the adsorbate.

The relatively recent development of single-walled and multiwalled carbon nanotubes[8–12] and synthetic zeolites ($AlPO_4-5$, $SAPO-5$),[13] along with their potential technological application as unique reference systems, molecular sieves and storage systems, has raised new questions about the equilibrium and transport properties of gases in low-dimensional adsorption potentials.

Various studies have been carried out on conductivity, electronic structure and mechanical strength of nanotubes. However, theoretical and experimental research focused in the interaction, equilibrium and dynamical properties of noble, simple (H_2, N_2, O_2, CO)[14–32] and polyatomic (CO_2, CH_4, hydrocarbons) gases within nanotubes is relatively more scarse.[33–50]

From a fundamental point of view, it is expected that adlayers of linear and branched molecules will exhibit a rich phase behavior that is not possible in films of spherical adsorbates. The ultimate behavior of adsorbed layers of polyatomic species will be strongly affected by quantities such as molecular size, aspect ratio, possible orientation of the molecular axis with respect to the surface and flexibility.

Although, many relevant studies of linear adsorbates on particular planar surfaces such as graphite have shed light on two-dimensional ordered phases,[51–58] solid phases of the adsorbate with different orientation of the molecular axis with respect to the surface,[54–56,59,60] and two-dimensional melting mechanisms,[60–69] there is still not well understood the complexity of the entropic/energetic balance arising from the non-spherical character and various degrees of freedom of the adsorbate.

Here we present a comprehensive description of recent advances in the theoretical description of adsorption of structured particles on regular (usually referred as multisite occupancy adsorption) with emphasis in the role and effect of the particle size and structure on the configurational entropy of the adlayer; an aspect that almost none thermodynamic adsorption description has ever taken properly and comprehensively into account. Insight into the entropic behavior of model polyatomic systems is of major interest to understand the complex properties of alkanes and hydrocarbons mixture adsorption with significant impact in petrochemical separation technology. Analytical and lattice-like simulations result are reported and compared as to disclose the degree of accuracy of the various formalisms. Peculiar critical properties of interacting linear species are addressed as well. When available, comparison and interpretation of experimental results in the light of the described approximations are presented. The work is organized as follows: the thermody-

namic functions for a one dimensional lattice-gas of interacting linear particles is addressed in Sec. 2. Section 3 is devoted to present the approximations for the thermodynamic functions of polyatomic model species in two dimensions, namely, an extension ansatz (EA) of the exact one-dimensional functions, the Flory–Huggins (FG) and the modified Flory–Huggins (FGL) for linear species, the Guggenheim–DiMarzio (GD) approximation, the recently presented Fractional Statistical Theory of Adsorption (FSTA) based on the Haldanes statistics conjecture; the Ocuppation Balance (OB) approximation and the Semiempirical Adsorption Model (SE). Comparison between analytical predictions and Monte-Carlo simulations are presented and analyzed in this section. Two dimensional lattice gases of interacting linear species in two dimensions are dealt with in section 4 through mean-field, quasi-chemical and Monte-Carlo techniques. Applications of the various theoretical description to monolayer and multilayer adsorption of polyatomics are shown and discussed in Sec. 5. Conclusions are drawn in Sec. 6.

2. Exact Thermodynamic Functions in One Dimension

2.1. *Non-interacting k-mers*

Let us assume a one-dimensional lattice of M sites with lattice constant a ($M \to \infty$) where periodic boundary conditions apply. Under this condition all lattice sites are equivalent hence border effects will not enter our derivation. From the experimental point of view, the adsorption potential within the narrowest nanotubes can be matched to a homogeneous one-dimensional lattice of adsorption sites. It has also been reported the one-dimensional character of adsorption in grooves of surface crystal planes of TiO_2.[70]

N linear k-mers (molecules containing k identical units) are adsorbed on the lattice. The distance between k-mer units is assumed in registry with the lattice constant a; hence exactly k sites are occupied by a k-mer when adsorbed. Small adsorbata with spherical symmetry would correspond to the monomers limit ($k = 1$). Double site occupancy is not allowed as to represent properties in the monolayer regime. Since different k-mers do not interact each other through their ends, all configurations of N k-mers on M sites are equally probable; henceforth, the canonical partition function $Q(M, N, T)$ results

$$Q(M, N, T) = \Omega(M, N) \exp(-\beta k U_0 N) \tag{1}$$

where $\Omega(M, N)$ is the number of ways to arrange N k-mers on M sites; U_0 is the interaction energy between every unit forming a k-mer and the substrate and $\beta = 1/k_B T$, being k_B the Boltzmann constant [for simplicity, we have also assumed the internal and vibrational contributions to the partition factor to be a unitary factor in Eq. (1)].

$\Omega(M,N)$ can be readily calculated as the total number of permutations of the N indistinguishable k-mers out of n_e entities, being n_e[71]

$$\begin{aligned} n_e &= \text{number of } k\text{-mers+number of empty sites} \\ &= N + M - kN = M - (k-1)N\,. \end{aligned} \tag{2}$$

Accordingly,

$$\Omega(M,N) = \binom{n_e}{N} = \frac{[M-(k-1)N]!}{N![M-kN]!} \tag{3}$$

(a particular solution for dimers was presented in Ref. 72).

In the canonical ensemble the Helmholtz free energy $F(M,N,T)$ relates to $\Omega(M,N)$ through

$$\beta F(M,N,T) = -\ln Q(M,N,T) = -\ln \Omega(M,N) + \beta k U_0 N\,. \tag{4}$$

The remaining thermodynamic functions can be obtained from the general differential form[73]

$$dF = -SdT - \Pi dM + \mu dN \tag{5}$$

where S, Π and μ designate the entropy, spreading pressure and chemical potential respectively, which, by definition, are

$$S = -\left(\frac{\partial F}{\partial T}\right)_{M,N} \quad \Pi = -\left(\frac{\partial F}{\partial M}\right)_{T,N} \quad \mu = \left(\frac{\partial F}{\partial N}\right)_{T,M}\,. \tag{6}$$

Thus, from Eqs. (3) and (4)

$$\beta F(M,N,T) = -\{\ln[M-(k-1)N]! - \ln N! - \ln[M-kN]!\} + \beta k U_0 N \tag{7}$$

which can be accurately written in terms of the Stirling approximation

$$\begin{aligned} \beta F(M,N,T) &= -[M-(k-1)N]\ln[M-(k-1)N] + [M-(k-1)N] \\ &\quad + [N\ln N - N] + [(M-kN)\ln(M-kN) \\ &\quad - (M-kN)] + \beta k U_0 N \\ &= -[M-(k-1)N]\ln[M-(k-1)N] + N\ln N \\ &\quad + (M-kN)\ln(M-kN) + \beta k U_0 N\,. \end{aligned} \tag{8}$$

Henceforth, from Eqs. (6) and (8)

$$\begin{aligned} \frac{S(M,N)}{k_B} &= [M-(k-1)N]\ln[M-(k-1)N] - N\ln N \\ &\quad - (M-kN)\ln(M-kN) \end{aligned} \tag{9}$$

$$\begin{aligned} \beta\mu &= \ln\frac{kN}{M} + (k-1)\ln\left[1-(k-1)\frac{N}{M}\right] - k\ln\left[1-\frac{kN}{M}\right] \\ &\quad + \beta k U_0\,. \end{aligned} \tag{10}$$

Then, by defining the lattice coverage $\theta = kN/M$, molar free energy $f = F/M$ and molar entropy $s = S/M$, Eqs. (8)–(10) can be rewritten in terms of the intensive variables θ and T.

$$\beta f(\theta,T) = -\left\{\left[1-\frac{(k-1)}{k}\theta\right]\ln\left[1-\frac{(k-1)}{k}\theta\right] - \frac{\theta}{k}\ln\frac{\theta}{k} - (1-\theta)\ln(1-\theta)\right\} + \beta U_0\theta \tag{11}$$

$$\frac{s(\theta)}{k_B} = \left[1-\frac{(k-1)}{k}\theta\right]\ln\left[1-\frac{(k-1)}{k}\theta\right] - \frac{\theta}{k}\ln\frac{\theta}{k} - (1-\theta)\ln(1-\theta) \tag{12}$$

$$C_k \exp[\beta(\mu - kU_0)] = \frac{\theta\left[1-\frac{(k-1)}{k}\theta\right]^{k-1}}{(1-\theta)^k} \tag{13}$$

where $C_k = k$.

2.2. *Interacting k-mers*

Now, we address the general case of interacting adsorbata.[74] Thus, two k-mers interact through their ends with an interaction energy that amounts w when the ends are nearest-neighbors. Without any loss of generality, we assume the interaction energy between a chain unit and a lattice site to be zero ($U_0 = 0$). We can now think of a mapping $\mathbf{L} \to \mathbf{L}'$ from the original lattice $\mathbf{L}$ to an effective lattice $\mathbf{L}'$ where each empty site of $\mathbf{L}$ transforms into an empty one of $\mathbf{L}'$, while each set of k sites occupied by a k-mer in $\mathbf{L}$ is represented by an occupied site in $\mathbf{L}'$.[75] Thus, the total number of sites in $\mathbf{L}'$ is

$$M' = M - (k-1)N \tag{14}$$

and the coverage of $\mathbf{L}'$

$$\theta' = N/M' = (\theta/k)\Big/\left[1-\frac{(k-1)}{k}\theta\right]. \tag{15}$$

The canonical partition functions $Q(kN, M, T)$, $Q'(N, M', T)$ in the original and effective lattice must be equal. Thus,

$$Q(kN,M,T) = \sum_{\{\mathbf{X}\}} \exp\left[-\beta E(\mathbf{X})\right] = Q'(N,M',T) = \sum_{\{\mathbf{X}'\}} \exp\left[-\beta E(\mathbf{X}')\right] \tag{16}$$

where $\{\mathbf{X}\}$ and $\{\mathbf{X}'\}$ refer to a sum over all possible configurations in $\mathbf{L}$ and $\mathbf{L}'$ respectively.

Accordingly, the Helmholtz free energies per site in $\mathbf{L}$ and $\mathbf{L}'$, f and f', respectively, are related through

$$\begin{aligned} f(kN, M, T) &= -\frac{1}{\beta M} \ln[Q(kN, M, T)] \\ &= -\frac{1}{\beta M} \ln[Q'(N, M', T)] \\ &= \frac{M'}{M} f'(N, M', T) \\ f(kN, M, T) = \frac{M'}{M} f' &= \left\{ 1 - \left[\frac{(k-1)}{k} \theta \right] \right\} f'(N, M', T) \,. \end{aligned} \tag{17}$$

This relationship makes complete the mapping from the original problem of k-mer adsorption on $\mathbf{L}$ to an effective Ising-like one (monomer adsorption) on $\mathbf{L}'$. f' can then be written in terms of the probability y of having two nearest-neighbor sites occupied in $\mathbf{L}'$, by means of the cumulant variation method,[73,76] as

$$\begin{aligned} \beta f \left(\frac{N}{M'}, T \right) = \beta w y &- [\theta' \ln \theta' + (1-\theta') \ln(1-\theta') - y \ln y] \\ &- [-2(\theta' - y) \ln(\theta' - y) - (1 - 2\theta' - y) \ln(1 - 2\theta' - y)] \,. \end{aligned} \tag{18}$$

For each set of values θ', T, y is obtained by minimizing f'. Thus,

$$y = \theta' - \left(\frac{A}{2} \right) + \left[\frac{A^2}{4} - \theta'(1-\theta') A \right]^{1/2} \tag{19}$$

where $A = [1 - \exp(-\beta w)]^{-1}$. In the infinite temperature limit $\beta w \to 0$, $A \approx 1/\beta w$ and $y \approx {\theta'}^2 + O(\beta w)$, as expected for a totally random distribution of units on the lattice. For infinitely repulsive interactions $\beta w \to \infty$, $A \to 1$ and $y = 0$ if $\theta' \leq 1/2$. (i.e. no two nearest-neighbor occupied sites are present on the lattice), or $y = 2\theta' - 1$ if $\theta' \geq 1/2$. For infinitely attractive interactions, $\beta w \to -\infty$, it yields $y = \theta'$, as physically expected.

By using the relationship between θ' and θ [from Eq. (15)] in Eq. (19), and replacing Eq. (19) in Eq. (18), the exact form of f is obtained

$$\begin{aligned} \beta f(\theta, T) = \beta w \left[\frac{\theta}{k} - \alpha \right] &- \left[\frac{\theta}{k} \ln \frac{\theta}{k} + (1-\theta) \ln(1-\theta) - 2\alpha \ln \alpha \right] \\ &- \left\{ - \left[\frac{\theta}{k} - \alpha \right] \ln \left[\frac{\theta}{k} - \alpha \right] - (1 - \theta - \alpha) \ln(1 - \theta - \alpha) \right\} \end{aligned} \tag{20}$$

where α is given by

$$\alpha = \frac{2\theta(1-\theta)}{k \left[1 - \dfrac{(k-1)}{k} \theta + b \right]} \quad \text{and} \quad b = \left\{ \left[1 - \frac{(k-1)}{k} \theta \right]^2 - \frac{4}{kA} (\theta - \theta^2) \right\}^{1/2} . \tag{21}$$

All the equilibrium properties of the adlayer can be deducted from Eqs. (20) and (5). Then the coverage dependence of the chemical potential and the entropy per site s result

$$\beta\mu = k\left(\frac{\partial\beta f}{\partial\theta}\right)_{M,T} = \beta w + \ln[k(b-1+\theta)+\theta] + (k-1)\ln\left[1-\frac{(k-1)}{k}\theta+b\right] + (k-1)\ln k - \ln[k(b+1-\theta)-\theta] \tag{22}$$

$$s/k_B = -\left(\frac{\partial f}{\partial T}\right)_{M,N} = \frac{\theta}{k}\ln\frac{\theta}{k} + (1-\theta)\ln(1-\theta) - 2\alpha\ln\alpha - \left[\frac{\theta}{k}-\alpha\right]\ln\left[\frac{\theta}{k}-\alpha\right] - (1-\theta-\alpha)\ln(1-\theta-\alpha) \tag{23}$$

and finally the specific heat at constant volume

$$c_v/k_B = -\left(\frac{\partial^2 f}{\partial T^2}\right)_{M,N} = \frac{4\theta^2(1-\theta)^2}{bk^2\left[1-\frac{(k-1)}{k}\theta+b\right]^2}[\beta w]^2\exp[\beta w]\,. \tag{24}$$

Equation (22) represent the exact form for the adsorption isotherm of interacting adsorbates (k-mers) in one dimension. For non-interacting adsorbates ($w = 0$), Eq. (22) reduces to the rigorous isotherm of non-interacting chains [Eq. (13)].

The coverage dependence of the chemical potential (adsorption isotherm), molar entropy and specific heat are shown in Figs. 1–3 for various k-mer's sizes and interaction energies [attractive ($w < 0$) as well as repulsive ($w > 0$)]. MC simulations in

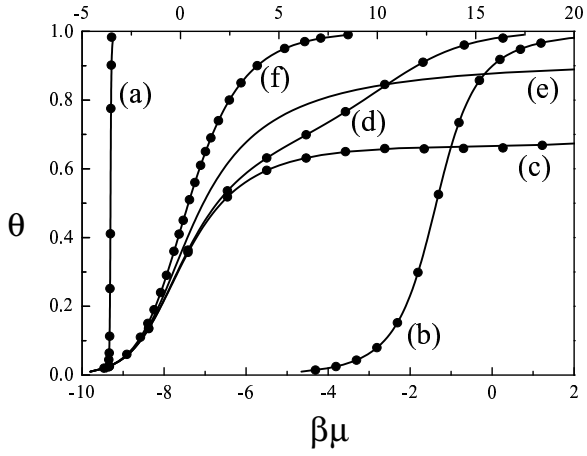

Fig. 1. Lattice coverage θ versus relative chemical potential $\beta\mu$ for interacting (repulsive as well attractive) dimers and 10-mers; (a) $k = 2$, $\beta w = -10$; (b) $k = 2$, $\beta w = -2$, (c) $k = 2$, $\beta w = +10$; (d) $k = 2$, $\beta w = +2$; (e) $k = 10$, $\beta w = +10$; (f) $k = 2$, $\beta w = 0$. The symbols represent results from Monte-Carlo Simulation in the lattice gas model with the parameters specified in the respective case. The upper axis corresponds to $\beta\mu$ for the repulsive case ($\beta w > 0$).

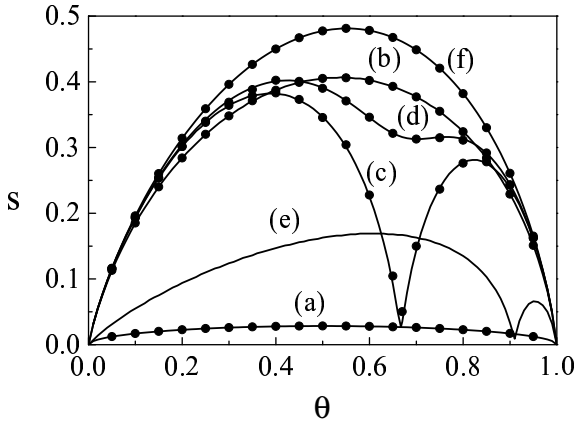

Fig. 2. Entropy per site, $s(\theta)$, versus lattice coverage, θ; the curves denoted (a) to (f), correspond one-to-one to the cases displayed in Fig. 1.

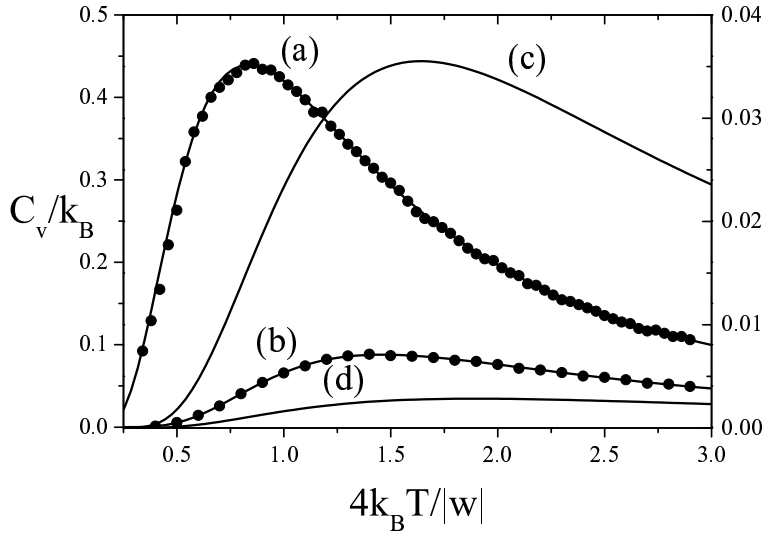

Fig. 3. Specific heat in units of k_B (at constants volume) versus $4k_BT/|w|$ at $\theta = 0.5$. (a) monomers ($k = 1$); (b) dimers ($k = 2$); (c) trimers ($k = 3$); (d) 10-mers ($k = 10$). The cases (a) and (b) correspond to the left hand side axis and the cases (c) and (d) correspond to the right hand side axis.

the grand canonical ensemble (shown in symbols) fully agree with the predictions from Eqs. (22)–(24).

The stronger the lateral interaction the more steeped the adsorption isotherm for attractive k-mers becomes. Qualitatively, no significant changes are observed as the k-mer size increases. However, the curves have a pronounced plateau at $\theta = (k-1)/k$ for strongly repulsive interactions, which smoothes out for already $\beta w = +2$. This type of isotherm has very recently been reported for Kr and CH_4 adsorbed in

$AlPO_4$-5, where, very likely, the mistmatch between the equilibrium separation of the intermolecular interaction and the lattice constant along the nanochannels give rises to repulsive interaction between NN molecules as assumed in our calculations. It is worth noticing that although the double-steep isotherm may be indicative of a second order phase transition (as speculated in Ref. 77), they may be not for an adsorbate whose size is comparable to the nanotube diameter that behaves as a one-dimensional confined fluid. It is well known that no phase transition develops in a one-dimensional lattice when weak coupling between neighboring particles exists.[73] Since our model of adsorbed k-mers is isomorphous to a one-dimensional Ising model it will not present phase transition either. This is clearly seen in Fig. 3 where the smooth dependence of the specific heat on temperature is depicted for various k-mers. More recently molecular simulations[78,79] of alkenes in $AlPO_4 - 5$ have also shown that a plateau in the adsorption isotherm arises along with a rearrangements of the adsorbate molecules within the channels. From isosteric heat of adsorption calculations is concluded that the plateau is due to a net repulsive potential felt by molecules. As the coverage approachs the typical value $\theta \approx 2/3$ the molecules rearrange within the channel to increase their ads-ads interaction; however, this forces the molecules to occupy new adsorption sites where their interaction with the $AlPO_4 - 5$ framework diminishes (become more repulsive) giving a net decrease of the isosteric heat of adsorption.

The general features of the coverage dependence of the entropy per site are shown in Fig. 2. The agreement between theory and MC simulation[80,81] is remarkable for weak as well as strong lateral interactions regarding the intrinsic difficulties of entropy calculation for polyatomic species at low temperatures. For attractive interactions s is symmetrical with a maximun at $\theta = 0.5$ for interacting as well as for non-interacting monomers ($k = 1$). For interacting k-mers ($k > 1$) the maximun shifts to higher coverages ($\theta > 0.5$). However, given a ratio $\beta w \leq 0$ the maximun shift to higher coverages such a way that the larger k the more apart the maximun gets from $\theta = 0.5$. This result differs from the one-dimensional limit of non-interacting k-mers ($\beta w = 0$) in the Flory–Huggins's approximation[73,82–86] for which the maximun of s shifts to lower coverages as k increases. Given a k-mer size the stronger the interaction the smaller the shift of the maximun from $\theta = 0.5$. For repulsive interactions, the entropy develops a local minimum at $\theta \geq 0.5$, which gets sharper as the ratio βw increases and shifts to higher coverages as the k-mer size increases. In all cases the minimum traces to a non-degenerate ground state where k-mers structure is an ordered sequence leaving one empty site between nearest-neighbor particles. None of the minima correspond to a second order phase transition as expected for particles with short-ranged interactions in one dimension.

The specific heat, from Eq. (24), is compared with MC simulations at $\theta = 0.5$ (see Fig. 3). A continuum variation of c_v/k_B on T is observed with a maximun that lowers and broadens as the k-mers size increases; accordingly no phase transition develops as expected.

3. Two-Dimensional Lattice Gas of Non-Interacting Polyatomics

The model is the same as in Sec. 2.1, except that the sites form a two-dimensional array instead of a one-dimensional lattice. Accordingly, the adsorbate molecules are assumed to be arranged in two type of configurations: (i) as a linear array of monomers, which we call "linear k-mer"[a]; and (ii) as a chain of adjacent monomers with the following sequence: once the first monomer is in place, the second monomer occupies one of the γ nearest-neighbor of the first monomer. Third and successive monomers occupy one of the $\gamma - 1$ nearest-neighbors of the preceding monomer. This process continues until k monomers are placed without creating an overlap. We call this feature "flexible k-mer".

From an analytical point of view, the problem in which a two-dimensional lattice contains isolated lattice points (vacancies) as well as k-mers has not been solved in closed form and approximated methods have been utilized to study this problem. Six of these methods are described in the present section: (i) the first (EA) is an extension to 2-D of the exact partition function obtained in 1-D;[71,87,88] (ii) the second is a virial expansion (VE);[88] (ii) the second is the Flory–Huggins's approximation (FH) and its modification to address linear adsorbates (FHL);[82−86] (iii) the third is the well-known Guggenheim–DiMarzio approximation (GD);[89,90] (iv) the fourth is a new theoretical description of adsorption phenomena ($FSTA$), which is based on Haldane's fractional statistics;[91,92] (v) the fifth, which we called Occupation Balance (OB), is based on the expansion of the reciprocal of the fugacity;[80,81,88] and (vi) the sixth is a simple semi-empirical adsorption model for polyatomics (SE), which is obtained by combining exact one-dimensional calculations and GD.[93]

3.1. *Exact thermodynamic functions in one dimension and extension to higher dimensions (EA)*

We address the calculation of approximated thermodynamical functions of chains adsorbed on lattices with connectivity γ higher than 2 (i.e. dimensions higher than one).

In general, the number of configurations of N k-mers on M sites, $\Omega(M, N, \gamma)$, depends on the lattice connectivity $\gamma \cdot \Omega(M, N, \gamma)$ can be approximated considering that the molecules are distributed completely at random on the lattice, and

[a]The concept of linear k-mer is trivial for square and triangular lattices. However, in a honeycomb lattice, the geometry does not allow the existence of a linear array of monomers with $k \geq 2$. In this case, we call linear k-mer to a chain of adjacent monomers with the following sequence: once the first monomer is in place, the second monomer occupies one of the three nearest-neighbors of the first monomer. Third monomer occupies one of the two nearest-neighbors of the second monomer. i-esime monomer (for $i \geq 4$) occupies one of the two nearest-neighbors of the preceding monomer, which maximizes the distance between first monomer and i-esime monomer. Then, once a site is chosen, there exists six equilibrium states available to a single k-mer ($k \geq 2$) on a honeycomb lattice at infinitely low density.

assuming the arguments given by different authors[73,82,83,94–97] to relate the configurational factor $\Omega(M,N,\gamma)$ for any γ with respect to the same quantity in one dimension ($\gamma = 2$). Thus

$$\Omega(M,N,\gamma) = K(\gamma,k)^N \Omega(M,N,2) \tag{25}$$

where $\Omega(M,N,2)$ can be readily calculated from Eq. (3) and $K(\gamma,k)$ represents the number of available configurations (per lattice site) for a k-mer at zero coverage. $K(\gamma,k)$ is, in general, a function of the connectivity and the size/shape of the adsorbate. It is easy demonstrate that,

$$K(\gamma,k) = \begin{cases} \gamma/2 & \text{for linear } k\text{-mers} \\ [\gamma(\gamma-1)^{(k-2)}]/2 - m' & \text{for flexible } k\text{-mers} \end{cases} \tag{26}$$

the term m' is subtracted in Eq. (26) since the first term overestimates $K(\gamma,k)$ by including m' configurations providing overlaps in the k-mer.

In this way, the entropy s and the adsorption isotherm corresponding to an adsorbed molecule/surface geometry result,

$$\frac{s(\theta,\gamma)}{k_B} = \left[1 - \frac{(k-1)}{k}\theta\right] \ln\left[1 - \frac{(k-1)}{k}\theta\right] - \frac{\theta}{k}\ln\frac{\theta}{k} - (1-\theta)\ln(1-\theta) + \frac{\theta}{k}\ln K(\gamma,k) \tag{27}$$

$$kK(\gamma,k)\exp\left[\beta(\mu - kU_0)\right] = \frac{\theta\left[1 - \frac{(k-1)}{k}\theta\right]^{k-1}}{(1-\theta)^k}. \tag{28}$$

Equations (26)–(28) provide the basic thermodynamic functions for non-interacting polyatomics in lattices with general connectivity γ.

3.2. *Flory–Huggins's approximation for flexible (FH) and linear (FHL) adsorbates*

The theory to be presented here, due to Flory[82,83] and Huggins,[84–86] is a generalization of the lattice-gas theory of binary solutions,[73] but in this case, as a solvent molecule occupies only one site in the lattice, the polymer molecule occupies k sites.

We calculate first the number $\Omega(N_1,N_2)$ of possible configurations of N_2 polymers and N_1 molecules of a monoatomic solvent on a lattice with M sites and connectivity $\gamma \cdot \Omega(N_1,N_2)$ is just equal to the number of ways of arranging N_2 polymer molecules on M sites, for after we place the polymer molecules in the originally empty lattice, there is only one way to place the solvent molecules (i.e. we simply fill up all the remaining unoccupied sites). Imagine that we label the polymer molecules from 1 to N_2 and introduce them one at a time, in order, into the lattice. Let w_i be the number of ways of putting the i-th polymer molecule into the

lattice with $i-1$ molecules already there (assumed to be arranged in an average, random distribution). Then the approximation to $\Omega(N_1, N_2)$ which we use is

$$\Omega(N_1, N_2) = \frac{1}{N_2!} \prod_{i=1}^{N_2} w_i \tag{29}$$

The factor $(N_2!)^{-1}$ is inserted because we have treated the molecules as distinguishable in the product, whereas they are actually indistinguishable.

Next, we derive an expression for w_{i-1}. With i polymer molecules already in the lattice, the fraction of sites filled is $\theta_i = ki/M$. The first unit of the $(i+1)$th molecule can be placed in any one of the $M - ki$ vacant sites. The first unit has γ nearest neighbor sites, of which $\gamma(1-\theta_i)$ are empty (random distribution assumed). Therefore the number of possible locations for the second unit is $\gamma(1-\theta_i)$. Similarly, the third unit can go in $(\gamma-1)(1-\theta_i)$ different places. At this point we make the approximation that units $4, 5, \ldots, k$ also each have $(\gamma-1)(1-\theta_i)$ possibilities, though this is not quite correct. Multiplying all of these factors together, we have for w_{i+1},

$$\begin{aligned} w_{i+1} &= (M-ki)\gamma(\gamma-1)^{k-2}(1-\theta_i)^{k-1} \\ &= (M-ki)^k \left(\frac{\gamma-1}{M}\right)^{k-1} \end{aligned} \tag{30}$$

where we replaced γ by $\gamma - 1$ as a further approximation.

Now we will need

$$\ln \prod_{i=1}^{N_2} w_i = N_2(k-1) \ln\left(\frac{\gamma-1}{M}\right) + k \sum_{i=0}^{N_2-1} \ln(M-ki)\,. \tag{31}$$

We approximate the sum by an integral:

$$\begin{aligned} \sum &\approx \int_0^{N_2} \ln(M-ki)di = \frac{1}{k}\int_{N_1}^{M} \ln u du \\ &= \frac{1}{k}(M\ln M - M - N_1 \ln N_1 + N_1)\,. \end{aligned} \tag{32}$$

From Eqs. (29)–(32), we find

$$\begin{aligned} \ln \Omega(N_1, N_2) = &-N_2 \ln N_2 + N_2 - N_1 \ln N_1 + N_1 + M \ln M - M \\ &+ N_2(k-1) \ln\left[\frac{(\gamma-1)}{M}\right]. \end{aligned} \tag{33}$$

All results presented here can be straightforwardly applied to the corresponding k-mers adsorption problem, with $N_2 \equiv N$ (number of k-mers) and $N_1 \equiv M - kN$ (number of empty sites). Then, by rewriting $\Omega(N_1, N_2)$ in terms of $\theta \equiv kN/M$, and by using Eqs. (4), (6) and (8), we get,

$$\frac{s(\theta,\gamma)}{k_B} = -\frac{\theta}{k}\ln\frac{\theta}{k} - (1-\theta)\ln(1-\theta) + \left(\frac{k-1}{k}\right)\theta \ln\left(\frac{\gamma-1}{e}\right) \tag{34}$$

$$\exp[\beta(\mu - kU_0)] = \frac{\theta}{k(\gamma-1)^{k-1}(1-\theta)^k}\,. \tag{35}$$

The last equation is the classical adsorption isotherm in the framework of the Flory–Huggins's approximation, which was developed for flexible polymers. In the following, we will introduce appropriate modifications in the formalism, in order to obtain the adsorption isotherm corresponding to linear k-mers. In this case,

$$w_{i+1} = \frac{\gamma}{2}(M-ki)^k \left(\frac{1}{M}\right)^{k-1} \tag{36}$$

where two modifications have been included with respect to Eq. (30): (i) the number of possible locations for the third and successive units is $(1-\theta_i)$, instead of $\gamma(1-\theta_i)$, as it was considered for flexible k-mers, and (ii) a factor $1/2$ is inserted because we have treated the extremes of the k-mers as distinguishable, whereas they are actually indistinguishable. Under these considerations, the desired Flory–Huggins thermodynamic functions of linear k-mers results

$$\frac{s(\theta,\gamma)}{k_B} = -\frac{\theta}{k}\ln\frac{\theta}{k} - (1-\theta)\ln(1-\theta) - \left(\frac{k-1}{k}\right)\theta - \frac{\theta}{k}\ln\left(\frac{\gamma}{2}\right) \tag{37}$$

$$\times \exp\left[\beta(\mu - kU_0)\right] = \frac{2\theta}{k\gamma(1-\theta)^k}\,. \tag{38}$$

The validity of the last equation is restricted to the range $k \geq 2$. Note that Eq. (38) does not reproduce the Langmuir isotherm for monomers.[73]

3.3. *Guggenheim–Di–Marzio approximation (GD)*

In 1944, Guggenheim proposed an interesting method to calculate the combinatory term in the canonical partition function.[89] Later, in a valuable contribution, Di-Marzio obtained the Guggenheim's factor for a model of rigid rod molecules.[90] In this section we reproduce the calculations developed by DiMarzio, who obtained the number of ways to pack rigid rods onto a cubic lattice and its generalization to lattices of connectivity γ.

Let us place N straight rigid rods (linear k-mers) onto a cubic lattice. We will assume that only the three mutually perpendicular base vector directions in which the rigid rods lie. The number of molecules that lie in the direction i will be denoted by $N_i (i = 1, 2, 3)$. We ask for the number of ways, $\Omega(\{\cdots N_i \cdots\}, N_0)$ to pack the N molecules such that N_i of them lie in the direction i and there are N_0 holes. The advantage of allowing only those orientations for which the molecules fit exactly onto the lattice is that for the case of an isotropic distribution the value of Ω reduces to the value obtained previously by Guggenheim.[89]

Let us place N_1 molecules, one at a time, onto the lattice in orientation 1, and then the N_2 molecules, one at a time, in orientation 2 and then place the remaining N_3 molecules, one at a time, in orientation 3. In order to estimate the number of ways to place the (j_1+1)th molecule onto the lattice, given that j_1 molecules have

already been placed, we must know the probability that k contiguous sites lying in this orientation are empty. Here the subscript reminds us that we are discussing type 1 molecules. Consider a contiguous pair of sites arbitrarily chosen except for the fact that the line determined by the centers of these sites lies along orientation 1. Label the sites A and B. Site A has a probability of being empty equal to the fraction of sites that are unoccupied by molecular segments since site A can be thought of as chosen arbitrarily. If site A is empty, the ratio of the number of times it adjoins a polymer to the number of times it adjoins a vacant site is $2j_1/2(M-kj_1)$, where M is the total number of sites in the lattice. Notice that in writing this expression for the ratio we counted only those pairs of contiguous sites which lie along orientation 1. The pairs which lie along orientations 2 and 3 are of no consequence as far as the nearest-neighbor statistics along orientation 1 are concerned.

The above ratio is also the ratio of the number of times a polymer adjoins site A (presumed empty) to the number of times a vacant site adjoins site A. Thus the probability that site B is empty given that site A is empty is

$$\frac{2(M-kj_1)}{2(M+kj_1)+2j_1}\,. \tag{39}$$

We see that ν_{j_1+1}, the number of ways to place the (j_1+1)th molecule onto the lattice, is

$$\nu_{j_1+1} = (M-kj_1)\left[\frac{2(M-kj_1)}{2(M+kj_1)+2j_1}\right]^{k-1}\,. \tag{40}$$

The total number of ways to place N_1 indistinguishable molecules onto the lattice in this orientation is

$$\frac{\prod_{j_1=0}^{N_1-1}\nu_{j_1+1}}{(N_1)!} = \frac{M!\,(M-kN_1+N_1)!}{(M-kN_1)!M!\,(N_1)!} = \frac{(M-kN_1+N_1)!}{(M-kN_1)!\,(N_1)!}\,. \tag{41}$$

Note that this result so far is equal to the exact number. That is to say, the number of ways to pack the molecules is the number of ways to arrange N_1 linear molecules and N_0 holes on a linear lattice [see Eq. (3)].

In order to count the number of ways to pack the N_2 molecules in the second orientation, given that we have already placed the N_1 molecules, we need to know the statistics for those pairs of neighboring sites whose centers are connected by a line in this direction. The number of these kind of nearest-neighbors to polymer molecules is $2kN_1+2j_2$ where j_2 is the number of polymer molecules in the second orientation and the number of these kind of nearest-neighbors to holes is $2M-(2kN_1+2kj_2)$.

The first segment of the (j_2+1)th molecule can go into the lattice in $(M-kN_1-kN_2)$ places. The expectancy that a site is unoccupied when it is known that the adjacent site in the direction in which the molecules lies is unoccupied is

$$\frac{2(M-kN_1-kj_2)}{2(M-kN_1-kj_2)+2(kN_1+j_2)}\,. \tag{42}$$

We therefore have for ν_{j_2+1}

$$\nu_{j_2+1} = (M - kN_1 - kj_2)\left[\frac{(M - kN_1 - kj_2)}{(M - kN_1 - kj_2) + (kN_1 + j_2)}\right]^{k-1}. \tag{43}$$

The total number of ways to pack these indistinguishable molecules is

$$\frac{\prod_{j_2=0}^{N_2-1}\nu_{j_2+1}}{(N_2)!} = \frac{(M - kN_1)!\,(M - kN_2 + N_2)!}{(M - kN_1 - kN_2)!M!\,(N_2)!}. \tag{44}$$

By an exactly analogous reasoning process we obtain for ν_{j_3+1},

$$\nu_{j_3+1} = (M - kN_1 - kN_2 - kj_3) \times \left[\frac{(M - kN_1 - kN_2 - kj_3)}{(M - kN_1 - kN_2 - kj_3) + (kN_1 + kN_2 + j_3)}\right]^{k-1}, \tag{45}$$

$$\frac{\prod_{j_3=0}^{N_3-1}\nu_{j_3+1}}{(N_3)!} = \frac{(M - kN_1 - kN_2)!\,(M - kN_3 + N_3)!}{(M - kN_1 - kN_2 - kN_3)!M!\,(N_3)!}. \tag{46}$$

The product obtained from Eqs. (41), (44) and (46) gives the total number of ways to pack the molecules

$$\begin{aligned}\Omega(N_0, N_1, N_2, N_3) &= \frac{(M - kN_1 + N_1)!}{(M - kN_1)!(N_1)!}\,\frac{(M - kN_1)!(M - kN_2 + N_2)!}{(M - kN_1 - kN_2)!M!(N_2)!} \\ &\quad \times \frac{(M - kN_1 - kN_2)!(M - kN_3 + N_3)!}{(M - kN_1 - kN_2 - kN_3)!M!(N_3)!} \\ &= \frac{\prod_{j=1}^{3}[M - (k-1)N_i]!}{(N_0)!\prod_{i=1}^{3}(N_i)!(M!)^2}.\end{aligned} \tag{47}$$

As remarked before, this expression is exact when all the molecules are in one direction. Eq. (47) has the proper symmetry requirements. It is invariant under the permutation of the N_i. For the case $N_1 = N_2 = N_3 = N/3$ we obtain

$$\Omega = \frac{\{[N_0 + (2kN/3) + (N/3)]!\}^3}{N_0![(N/3)!]^3(M!)^2}. \tag{48}$$

Equation (47) can be generalized for a lattice of connectivity γ. If ones uses a mole fraction for molecules that are parallel to one another and a volume fraction for molecules that are perpendicular (it is assumed that the base vectors of the new space are orthogonal) then the appropriate generalization of Eq. (47) is

$$\Omega(N_0, \{N_i\}) = \frac{\prod_{i=1}^{\gamma/2}[M - (k-1)N_i]!}{(N_0)!\prod_{i=1}^{\gamma/2}(N_i)!(M!)^{\gamma/2-1}}, \tag{49}$$

where $\gamma/2$ is the dimensionality of the space. Again, if we allow $N_i = (2/\gamma)N$ (and $N_0 = M - kN$) then Eq. (47) reduces to the well-known Guggenheim's factor

$$\Omega(M, N, \gamma) = \left(\frac{\gamma}{2}\right)^N \frac{M!}{N!(M - kN)!}\left[\frac{\{M - kN + [(\gamma - 2)k + 2]N\}!}{M!}\right]^{\gamma/2}. \tag{50}$$

By operating as in previous sections, configurational entropy per site and adsorption isotherm can be obtained from Eq. (50)

$$\frac{s(\theta,\gamma)}{k_B} = \left[\frac{\gamma}{2} - \frac{(k-1)}{k}\theta\right]\ln\left[\frac{\gamma}{2} - \frac{(k-1)}{k}\theta\right] - \frac{\theta}{k}\ln\frac{\theta}{k} - (1-\theta)\ln(1-\theta) + \left(\theta - \frac{\gamma}{2}\right)\ln\frac{\gamma}{2} \tag{51}$$

$$k\frac{\gamma}{2}\exp[\beta(\mu - kU_0)] = \frac{\theta\left[1 - \dfrac{(k-1)}{k}\dfrac{2\theta}{\gamma}\right]^{k-1}}{(1-\theta)^k}\,. \tag{52}$$

3.4. *Fractional statistics thermodynamic theory of adsorption of polyatomics (FSTA)*

We present the basis of the phenomenological fractional statistic thermodynamic theory of adsorption of polyatomics[91,92] from a novel conceptual framework inspired in the formalism of the recently developed Haldane's Statistics,[98,99] on a generalization of the Pauli's Principle. For the sake of simplicity we contrive our formulation to adsorption in a homogeneous adsorption field. *FSTA* is based in the following conceptual framework: the interaction of one isolated molecule with a solid surface can be represented by an adsorption field[b] having a total number G of local minima in the space of coordinates necessary to define the adsorption configuration (we can think of G being the total number of a equilibrium states for a single molecule).

Depending on the typical size of the particle in the adsorbed state and on the adsorption configuration, some states out of G are prevented from being further occupied upon adsorption of a molecule. We characterize the mean number of states excluded per molecule upon adsorption by the quantity g, being a measure of the "statistical interactions" as it will be shown latter. The parameter g (or better the function g in general) is the fundamental phenomenological parameter of the theory that turns to have a precise physical meaning in either lattice and off-lattice systems; it can be obtained from thermodynamic experiments and relates straightforwardly to the configurational state of the adsorbed particle. Essentially, the configurational entropy of the system will be characterized by the parameter g making either the statistical as well as the thermodynamic properties of complex adsorbed polyatomics much simpler and understandable. Because of possible concurrent exclusion of states by two or more particles g depends in general on the density. Thus, $g \equiv g(N)$ in general.

[b]This adsorption field is usually represented by a lattice of adsorption sites although in the case of particles or molecules composed by more than one elementary unit there is not a one-to-one correspondence between an equilibrium state and a lattice as will be made clear later.

Let us assume $(N-1)$ identical particles within a fixed volume V containig G equilibrium states. The number of states available to the Nth particle when added to the volume is[98]

$$d_N = G - \sum_{N'=1}^{N-1} g(N') = G - G_0(N)\,. \tag{53}$$

This is basically the definition proposed by Haldane[98] as a generalization of Pauli's Exclusion Principle, from which the Haldane's Statistics follows (so called Quantum Fractional Statistics). Accordingly, we propose to describe the general class of physical system addressed here by means of a generalized statistics with $g(N) \geq 1$ for which the number of configurations of a system of N molecules and G states is

$$W(N) = \frac{(d_N + N - 1)!}{[N!(d_N - 1)!]} = \frac{[G - G_0(N) + N - 1]!}{\{N![G - G_0(N) - 1]!\}}\,. \tag{54}$$

It is clear that, for particles that exclude only one state $g(N) = 1$ and $G_0(N) = (N-1)$ $\forall N$, and $W(N)$ reduces to the one expected for fermion-like particles, $W(N) = G!/[N!(G-N)!]$. On the other hand, no exclusion at all, i.e. $g(N) = 0$ $\forall N$, the boson-like form of $W(N)$, $W(N) = (G+N-1)!/[N!(G-N)!]$ is recovered.

In general, configurational entropy per site and adsorption isotherm of non-interacting adsorbed polyatomics can be obtained from Eq. (54)

$$\frac{s(n,\gamma)}{k_B} = -\frac{n}{ak}\ln n + \frac{1}{ak}[1 - \tilde{G}_0(n) + n]\ln[1 - \tilde{G}_0(n) + n] - \frac{1}{ak}[1 - \tilde{G}_0(n)]\ln[1 - \tilde{G}_0(n)] \tag{55}$$

$$\exp[\beta(\mu - kU_0)] = \frac{n[1 - \tilde{G}_0(n) + n]^{(\tilde{G}_0' - 1)}}{[1 - \tilde{G}_0(n)]^{\tilde{G}_0'}} \tag{56}$$

where $n = N/G$ is the density (n finite as N, $G \to \infty$), which is proportional to the standard surface coverage θ, $n = a\theta$, θ being either the ratio N/N_m or the ratio v/v_m, where N (v) is the number of admolecules (adsorbed amount) at given μ, T and N_m (v_m) is the one corresponding to monolayer completion. In addition, $\tilde{G}_0(n) \equiv \lim_{N,G\to\infty} G_0(N)/G$ and $\tilde{G}_0' \equiv d\tilde{G}_0/dn$. Hereafter we examine the simplest approximation within FSTA, namely g =constant,[c] which is rather robust as it will be shown below. Considering that $\tilde{G}_0 = gn$ and $\tilde{G}_0' = g$, a particular isotherm function arises from Eq. (56)

$$\exp[\beta\mu] = \frac{a\theta[1 - a\theta(g-1)]^{g-1}}{[1 - a\theta g]^g}\,. \tag{57}$$

[c]It is worth to note that in general adsorbed molecules may adopt different configurations as the density increases. In this case the values obtained for g from experiments will depend on the pressure range analyzed, according to the general form of Eq. (56). In turn, a relates to the low density limit $\theta \to 0$, $\beta\mu \approx \ln a\theta$.

Equation (57) has well-known adsorption isotherms as limiting cases. Namely, for spherical particles (or single-site occupation in the lattice fashion of the adsorption field) which exclude only one state (one minimum), $g = 1$ and Eq. (57) corresponds to the Langmuir isotherm.[73] On the other hand, it can be demonstrated that Eq. (57) reduces to the rigorous isotherm of non-interacting chains adsorbed flat on a one-dimensional lattice [see Eq. (3)] if g equals the number of chain units (size) k. This is already a simple example of the underlaying relationship between the statistical exclusion parameter g and the spatial configuration of the admolecule.

Finally, we shortly mention some examples out of a whole variety of adsorption configurations that the proposed formalism allows to deal with. Let us consider adparticles composed by k elementary units in which k' out of k units of the molecule are attached to surface sites and $(k - k')$ units are detached and tilted away from them. For a lattice of M sites, $\theta = k'N/M$. Thus, for a molecule with k units, each of which occupying an adsorption site, $k' = k$ and $G = Mm$, where m is the number of distinguishable configurations of the molecule per lattice site (at zero density) and depends on the lattice/molecule geometry. Then $1/a = k'm$. For instance, straight k-mers adsorbed flat on sites of a square lattice would correspond to $m = 2$, $g = 2k$ and $a = 1/(2k)$. On the other hand, $m = 1$, $g = 1$ and $a = 1$ represents the case of end-on (normal to the surface) adsorption of k-mers. Instead, $m = 1$, $g = k'$ and $a = 1/k'$ represents an adsorption configuration in which k' units of the k-mer are attached to a one-dimensional lattice and $(k - k')$ units at the ends are detached.

3.5. *Occupation balance approximation (OB)*

As it is well known, the mean number of particles in the adlayer $\bar{N}$ and the chemical potential μ are related through the following general relationship in the grand canonical ensemble

$$\bar{N} = \lambda \left[\frac{\partial \ln \Xi(M, \lambda)}{\partial \lambda} \right]_M \tag{58}$$

where $\lambda = \exp(\beta\mu)$ and Ξ is the grand partition function. By solving λ^{-1} from Eq. (58)

$$\lambda^{-1} = \frac{1}{\bar{N}} \left[\frac{\partial \ln \Xi(M, \lambda)}{\partial \lambda} \right]_M = \frac{\bar{R}(M, \lambda)}{\bar{N}} \tag{59}$$

where the quantity $\bar{R}(M, \lambda)$ can be proven to be the mean number of states available to a particle on M sites at λ. If $Y_t(M, N)$ and $R_i(M, N)$ denote, the total number of configurations of N distinguishable particles on M sites, and the number of states available to the $(N+1)$th particle in the ith configuration [out of $Y_t(M, N)$], respectively, then

$$Y_t(M, N+1) = \sum_{i=1}^{Y_t(M,N)} R_i(M, N)\,. \tag{60}$$

The total number of configurations of $(N+1)$ indistinguishable particles on M sites, $G_t(M, N+1)$ can be obtained from Eq. (60).

$$G_t(M,N+1) = \frac{Y_t(M,N+1)}{(N+1)!} = \frac{\sum_{i=1}^{Y_t(M,N)} R_i(M,N)}{(N+1)!}$$
$$= \frac{N!}{(N+1)!} \sum_{i=1}^{G_t(M,N)} R_i(M,N) = \frac{1}{N+1} \sum_{i=1}^{G_t(M,N)} R_i(M,N)\,. \quad (61)$$

In the last arguments, we consider that for each configuration of N indistinguishable particles there exist $N!$ configurations of N distinguishable particles.

The average of $R_i(M,N)$ over a grand canonical ensemble is

$$\bar{R}(M,\lambda) = \langle R_i(M,N)\rangle = \frac{1}{\Xi} \sum_{N=0}^{N_m} \left\{ \lambda^N \sum_{i=1}^{G_t} R_i(M,N) \right\}$$
$$= \frac{1}{\Xi} \sum_{N=0}^{N_m-1} (N+1)\lambda^N G_t(M,N+1)$$
$$= \frac{\lambda^{-1}}{\Xi} \sum_{N'=1}^{N_m} \lambda^{N'} N' G_t(M,N') = \frac{\bar{N}}{\lambda} \quad (62)$$

as already advanced in Eq. (59). $N' = N+1$, N_m being the maximum number of particles that fit in the lattice, and $R_i(M,N_m) = 0$.

The advantage of using Eq. (59) to calculate the coverage dependence of the fugacity λ can be seen by dealing with adsorption of dimers in the monolayer regime. $\bar{R}[M,\lambda(\bar{N})] = \bar{R}(M,\bar{N})$ for dimers (occupying two nearest neighbor lattice sites) is, at first order[d], $\bar{R}(M,\bar{N}) \approx \gamma M/2 - (2\gamma-1)\bar{N}$, where the second terms account for the mean number of states excluded by the adsorbed dimers on a lattice with connectivity γ. Thus,

$$\lim_{M\to\infty} \lambda^{-1} \approx \lim_{M\to\infty} \frac{\gamma M/2 - (2\gamma-1)\bar{N}}{\bar{N}} = \frac{\gamma}{\theta} - (2\gamma-1) \quad (63)$$

where $\lim_{M\to\infty} 2\bar{N}/M = \theta$.

The term $(2\gamma-1)$ overestimates the number of excluded states because of simultaneous exclusion of neighboring particles. Then, the approximation can be further refined by considering the mean number of states that are simultaneously excluded by $\bar{N}$ dimers, $\bar{L}(M,\bar{N})$. It is possible to demonstrate that, in general, $\bar{R}(M,\bar{N}) = \gamma M/2 - (2\gamma-1)\bar{N} + \bar{L}(M,\bar{N})$ for linear k-mers.

[d]If it is assumed that each dimer is independent from the neighboring ones, each dimer excludes $(2\gamma-1)$ states out of total $\gamma M/2$

For dimers, $\bar{L}(M,\bar{N})$ is the average number of occupied nearest-neighbor. Due to it is not possible to obtain exacts solutions for $\bar{L}(M,\bar{N})$, we approximate

$$\bar{L}(M,\bar{N}) \approx \frac{\bar{N}\left(\bar{N}-1\right)}{2}\bar{L}(M,2) \tag{64}$$

where $\bar{N}(\bar{N}-1)/2$ is the number of possible pairs for $\bar{N}$ indistinguishable particles.

Considering a system of two adsorbed dimers on a square lattice ($\gamma = 4$), we can write

$$\bar{L}(M,2) = \frac{g_1(M,2)+2g_2(M,2)}{G_t(M,2)} = \frac{18}{(2M-7)} \tag{65}$$

where $G_t(M,2) = M(2M-7)$. In addition, $g_1(M,2) = 14M$ and $g_2(M,2) = 2M$, are the number of states with one and two occupied nearest-neighbor. Finally, we can write

$$\begin{aligned}\lim_{M\to\infty}\lambda^{-1} &= \lim_{M\to\infty}\frac{2M-7\bar{N}+\bar{L}(M,\bar{N})}{\bar{N}}\\ &\approx \lim_{M\to\infty}\frac{1}{\bar{N}}\left[2M-7\bar{N}+\frac{9\bar{N}(\bar{N}-1)}{(2M+7)}\right]\\ &\approx \frac{4}{\theta}-7+\frac{9}{4}\theta+\mathrm{O}(\theta^2)\,.\end{aligned} \tag{66}$$

Finally, by considering that the terms neglected in Eq. (66) are $O(\theta^2)$, it becomes

$$\lambda^{-1} = \frac{4}{\theta}-7+\frac{9}{4}\theta+a\theta^2 \qquad \text{(square lattice)} \tag{67}$$

and the constant $a = 3/4$ can be determined from the limiting condition $\lambda\to\infty$ for $\theta\to 1$. Similarly,

$$\lambda^{-1} = \frac{3}{\theta}-5+\frac{4}{3}\theta+\frac{2}{3}\theta^2 \qquad \text{(honeycomb lattice)} \tag{68}$$

$$\lambda^{-1} = \frac{6}{\theta}-11+\frac{23}{6}\theta+\frac{7}{6}\theta^2 \qquad \text{(triangular lattice)}\,. \tag{69}$$

The entropy per lattice site can be evaluated in the limit $T\to\infty$ as follows

$$\frac{\mu}{k_BT} = \ln\lambda = -\frac{1}{k_B}\lim_{M,T\to\infty}\left[\frac{\partial S(M,N,T)}{\partial N}\right]_{M,T} = -\frac{2}{k_B}\left[\frac{ds(\theta)}{d\theta}\right] \tag{70}$$

then

$$\frac{s(\theta)}{k_B} = -\frac{1}{2}\int_0^\theta \ln\lambda(\theta')d\theta'\,. \tag{71}$$

From Eqs. (67)–(69) and (71) we obtain

$$\begin{aligned}\frac{s(\theta)}{k_B} &= \frac{\theta}{2}\left[\ln C-\ln\theta-2\right]-\frac{(1-\theta)}{2}\ln(1-\theta)-\frac{(A-\theta)}{2}\ln(A-\theta)\\ &\quad+\frac{(B+\theta)}{2}\ln(B+\theta)+\frac{A}{2}\ln A-\frac{B}{2}\ln B\end{aligned} \tag{72}$$

where $A = 2(\sqrt{7/3}-1)$, $(3/2)(\sqrt{3}-1)$ and $(15/7)(\sqrt{53}/5-1)$; $C = 3/4$, $2/3$ and $7/6$; $B = 2(\sqrt{7/3}+1)$, $(3/2)(\sqrt{3}+1)$ and $(15/7)(\sqrt{53}/5+1)$ for square, honeycomb and triangular lattices, respectively.

3.6. *Semi-empirical adsorption model for polyatomics (SE)*

In this section, we propose an approximation of the adsorption isotherm for non-interacting k-mers on a regular lattice, based on semi-empirical arguments, which leads to very accurate results.

We start from Eq. (59), which is called Occupation Balance, and approximate R by using a variant of the method developed by Flory to obtain $\Omega(N_1, N_2)$ as a function of the w_i's [Eq. (29)]. Thus, $R(M, \lambda)$, can be written as,

$$R = \left(\frac{\gamma}{2}M\right)\prod_{i=1}^{k} P_i \,. \tag{73}$$

Equation (73) can be interpreted as follows. The term between parentheses corresponds to the total number of linear k-uples on the surface. These k-uples can be separated in three groups: full k-uples (occupied by k-mers), empty k-uples (available for adsorption) and frustrated k-uples (partially occupied or occupied by segments belonging to different adsorbed k-mers). Then, an additional factor must be incorporated, which takes into account the probability of having a empty k-uple. We suppose that this factor can be written as a product of k functions (P_i's), being P_i the conditional probability of finding the i-th empty site into the lattice with $i-1$ already vacant sites (the i sites are assumed to be arranged in a linear k-uple). In the particular case of $i = 1$,

$$P_1 = 1 - \theta \,, \tag{74}$$

which represents an exact result.

Now, let us consider the simplest approximation within this scheme, namely, $P_i = P_1$ for all i. Then, from Eqs. (59)–(74) result,

$$\lambda^{-1} = \frac{R}{\bar{N}} = \frac{\gamma k}{2}\frac{M}{k\bar{N}}{P_1}^k = \frac{\gamma k(1-\theta)^k}{2\theta} \,. \tag{75}$$

Equation (75) reduces to the *FHL* isotherm of non-interacting linear k-mers adsorbed flat on homogeneous surfaces. This is already a simple example out of a whole variety of multisite adsorption models that the proposed formalism allows to deal with.

In general, the P_i's can be written as

$$P_i = (1-\theta)C_i \,, \tag{76}$$

where a correction factor, C_i, has been included (being $C_1 = 1$ and $C_i \to 1$ as $\theta \to 0$). From Eqs. (73)–(76), we obtain

$$R = \frac{\gamma}{2}M(1-\theta)^k\prod_{i=2}^{k} C_i = \frac{\gamma}{2}M(1-\theta)^k\tilde{C}^{k-1} \tag{77}$$

and

$$\tilde{C} = \left(\prod_{i=2}^{k} C_i \right)^{\frac{1}{k-1}} \tag{78}$$

being $\tilde{C}$ the average correction function, which is calculated as the geometrical mean of the C_i's. Then, from Eqs. (59) and (77), the general form of the adsorption isotherm of linear k-mers can be obtained:

$$\lambda^{-1} = \frac{\gamma k (1-\theta)^k \tilde{C}^{k-1}}{2\theta} \tag{79}$$

or

$$\beta(\mu - kU_0) = \ln\left(\frac{\theta}{k}\right) - k\ln(1-\theta) \ln\left(\frac{\gamma}{2}\right) (k-1) \ln -\tilde{C}\,. \tag{80}$$

It is interesting to compare Eq. (80), obtained in the framework of the OB formalism, with the corresponding ones from the main theories of adsorption of linear polyatomics described in previous sections. For this purpose, we rewrite Eqs. (28), (35), (38), (52) and (25) in a convenient form

$$\beta(\mu - kU_0) = \ln\left(\frac{\theta}{k}\right) - k\ln(1-\theta) - \ln\left(\frac{\gamma}{2}\right) + (k-1)\ln\left[1 - \frac{(k-1)\theta}{k}\right] \quad EA \tag{81}$$

$$\beta(\mu - kU_0) = \ln\left(\frac{\theta}{k}\right) - k\ln(1-\theta) - \ln\left(\frac{\gamma}{2}\right) \quad FHL \quad (k \geq 2) \tag{82}$$

$$\beta(\mu - kU_0) = \ln\left(\frac{\theta}{k}\right) - k\ln(1-\theta) - \ln\left(\frac{\gamma}{2}\right) + (k-1)\ln\left[1 - \frac{(k-1)}{k}\frac{2\theta}{\gamma}\right] \quad GD \tag{83}$$

$$\beta(\mu - kU_0) = \ln\left(\frac{\theta}{k}\right) - \frac{k\gamma}{2}\ln(1-\theta) \ln\left(\frac{\gamma}{2}\right) + \left(\frac{k-\gamma}{2} - 1\right)\ln\left[1 - \theta\frac{(k\gamma - 2)}{k\gamma}\right] \quad FSTA\,. \tag{84}$$

As it can be observed, EA, FHL and GD have already the structure of Eq. (80). In the case of $FSTA$ (and its simplest approximation to linear k-mers), an identical structure can be obtained after simple algebraic operations. From this new perspective, the differences between the theoretical models arise from the distinct strategies of approximating $\tilde{C}$. These arguments can be better understood with an example: EA and GD provide the exact solution for the one-dimensional case.

Then, the comparison between Eq. (80) and the adsorption isotherm from EA (or GD with $\gamma = 2$) allows us to obtain:

$$\tilde{C}^{-1} = 1 - \frac{k-1}{k}\theta \qquad (\gamma = 2)\,. \tag{85}$$

The result in Eq. (85) is exact. Moreover, it can be demonstrated that $C_i = \tilde{C}$ for all i.[90]

On the other hand, previous work[93,100] (comparisons between theoretical models and simulation results in two-dimensional systems) shown that GD fits very well the numerical data at low coverage, while EA behaves excellently at high coverage. Once the equations are written as in Eqs. (81) and (83), it is clear that the differences between EA and GD can be only associated to the average correction function $\tilde{C}$. These findings, along with the structure proposed for the adsorption isotherm [Eq. (80)], allow us to build a new semi-empirical adsorption isotherm for polyatomics (SE),

$$\begin{aligned}\beta\,(\mu - kU_0) = \ln\left(\frac{\theta}{k}\right) - k\ln\,(1-\theta)\ln\left(\frac{\gamma}{2}\right) \\ + (1-\theta)(k-1)\ln\left[1 - \frac{(k-1)}{k}\frac{2\theta}{\gamma}\right] \\ + \theta(k-1)\ln\left[1 - \frac{(k-1)\theta}{k}\right]\,.\end{aligned} \tag{86}$$

The last equation can be interpreted as follows. First line includes three terms, which are identical in both EA and GD. Second and third lines represent a combination of the average correction functions corresponding to GD and EA, with $(1-\theta)$ and θ as weights, respectively. The behavior of SE will be discussed in the next section, in comparison with MC simulation results.

3.7. *Comparison between theory and Monte-Carlo simulations*

We shall discuss some basic characteristics of the adsorption isotherms. For this purpose, Fig. 4 shows a comparison between the exact adsorption isotherm of monomers and the simulation adsorption isotherms of dimers on honeycomb, square and triangular lattices. As it can be observed, the symmetry particle-vacancy, valid for monoatomic species, is broken for $k \geq 2$. In addition, even though adsorption isotherms of dimers look very similar for all connectivities, curves shift to lower values of $\beta(\mu - 2U_0)$ as γ is increased. In other words, for a given value of $\beta(\mu - 2U_0)$, the equilibrium surface coverage increases as γ is increased. This behavior can be easily understood from the following equation:

$$\ln\theta = \ln\gamma + \beta(\mu - kU_0) \tag{87}$$

which is valid for linear k-mers at low concentrations [see Eq. (80)]. The effect diminishes as chemical potential is increased and consequently, the slope of the isotherms diminishes as γ is increased.

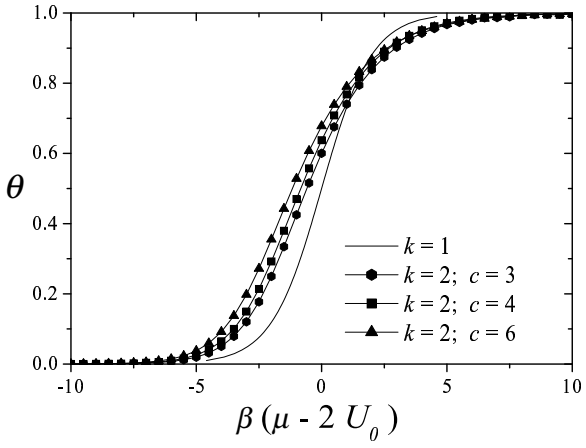

Fig. 4. Comparison between the exact adsorption isotherm of monomers and the simulation adsorption isotherms of dimers on honeycomb, square and triangular lattices.

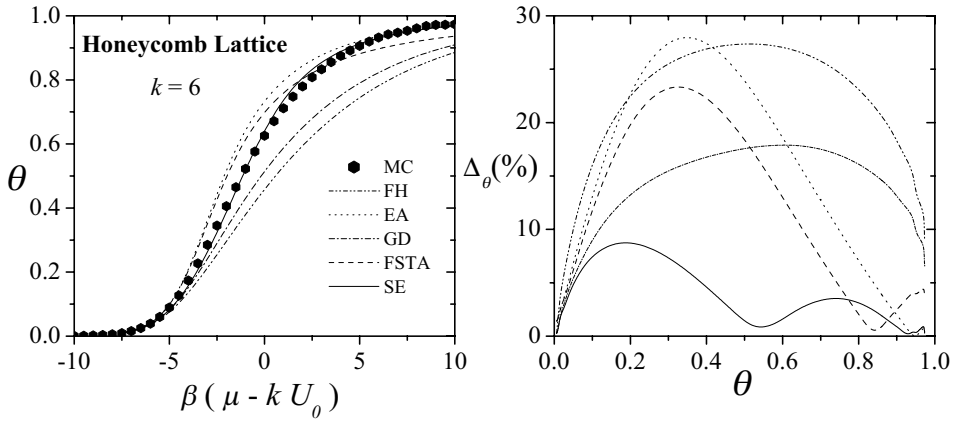

(a) (b)

Fig. 5. (a) Adsorption isotherms of 6-mers on a honeycomb lattice. Symbols represent MC results, and lines correspond to different approaches (see inset). (b) Percentage reduced coverage, $\Delta_\theta(\%)$, versus surface coverage. The symbols are as in part (a).

We now analyze the case corresponding to linear adsorbates larger than dimers. In the case of honeycomb lattices, the k-mers are adsorbed as indicated in Sec. 3. Then, once a site is chosen, there exists six equilibrium states available to a single k-mer ($k \geq 2$) on a honeycomb lattice at infinitely low density. Consequently, the term between parentheses in Eq. (73), which corresponds to the total number of k-uples on the surface, results $3M$ ($\gamma = 6$), as in the case of triangular lattices.

Under these considerations, an extensive work of simulation has been carried out for linear adsorbates with k ranging between 2 and 10. As an example, Figs. 5(a), 6(a) and 7(a) show the comparison between simulation adsorption isotherms and

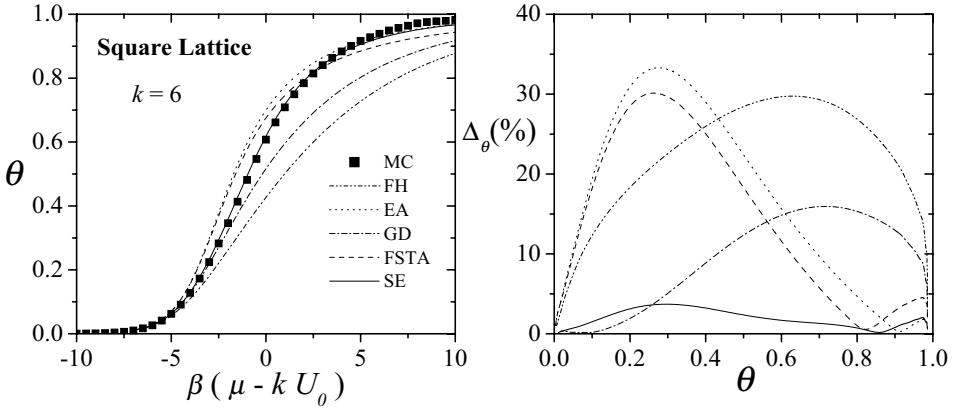

(a) (b)

Fig. 6. As per Fig. 5 for a square lattice.

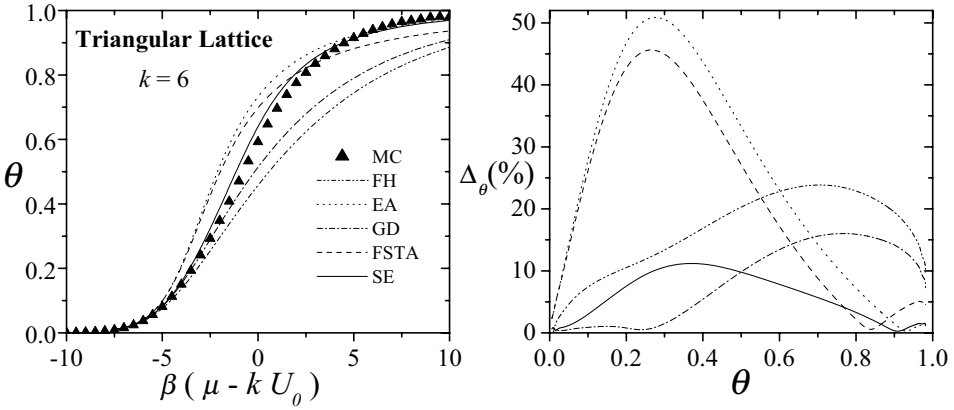

(a) (b)

Fig. 7. As per Fig. 5 for a triangular lattice.

the corresponding ones obtained from theoretical approaches for 6-mers adsorbed on honeycomb, square, and triangular lattices, respectively. In all cases, the agreement between simulation and analytical data is very well for small values of the coverage. However, as surface coverage is increased, the classical theories fail to reproduce adsorption results.

The differences between simulation and theoretical results can be expressed by mean of the percentage reduced coverage, which is defined as[88]

$$\Delta_\theta(\%) = 100 \left| \frac{\theta_{\text{sim}} - \theta_{\text{appr}}}{\theta_{\text{sim}}} \right|_\mu \tag{88}$$

where θ_{sim} (θ_{appr}) represents the coverage obtained by using MC simulation (analytical approach). Each pair of values $(\theta_{\text{sim}}, \theta_{\text{appr}})$ is obtained at fixed μ.

The dependence of $\Delta_\theta(\%)$ on the surface coverage is shown in Figs. 5(b), 6(b) and 7(b) for the different connectivities. The behavior of the analytical approaches can be explained as follows. *FSTA* (dash line) provides a good approximation with very small differences between simulated and theoretical results. *FHL* (dash dot dot line) and *GD* (dash dot line) predict a smaller θ than the simulation data over all range of coverage. In the case of *EA* (dot line), the disagreement turns out to be large for intermediate θ's and a good approximation is recovered for high coverage. With respect to the connectivity, *EA* and *FSTA* (*FHL* and *GD*) become more accurate as γ diminishes (increases). The behavior of *GD* and *EA* justifies the methodology used to build the *SE* isotherm (solid line) in Eq. (86). This situation is also reflected in Figs. 8–10, where the percentage reduced coverage is plotted as a function of concentration for *SE* approximation and different values of γ and k.

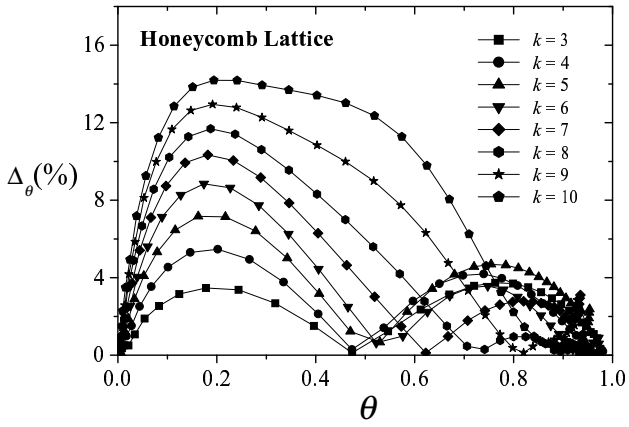

Fig. 8. Percentage reduced coverage versus concentration for k-mers adsorbed on a honeycomb lattice and *SE* approximation. Symbols are indicated in the inset.

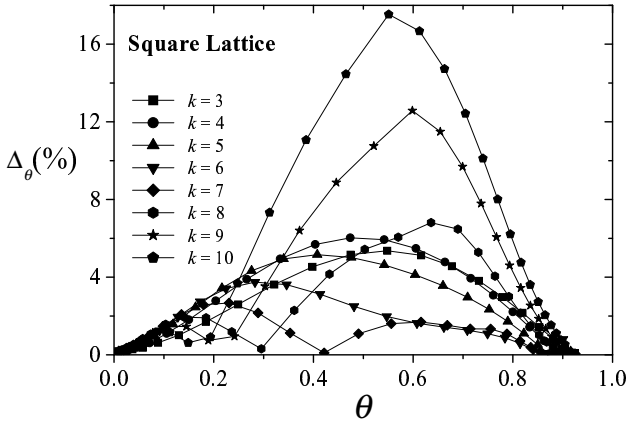

Fig. 9. As per Fig. 8 for a square lattice.

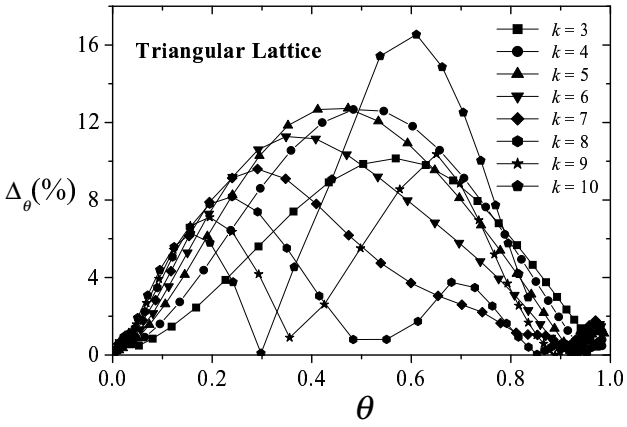

Fig. 10. As per Fig. 8 for a triangular lattice.

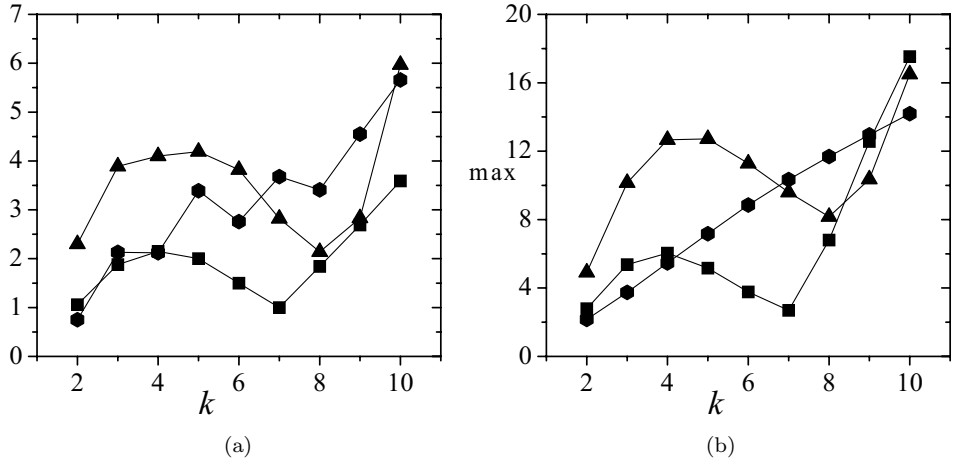

Fig. 11. (a) Average percentage reduced coverage $\bar{\Delta}_\theta$, as a function of k for different connectivities. (b) As in part (a) for the maximum percentage reduced coverage $\Delta_\theta^{\max}$. The symbols are the same as Fig. 4.

The results in Figs. 8–10 can be much easily rationalized with the help of: (1) the average of the absolute values of the difference between simulation and analytical results, $\bar{\Delta}_\theta$; and (2) the maximum value of the percentage reduced coverage, $\Delta_\theta^{\max}$. These quantities are shown in Fig. 11. Several conclusions can be drawn from the figure: (i) in general, the theoretical isotherm performs better for square lattices; (ii) $\bar{\Delta}_\theta$ and $\Delta_\theta^{\max}$ remain practically constant for k ranging between 2 and 8; and (iii) $\bar{\Delta}_\theta$ and $\Delta_\theta^{\max}$ increase for $k > 8$. Finally, the values obtained for $\bar{\Delta}_\theta$, which are lower than 6%, imply that SE is a very good approximation for representing multisite occupancy adsorption, at least for the sizes considered here.

4. Two-Dimensional Lattice-Gas of Interacting Polyatomics

The introduction of intermolecular forces brings about the possibility of phase transitions.[101−104] Among the common types of phase transitions are, condensation of gases, melting of solids, transitions from paramagnet to ferromagnet and order-disorder transitions. From a theoretical point of view, when nearest-neighbor interactions are present, an extra term in the partition function for interaction energy is required. With this extra term, only partition functions for the whole system can be written. Ising[105] gave an exact solution to the one-dimensional lattice problem in 1925. All other cases are expressed in terms of series solution,[73,106,107] except for the special case of two-dimensional lattices at half-coverage, which was exactly solved by Onsager[108] in 1944. For the one-dimensional lattice, there is no evidence of phase transitions. Close approximate solutions in dimensions higher than one can be obtained, and the two most important of these are the Bragg–Williams approximation (BWA)[73] and the quasi-chemical approximation (QCA).[73,109] Both show phase transitions in two-dimensional systems and the BWA incorrectly predicts a phase transition for a linear lattice. These leading models, along with much recent contributions, have played a central role in the study of adsorption systems in presence of lateral interactions between the adatoms. One fundamental feature is preserved in all these theories. This is the assumption that an adsorbed molecule occupies one adsorption site. In this section, we generalize BWA and QCA in order to include multisite-occupancy.

4.1. *Mean-field approximation for k-mers*

The Bragg–Williams approximation is the simplest mean-field treatment for interacting adsorbed particles, even in the case of multisite occupancy. In this context, the canonical partition function $Q(N,M,T)$ for a system of N k-mers adsorbed on M sites at a temperature T, considering nearest neighbor lateral interaction of magnitude w between adsorbed molecules is given by,

$$Q(N,M,T)=\sum_{\{E_k\}}\Omega(E_k)e^{-\beta E_k(N,M)} \tag{89}$$

where $\Omega(E_k)$ is the number of configurations of N k-mers on M sites with energy E_k. If a mean-field approximation is introduced at this point

$$Q(N,M,T)=e^{-\beta\overline{E_k(N,M)}}\sum_{\{E_k\}}\Omega(E_k)=e^{-\beta\overline{E_k(N,M)}}\Omega(N,M,\gamma) \tag{90}$$

where $\overline{E_k(N,M)}$ is the mean total energy of the system assuming that the kN occupied sites of the lattice are randomly distributed over M sites. On the other hand, $\Omega(N,M,\gamma)$ depends on the spatial configuration of the k-mer and the surface geometry. Even in the simplest case of linear k-mers, there not exist the exact form of $\Omega(N,M,\gamma)$ in two (or more) dimensions. However, as it was discussed in Sec. 3,

different approximations have been developed for $\Omega(N, M, \gamma)$. In this case, we will calculate $\Omega(N, M, \gamma)$ in the framework of EA model [Eq. 25].

On the other hand,

$$\overline{E_k(N, M)} = kNU_0 + \frac{1}{2}\lambda N \left(\frac{kN}{M}\right) w \tag{91}$$

where the first and second terms in the RHS of Eq. (16) account for the k-mer-lattice and k-mer-k-mer interactions, respectively; and $\lambda = [2(\gamma-1)+(k-2)(\gamma-2)]$ is the number of nearest neighbor sites of an adsorbed k-mer (in a linear configuration).

Hence, the canonical partition function $Q(N, M, T)$ can be written as

$$Q(N, M, T) = K(\gamma, k)^N \frac{[M-(k-1)N]!}{N![M-kN]!} e^{-(kNU_0+\frac{1}{2}\lambda k\frac{N^2}{M}w)/k_BT}\,. \tag{92}$$

The Helmholtz free energy $F(N, M, T)$ is given by:

$$\begin{aligned}\beta F(N, M, T) &= \ln Q(N, M, T)\\ &= \ln \Omega(N, M, \gamma) - \beta kNU_0 - \frac{1}{2}\beta w\lambda k\frac{N^2}{M}\\ &= \ln[M-(k-1)N]! - \ln N! - \ln[M-kN]!\\ &\quad + N\ln K(\gamma, k) - \beta kNU_0 - \frac{1}{2}\beta w\lambda k\frac{N^2}{M}\,.\end{aligned} \tag{93}$$

The Helmholtz free energy per site can be obtained as a function of coverage and temperature,

$$\begin{aligned}\beta f(\theta, T) = &-\left[1-\frac{k-1}{k}\theta\right]\ln\left[1-\frac{k-1}{k}\theta\right] + \frac{\theta}{k}\ln\frac{\theta}{k} + (1-\theta)\ln(1-\theta)\\ &-\frac{\theta}{k}\ln K(\gamma, k) + \beta\theta\epsilon_o + \frac{1}{2}\beta\lambda w\frac{\theta^2}{k}\,.\end{aligned} \tag{94}$$

Accordingly, from Eq. (19) and the formalism presented in Sec. 2.1, s is given by

$$\frac{s(\theta)}{k_B} = \left[1-\frac{k-1}{k}\theta\right]\ln\left[1-\frac{k-1}{k}\theta\right] - \frac{\theta}{k}\ln\frac{\theta}{k} - (1-\theta)\ln(1-\theta) + \frac{\theta}{k}\ln K(\gamma, k) \tag{95}$$

In addition, the isotherm equation takes the form

$$\begin{aligned}y(\theta, T) &= C_k K(\gamma, k) e^{[\beta(\mu-kU_0)]}\\ &= \frac{\theta\left[1-\dfrac{(k-1)}{k}\theta\right]^{(k-1)}}{(1-\theta)^k} e^{\beta\lambda w\theta}\end{aligned} \tag{96}$$

where $C_k = k$. Finally, the differential heat of adsorption, q_d, and total adsorption energy per site u result

$$q_d(\theta) = -\lambda w\theta - kU_0 \tag{97}$$

and

$$u(\theta) = \frac{1}{2}\lambda\frac{\theta^2}{k}w + \theta U_0\,. \tag{98}$$

4.2. *Quasi-chemical approximation for polyatomics*

Here, we address the general case of interacting adsorbates assumed as linear molecules in the framework of the quasi-chemical approach. As in the previous section, two different energies are considered in the adsorption process: (1) U_0, constant interaction energy between a k-mer unit and an adsorption site and (2) w, lateral interaction energy between two nearest-neighbor units belonging to different k-mers. Then, the canonical partition function can be written as:[73]

$$Q(N,M,T) = \sum_{N_{11}} \Omega(N,M,N_{11}) \exp\left[-\beta\left(wN_{11} + k\ N\ U_0\right)\right] \tag{99}$$

where N_{11} is the number of pairs of nearest-neighbor units belonging to different k-mers and $\Omega(N,M,N_{11})$ is the number of ways to array N k-mers on M sites with N_{11} pair of occupied sites. In addition, U_0 can be arbitrarily chosen equal to zero without losing generality.

As it is usual in the case of single-site occupation, it is convenient to write the canonical partition function as a function of N_{01}, being N_{01} the number of pairs formed by an empty site adjacent to a occupied site. For this purpose, we calculate the relations between N_{11}, N_{01} and N_{00} (being N_{00} the number of pairs of empty nearest-neighbor sites):

$$2N_{11} + N_{01} + 2N(k-1) = \gamma k N\,, \tag{100}$$

$$2N_{00} + N_{01} = \gamma(M - kN)\,, \tag{101}$$

where "number of 01 pairs" = "number of 10 pairs" = $N_{01}/2$. In the case of $k = 1$, the well-known relations for single-site occupation are recovered.[73]

Now, the canonical partition function can be written in terms of N_{01}

$$Q(N,M,T) = \exp\left[-\beta N\left(\lambda w/2\right)\right] \sum_{N_{01}} \Omega(N,M,N_{01}) \exp\left(\beta w N_{01}/2\right) \tag{102}$$

and $\lambda = (\gamma - 2)k + 2$.

By using the standard formalism of the QCA, the number of ways of assigning a total of $[\gamma M/2 - N(k-1)]$ independent pairs[e] to the four categories, 11, 10, 01, and 00, with any number 0 through $[\gamma M/2 - N(k-1)]$ per category consistent with the total, is

$$\tilde{\Omega}(N,M,N_{01}) = \frac{[\gamma M/2 - N(k-1)]!}{\left[(N_{01}/2)!\right]^2 [\gamma(M-kN)/2 - N_{01}/2]!\,[\lambda N/2 - N_{01}/2]!}\,. \tag{103}$$

[e]The term $N(k-1)$ is subtracted since the total number of nearest-neighbor pairs, $\gamma M/2$, includes the $N(k-1)$ bonds belonging to the N adsorbed k-mers.

This cannot be set equal to $\Omega(N, M, N_{01})$ in Eq. (102), because treating the pairs as independent entities leads to some unphysical configurations (see Ref. 73, p. 253). Thus $\tilde{\Omega}$ overcounts the number of configurations. To take care of this, we must normalize $\tilde{\Omega}$:

$$\Omega(N, M, N_{01}) = C(N, M, \gamma)\tilde{\Omega}(N, M, N_{01}) \tag{104}$$

and

$$\Omega(N, M) = \sum_{N_{01}} \Omega(N, M, N_{01}) = C(N, M, \gamma) \sum_{N_{01}} \tilde{\Omega}(N, M, N_{01})\,. \tag{105}$$

Once $\Omega(N, M)$ is approximated in some of the forms given in Sec. 3, $C(N, M, \gamma)$ can be obtained.

In order to calculate $C(N, M, \gamma)$, we replace $\sum_{N_{01}} \tilde{\Omega}(N, M, N_{01})$ by the maximum term in the sum, $\tilde{\Omega}(N, M, N_{01}^*)$. By taking logarithm in Eq. (103), using the Stirling's approximation and operating, it results,

$$\begin{aligned}\ln \tilde{\Omega}(N, M, N_{01}) = {} & [\gamma M/2 - (k-1)N] \ln[\gamma M/2 - (k-1)N] - N_{01} \ln N_{01}/2 \\ & - [\gamma(M - kN)/2 - N_{01}/2] \ln[\gamma(M - kN)/2 - N_{01}/2] \\ & - (\lambda N/2 - N_{01}/2) \ln(\lambda N/2 - N_{01}/2)\,. \end{aligned} \tag{106}$$

By differentiating the last equation with respect to N_{01}

$$\tilde{\Omega}'(N, M, N_{01}) = \frac{\tilde{\Omega}(N, M, N_{01})}{2} \ln\left\{\frac{[\gamma(M - kN) - N_{01}](\lambda N - N_{01})}{N_{01}^2}\right\}. \tag{107}$$

Setting $\tilde{\Omega}'(N, M, N_{01}) = 0$ and solving for N_{01}^*, the value of N_{01} in the maximum term of $\tilde{\Omega}$,

$$N_{01}^* = \frac{\gamma\lambda N(M - kN)}{\gamma M - 2(k-1)N} = \lambda N - \frac{\lambda^2 N^2}{\gamma B}\,, \tag{108}$$

and

$$B = M - 2(k-1)N/\gamma\,. \tag{109}$$

Then,

$$\tilde{\Omega}(N, M, N_{01}^*) = \frac{(\gamma B/2)!}{\left[\left(\lambda N/2 - \dfrac{\lambda^2 N^2}{2\gamma B}\right)!\right]^2 \left(\gamma B/2 - \lambda N + \dfrac{\lambda^2 N^2}{2\gamma B}\right)! \left(\dfrac{\lambda^2 N^2}{2\gamma B}\right)!}\,, \tag{110}$$

and, by simple algebra,

$$\tilde{\Omega}(N, M, N_{01}^*) = \left[\frac{B!}{(B - \lambda N/\gamma)!\,(\lambda N/\gamma)!}\right]^{\gamma}. \tag{111}$$

Equation (111) allows us to calculate $C(N, M)$,

$$C(N, M, \gamma) = \frac{\Omega(N, M, \gamma)}{\tilde{\Omega}(N, M, N_{01}^*)}$$
$$= \Omega(N, M, \gamma) \left[\frac{(B - \lambda N/\gamma)!\,(\lambda N/\gamma)!}{B!} \right]^{\gamma} . \quad (112)$$

Now, $\ln Q(N, M, T)$ [see Eq. (102)] can be written as

$$\ln Q(N, M, T) = -\beta N \lambda w/2 + \ln \left\{ \sum_{N_{01}} C(N, M, \gamma) \tilde{\Omega}(N, M, N_{01}) \exp(\beta w N_{01}/2) \right\} . \quad (113)$$

As in Eq. (105), we replace $\sum_{N_{01}} C(N, M, \gamma)\tilde{\Omega}(N, M, N_{01}) \exp(\beta w N_{01}/2)$ by the maximum term in the sum, $C(N, M, \gamma)\tilde{\Omega}(N, M, N_{01}^{**}) \exp(\beta w N_{01}^{**}/2)$. Thus,

$$C(N, M, \gamma)\tilde{\Omega}'(N, M, N_{01}^{**}) \exp(\beta w N_{01}^{**}/2) + C(N, M, \gamma)\tilde{\Omega}(N, M, N_{01}^{**})$$
$$\times \exp(\beta w N_{01}^{**}/2)\beta w/2 = 0 , \quad (114)$$

and

$$\frac{\tilde{\Omega}'(N, M, N_{01}^{**})}{\tilde{\Omega}(N, M, N_{01}^{**})} = -\beta w/2 . \quad (115)$$

From Eqs. (107) and (115),

$$(\gamma B - \lambda N - N_{01}^{**})(\lambda N - N_{01}^{**}) = {N_{01}^{**}}^2 \exp(-\beta w) \quad (116)$$

and

$$[1 - \exp(-\beta w)]{N_{01}^{**}}^2 - \gamma B N_{01}^{**} + (\gamma B - \lambda N)\lambda N = 0 . \quad (117)$$

Solving Eq. (117) we obtain[f]

$$\frac{N_{01}^{**}}{\gamma B} = \frac{1 - \sqrt{1 - 4A(1 - \lambda N/\gamma B)(\lambda N/\gamma B)}}{2A} . \quad (118)$$

where $A = 1 - \exp(-\beta w)$.

Finally, the canonical partition function can be written in terms of N_{01}^{**},

$$Q(N, M, T) = \exp(-\beta N \lambda w/2)\Omega(N, M, \gamma) \left[\frac{(B - \lambda N/\gamma)!(\lambda N/\gamma)!}{B!} \right]^{\gamma}$$
$$\times \tilde{\Omega}(N, M, N_{01}^{**}) \exp(\beta w N_{01}^{**}/2) . \quad (119)$$

As in the previous section, we will use the following expression for $\Omega(N, M, \gamma)$,

$$\Omega(N, M, \gamma) = K(\gamma, k)^N \frac{(B - \lambda N/\gamma + N)!}{N!(B - \lambda N/\gamma)!} , \quad (120)$$

[f]The solution $N_{01}^{**}/\gamma B = \left(1 + \sqrt{\cdots}\right)/2A$ is discarded for physical reasons.

which is an extension to two dimensions of the exact configurational factor obtained in one dimension. In the particular case of rigid straight k-mers, the simplest approximation provides $K(\gamma,k)=\gamma/2$.

Introducing Eq. (120) in Eq. (119), taking logarithm and using the Stirling's approximation, it results

$$\begin{aligned}\ln Q(N,M,T) = &-\beta N\lambda w/2 + N\ln K(\gamma,k) + \beta w N_{01}^{**}/2\\ &+(B-\lambda N/\gamma+N)\ln(B-\lambda N/\gamma+N) - N\ln N\\ &+(\gamma-1)(B-\lambda N/\gamma)\ln(B-\lambda N/\gamma)+\lambda N\ln\lambda N/\gamma\\ &-\gamma B\ln B+\gamma B/2\ln\gamma B/2 - N_{01}^{**}\ln N_{01}^{**}/2\\ &-(\gamma B/2-\lambda N/2-N_{01}^{**}/2)\ln(\gamma B/2-\lambda N/2-N_{01}^{**}/2)\\ &-(\lambda N/2-N_{01}^{**}/2)\ln(\lambda N/2-N_{01}^{**}/2)\,. \end{aligned} \tag{121}$$

From Eq. (121), the Helmholtz free energy per site, $f(N,M,T)$, can be obtained as a function of surface coverage and temperature,

$$\begin{aligned}\beta f(\theta,T) = &-\frac{\theta}{k}\ln K(\gamma,k)+\beta w\left(\frac{\lambda\theta}{2k}-\alpha\right)-\left[\frac{\gamma}{2}-\left(\frac{k-1}{k}\right)\theta\right]\\ &\times\ln\left\{\frac{\left[1-\left(\frac{k-1}{k}\right)\theta\right]^{2/\gamma}(1-\theta)^{2(\gamma-1)/\gamma}\left[\frac{\gamma}{2}-\left(\frac{k-1}{k}\right)\theta\right]}{\left[1-\frac{2}{\gamma}\left(\frac{k-1}{k}\right)\theta\right]^{2}\left[\frac{\gamma}{2}(1-\theta)-\alpha\right]}\right\}\\ &-\frac{\theta}{k}\ln\left\{\frac{\left(\frac{\lambda\theta}{\gamma k}\right)^{\lambda}\left[\frac{\gamma}{2}(1-\theta)-\alpha\right]^{\lambda/2}}{\frac{\theta}{k}\left[1-\left(\frac{k-1}{k}\right)\theta\right]^{(\lambda-\gamma)/\gamma}(1-\theta)^{(\lambda\gamma-\lambda)/\gamma}\left[\frac{\lambda\theta}{2k}-\alpha\right]^{\lambda/2}}\right\}\\ &-2\alpha\ln\left\{\frac{\left[\frac{\gamma}{2}(1-\theta)-\alpha\right]^{1/2}\left[\frac{\lambda\theta}{2k}-\alpha\right]^{1/2}}{\alpha}\right\}\end{aligned} \tag{122}$$

where α is

$$\alpha=\frac{N_{01}^{**}}{2M}=\frac{\lambda\gamma}{2k}\frac{\theta(1-\theta)}{\left[\frac{\gamma}{2}-\left(\frac{k-1}{k}\right)\theta+b\right]}\,. \tag{123}$$

and

$$b=\left\{\left[\frac{\gamma}{2}-\left(\frac{k-1}{k}\right)\theta\right]^{2}-\frac{\lambda\gamma}{k}A\theta(1-\theta)\right\}^{1/2}\,. \tag{124}$$

The coverage dependence of the chemical potential arises straightforwardly from Eqs. (5) and (122)

$$K(\gamma,k)\left(\frac{2}{\gamma}\right)^{2(k-1)}\exp\left[\beta\left(\mu-w\lambda/2\right)\right]$$

$$=\frac{\theta}{k}\frac{(1-\theta)^{k(\gamma-1)}\left[k-(k-1)\theta\right]^{k-1}\left[\dfrac{\lambda\theta}{2k}-\alpha\right]^{\lambda/2}}{\left[\dfrac{\gamma k}{2}-(k-1)\theta\right]^{k-1}\left[\dfrac{\gamma}{2}(1-\theta)-\alpha\right]^{k\gamma/2}\left(\dfrac{\lambda\theta}{\gamma k}\right)^{\lambda}}. \tag{125}$$

The configurational energy per site, u, can be calculated as

$$u=w\frac{N_{01}^{**}}{M}=w\left(\frac{\lambda N}{2M}-\frac{N_{01}^{**}}{2M}\right)$$

$$=w\left(\frac{\lambda\theta}{2k}-\alpha\right). \tag{126}$$

In addition, $f=u-Ts$ and the entropy per site, s, can be obtained from Eqs. (122) and (126) as

$$\frac{s}{k_B}=\frac{\theta}{k}\ln K(\gamma,k)+\left[\frac{\gamma}{2}-\left(\frac{k-1}{k}\right)\theta\right]$$

$$\times\ln\left\{\frac{\left[1-\left(\dfrac{k-1}{k}\right)\theta\right]^{2/\gamma}(1-\theta)^{2(\gamma-1)/\gamma}\left[\dfrac{\gamma}{2}-\left(\dfrac{k-1}{k}\right)\theta\right]}{\left[1-\dfrac{2}{\gamma}\left(\dfrac{k-1}{k}\right)\theta\right]^{2}\left[\dfrac{\gamma}{2}(1-\theta)-\alpha\right]}\right\}$$

$$+\frac{\theta}{k}\ln\left\{\frac{\left(\dfrac{\lambda\theta}{\gamma k}\right)^{\lambda}\left[\dfrac{\gamma}{2}(1-\theta)-\alpha\right]^{\lambda/2}}{\dfrac{\theta}{k}\left[1-\left(\dfrac{k-1}{k}\right)\theta\right]^{(\lambda-\gamma)/\gamma}(1-\theta)^{(\lambda\gamma-\lambda)/\gamma}\left[\dfrac{\lambda\theta}{2k}-\alpha\right]^{\lambda/2}}\right\}$$

$$+2\alpha\ln\left\{\frac{\left[\dfrac{\gamma}{2}(1-\theta)-\alpha\right]^{1/2}\left[\dfrac{\lambda\theta}{2k}-\alpha\right]^{1/2}}{\alpha}\right\}. \tag{127}$$

1 The isosteric heat of adsorption q_{st} is defined as[110]

$$\left(\frac{\partial\beta\mu}{\partial T}\right)_{\theta}=\frac{q_{st}}{k_BT^2} \tag{128}$$

which can be calculated explicitly from Eq. (125),

$$q_{st}(\theta,T)=-\frac{\lambda w}{2}+\left\{\frac{\lambda}{2}\left(\frac{\lambda\theta}{2k}-\alpha\right)^{-1}-\frac{k\gamma}{2}\left[\frac{\gamma}{2}(1-\theta)-\alpha\right]^{-1}\right\}\frac{w\alpha^2\exp\left(-\beta w\right)}{b}. \tag{129}$$

Finally, the heat capacity per site, c_v, results

$$\frac{c_v}{k_B} = \frac{1}{k_B}\frac{\partial u}{\partial T} = (\beta w \alpha)^2 \, \frac{\exp(-\beta w)}{b} \, . \tag{130}$$

4.3. *Comparison between BWA, QCA and Monte-Carlo simulations*

In the present section, we will analyze the main characteristics of the thermodynamic functions given in *BWA* and *QCA*, in comparison with simulation results for a lattice-gas of interacting dimers on honeycomb, square and triangular lattices.[g]

The computational simulations have been developed for honeycomb, square and triangular $L \times L$ lattices, with $L = 144$, 144 and 150, respectively, and periodic boundary conditions.[111,112] With this lattice size we verified that finite-size effects are negligible. Note, however, that the linear dimension L has to be properly chosen such that the adlayer structure is not perturbed.

Typical adsorption isotherms obtained by MC simulations in the grand canonical ensemble (symbols) and comparison with *QCA* (solid lines) and *BWA* (dashed lines) are shown in Figs. 12–14, for honeycomb, square and triangular lattices, respectively.

For attractive interactions [Figs. 12(a), 13(a) and 14(a)], as the temperature decreases, the system undergoes a first-order phase transition that shows as the discontinuity in the simulated isotherms and as the typical loops in the theoretical isotherms. In this situation, which has been observed experimentally in numerous systems,[101,110] the only phase which one expects is a lattice-gas phase at low coverage, separated by a two-phase coexistence region from a "lattice-fluid" phase at higher coverage. This lattice-fluid can be considered as a version of the registered (1×1) phase (where every available site of the lattice is occupied) diluted with vacancies.

This condensation of a two-dimensional gas to a two-dimensional liquid is similar to that of a lattice-gas of attractive monomers. However, the symmetry particle-vacancy (valid for monoatomic particles) is broken for k-mers and the isotherms are asymmetric with respect to $\theta = 0.5$.

The isotherms in the repulsive case [Figs. 12(b), 13(b) and 14(b)] have more features because of the existence of ordered structures in the adlayer. These structures are clearly evidence of subcritical behavior [the systems undergoes continuous

[g]In one dimension, *QCA* reduce to the rigorous functions of interacting chains adsorbed flat on a one-dimensional lattice [see Sec. 2.2]. With respect to *BWA*, a characteristic van der Waals loop is observed in the adsorption isotherm for the attractive case and *BWA* incorrectly predicts a phase transition for $\gamma = 2$. For strong repulsive couplings, the *BWA* curves apart from the exact results and does not reproduce the plateau in the adsorption isotherm. The limitations of the *BWA* can be much easily ratinalized with the help of the entropy per site. In fact, the main assumption of the *BWA* say that the configurational degeneracy and average nearest-neighbor interaction energy are treated as though the molecules were distributed randomly among the sites. Consequently, the entropy per site does not depend on w and adopts the form of Eq. (12).

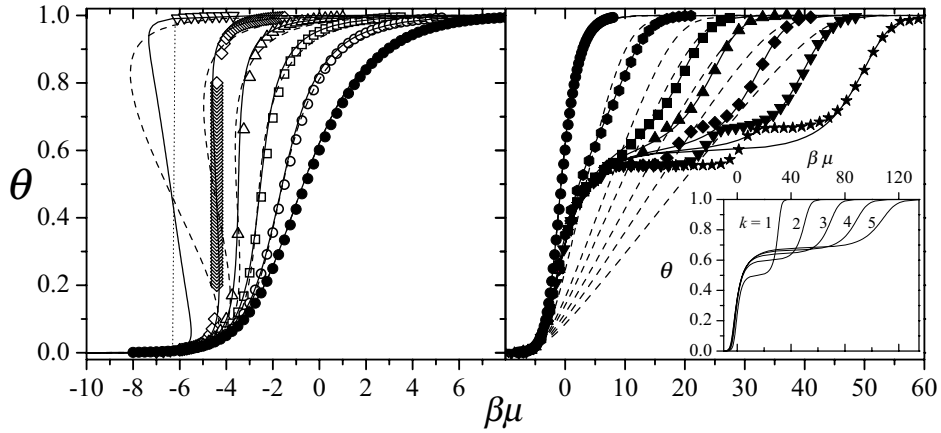

Fig. 12. Adsorption isotherms for homonuclear dimers adsorbed on a honeycomb lattice with nearest-neighbor interactions. Symbols, solid lines and dashed lines represent results from Monte-Carlo simulations, *QCA* and *BWA*, respectively. The dotted lines are included in the figure as a guide for the eyes. (a) Attractive case: full circles, $\beta w = 0$; open circles, $\beta w = -0.5$; open squares, $\beta w = -1.0$; open up triangles, $\beta w = -1.5$; open diamonds, $\beta w = -2.0$ and open down triangles, $\beta w = -3.0$. (b) Repulsive case: full circles, $\beta w = 0$; full hexagons, $\beta w = 2.0$; full squares, $\beta w = 4.0$; full up triangles, $\beta w = 5.0$; full diamonds, $\beta w = 6.5$; full down triangles, $\beta w = 8.0$ and full stars, $\beta w = 10.0$. Inset: Adsorption isotherms from *QCA* for $\beta w = 10.0$ and different values of k as indicated.

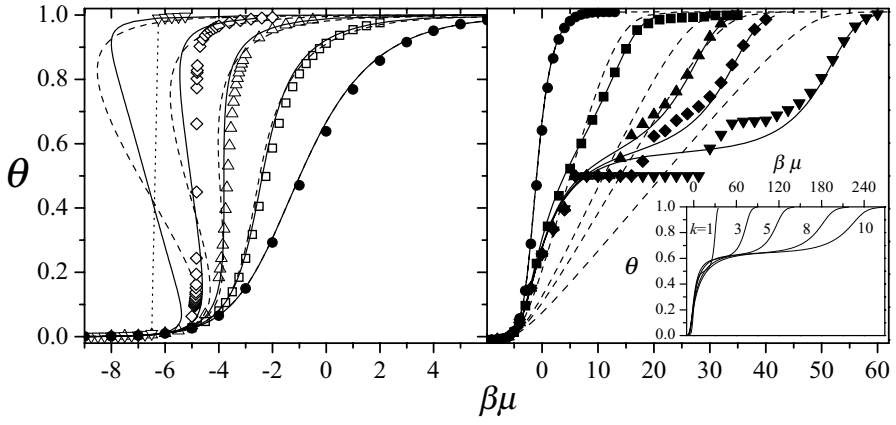

Fig. 13. Adsorption isotherms for homonuclear dimers adsorbed on a square lattice with nearest-neighbor interactions. Symbols, solid lines and dashed lines represent results from Monte-Carlo simulations, *QCA* and *BWA*, respectively. The dotted lines are included in the figure as a guide for the eyes. (a) Attractive case: full circles, $\beta w = 0$; open squares, $\beta w = -0.5$; open up triangles, $\beta w = -1.0$; open diamonds, $\beta w = -1.4$ and open down triangles, $\beta w = -2.0$. (b) Repulsive case: full circles, $\beta w = 0$; full squares, $\beta w = 2.0$; full up triangles, $\beta w = 4.0$; full diamonds, $\beta w = 5.0$ and full down triangles, $\beta w = 7.5$. Inset: Adsorption isotherms from *QCA* for $\beta w = 7.5$ and different values of k as indicated.

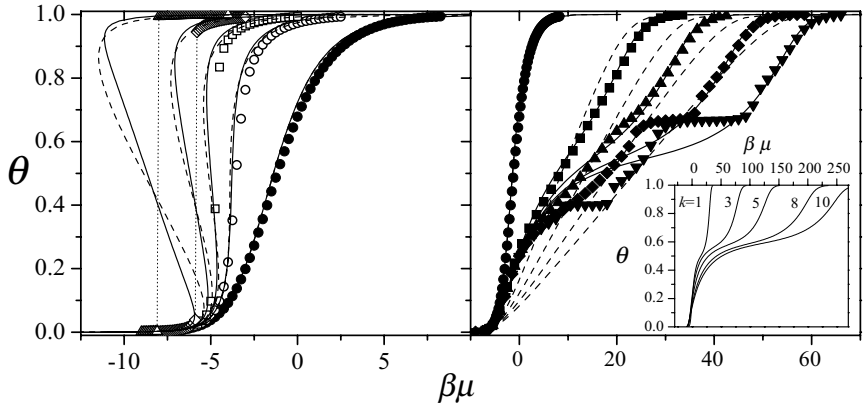

(a) (b)

Fig. 14. Adsorption isotherms for homonuclear dimers adsorbed on a triangular lattice with nearest-neighbor interactions. Symbols, solid lines and dashed lines represent results from Monte-Carlo simulations, *QCA* and *BWA*, respectively. The dotted lines are included in the figure as a guide for the eyes. (a) Attractive case: full circles, $\beta w = 0$; open circles, $\beta w = -0.5$; open squares, $\beta w = -0.75$; open diamonds, $\beta w = -1.0$ and open up triangles, $\beta w = -1.5$. (b) Repulsive case: full circles, $\beta w = 0$; full squares, $\beta w = 2.0$; full up triangles, $\beta w = 3.0$; full diamonds, $\beta w = 4.0$ and full down triangles, $\beta w = 5.0$. Inset: Adsorption isotherms from *QCA* for $\beta w = 5.0$ and different values of k as indicated.

phase transitions, from disorder to ordered structures].[111,112] At high temperatures, the isotherms do not present any peculiar behavior. For low temperatures, we can see the typical steps which correspond to the developing of some ordered phase structures and the shape of the isotherms is much dependent on the connectivity. In fact, as the chemical potential μ increases and θ varies from 0 to 1, we found two different ordered phases in the adsorbate: (1) a low-coverage ordered phase (LCOP), with 5/9, 1/2 and 2/5 of the sites occupied for honeycomb, square and triangular lattices, respectively; and (2) a high-coverage ordered phase (HCOP), with 2/3 of the sites filled for the three geometries. Snapshots corresponding to LCOP [part (a)] and HCOP [part (b)] for honeycomb, square and triangular lattices are shown in Figs. 15–17. For a more complete discussion of LCOP and HCOP, interested readers are referred to Refs. 111 and 112.

In the attractive cases, the two theoretical approximations agree qualitatively well and the adsorption isotherms for the *BWA* and *QCA* are hardly distinguishable from each other. However, it is known that the isotherms resulting distinctly different approximations can look very similar.[113] The differences between numerical and theoretical results can be much easily rationalized with the help of the absolute error, $\varepsilon^a(\theta)$, which is defined as

$$\varepsilon^a(\theta) = |\mu_{\text{theor}} - \mu_{\text{sim}}|_\theta \tag{131}$$

where μ_{sim} (μ_{theor}) represents the chemical potential obtained by using MC simulation (analytical approach). Each pair of values (μ_{sim}, μ_{theor}) is obtained at fixed θ.

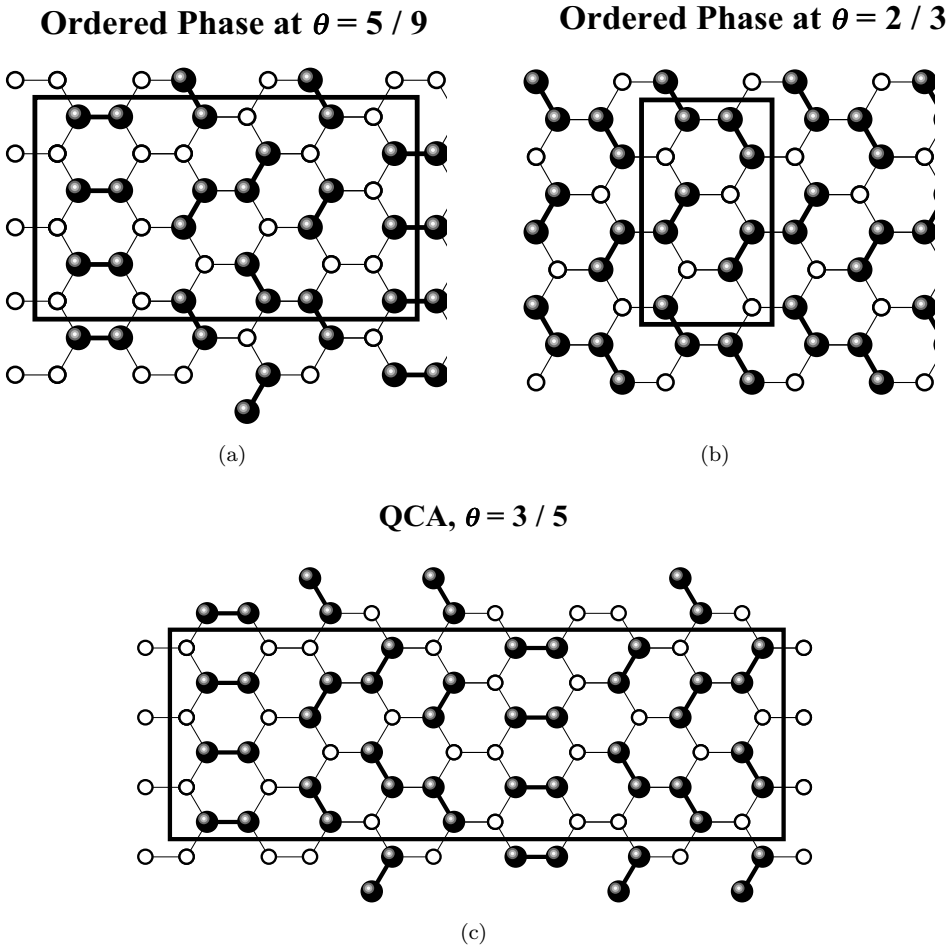

Fig. 15. Snapshots of the ordered phases corresponding to repulsive dimers adsorbed on a honeycomb lattice. (a) Low-coverage ordered structure (LCOP); (b) high-coverage ordered structure (HCOP) and (c) LCOP-HCOP mixture according to the predictions of QCA.

As an example, Fig. 18(a) shows $\varepsilon^a(\theta)$ for three typical attractive cases: squares, $\beta w = -3.0$; triangles, $\beta w = -1.5$ and circles, $\beta w = -0.5$. Full and open symbols represent results from *BWA* and *QCA*, respectively. In all cases, *QCA* leads to appreciably better results than *BWA*. The curves in Fig. 18 correspond to a honeycomb lattice. However, the behavior of $\varepsilon^a(\theta)$ for square and triangular lattices is very similar (data are not shown here for sake of simplicity).

With respect to repulsive interactions, the differences between *QCA* and *BWA* are very appreciable. This situation is clearly reflected in Fig. 18(b), where three repulsive cases are depicted: squares, $\beta w = 8.0$; triangles, $\beta w = 4.0$ and circles, $\beta w = 2.0$. Full and open symbols are as in part (a). Beyond the quantitative discrepancies between *QCA* and *BWA*, there exists qualitative differences between both

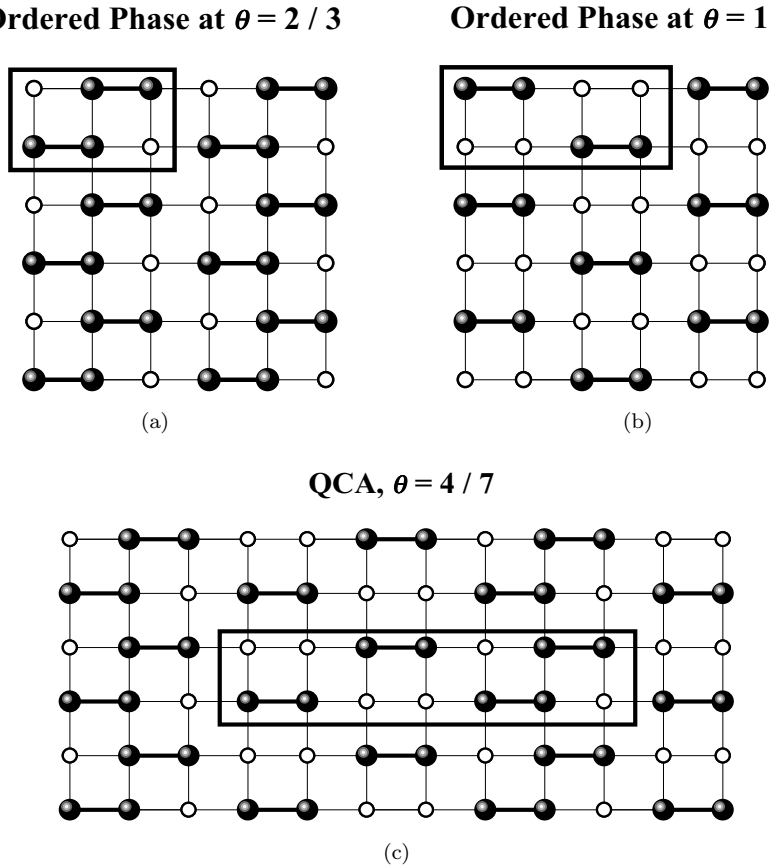

Fig. 16. As per Fig. 15 for square lattices.

approximations. Thus, while *BWA* does not predict the existence of ordered phases in the adsorbate, *QCA* isotherms present a pronounced plateau as the temperature lowers. This singularity or critical coverage θ_c^{QCA}, which appears at a intermediate coverage between the LCOP and the HCOP, depends on both the geometry of the substrate and the size of the adsorbate. The value of θ_c^{QCA} can be determined from the point of inflection in the adsorption isotherm equation [Eq. (125)], calculated in the limit as $\beta w \to \infty$. Thus,

$$\theta_c^{QCA} = \frac{(\gamma/2)\,k}{(\gamma-1)k+1}\,. \tag{132}$$

Figure 19 shows the behavior of θ_c^{QCA} as a function of the k-mer's size, for the different connectivities studied. In the particular case of $k = 2$, $\theta_c^{QCA} = 3/5, 4/7$ and $6/11$, for honeycomb, square and triangular lattices, respectively. The configuration of the adsorbate at θ_c^{QCA} "could be thought" as a mixture of LCOP and HCOP [see part (c) in Figs. 15–17].

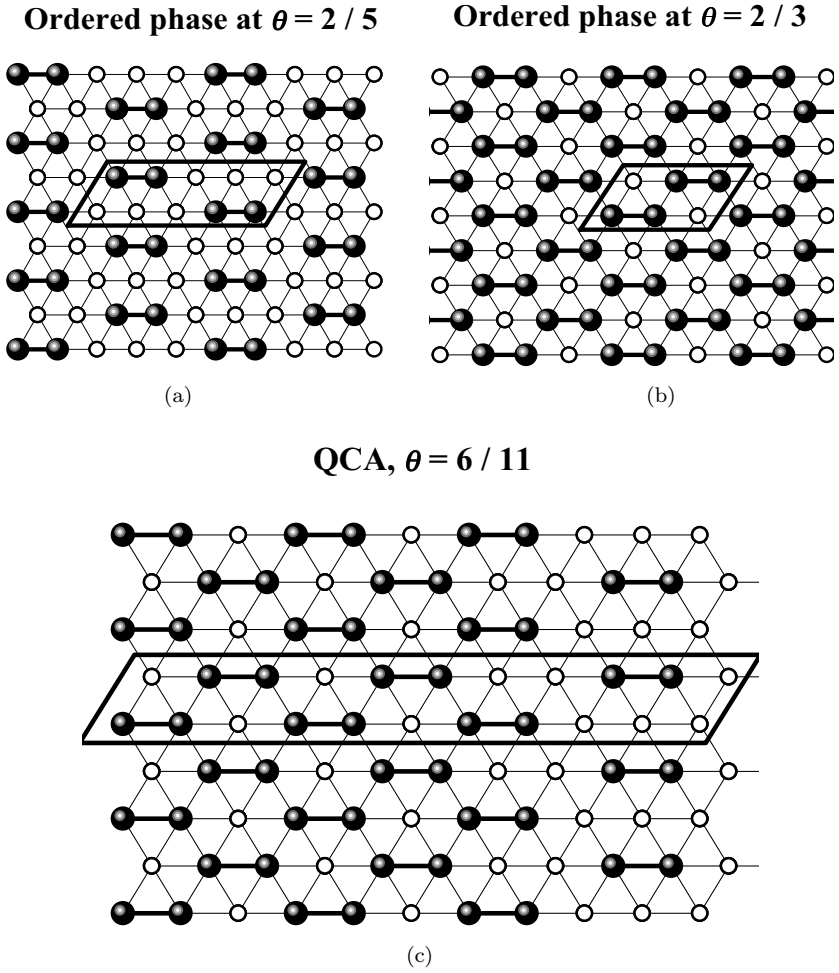

Fig. 17. As per Fig. 15 for triangular lattices.

Summarizing, we define the integral error ε^i, which takes into account the differences between theoretical and simulation data in all range of coverage,

$$\varepsilon^i = \int_0^1 \varepsilon^a(\theta) d\theta \,. \tag{133}$$

The integral error is shown in Fig. 20 for all studied geometries and for a wide range of values of βw. Several conclusions can be drawn from the figure:

- In all cases, *QCA* gives a much better description of the MC adsorption isotherms than the *BWA*. In the particular case of repulsive interactions, the disagreement between MC and *BWA* turns out to be significantly large, while *QCA* appears as the simplest approximation capable to take into account the main features of the multisite occupancy adsorption.

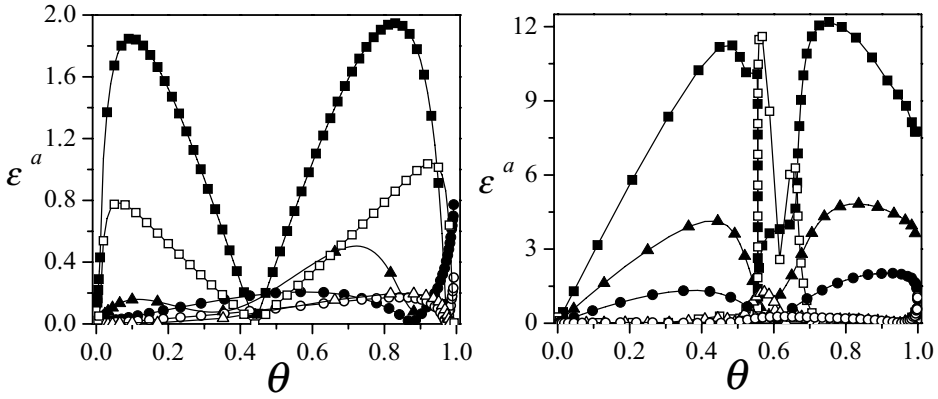

Fig. 18. Absolute error ε^a, versus surface coverage for adsorption isotherms of dimers. The symbology is as follows: (a) Squares, $\beta w = -3.0$; triangles, $\beta w = -1.5$ and circles, $\beta w = -0.5$. (b) Squares, $\beta w = 8.0$; triangles, $\beta w = 4.0$ and circles, $\beta w = 2.0$. Full and open symbols correspond to comparisons with QCA and BWA, respectively.

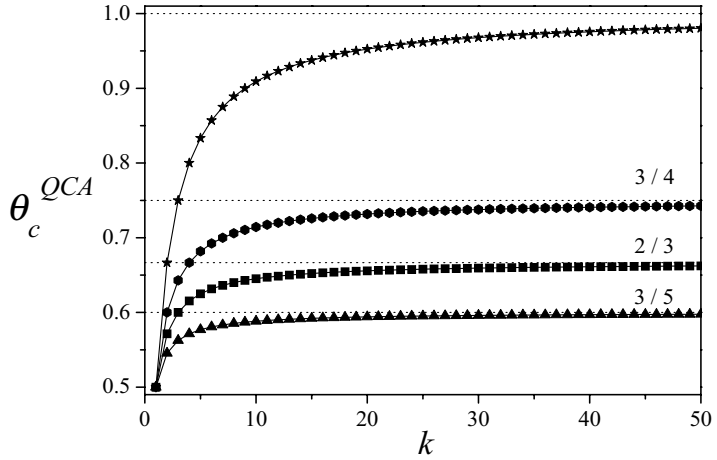

Fig. 19. Critical coverage θ_c^{QCA}, as a function of the adsorbate size k for different geometries: stars, one-dimensional lattices; hexagons, honeycomb lattices; squares, square lattices and triangles, triangular lattices.

- $\varepsilon^i(\theta)$ increases as the lattice connectivity is increased. A possible explanation for the deviation from QCA (and BWA) observed for high connectivity is associated with the choice of $\Omega(N, M, \gamma)$ in Eqs. (105) and (120). In fact, $\Omega(N, M, \gamma)$ is an extension to two dimensions of the exact configurational factor obtained in one dimension. Consequently, the accuracy of $\Omega(N, M, \gamma)$ diminishes as γ is increased.[88] In the future, other expressions for $\Omega(N, M, \gamma)$ will be investigated.
- There exists a wide range of βw's ($-1 \leq \beta w \leq 4$), where QCA provides an excellent fitting of the simulation data. In addition, most of the experiments in

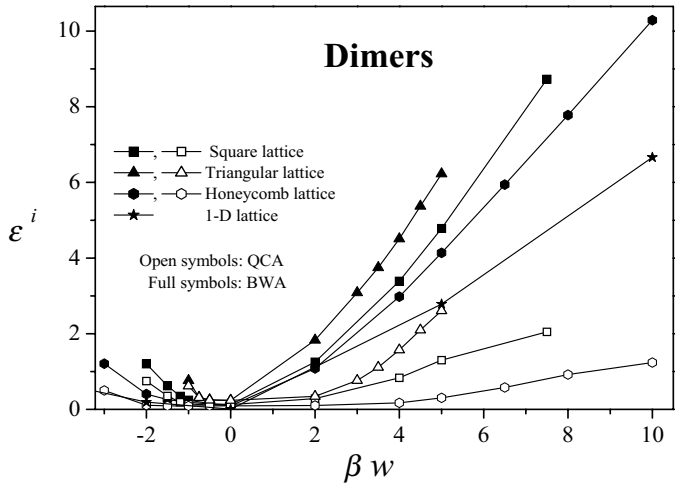

Fig. 20. Integral error ε^i, versus lateral interaction (in β units) for different geometries as indicated.

surface science are carried out in this range of interaction energy. Then, *QCA* not only represents a qualitative advance in the description of the adsorption k-mers with respect to the *BWA*, but also gives a framework and compact equations to consistently interpret thermodynamic adsorption experiments of polyatomics species such as alkanes, alkenes, and other hydrocarbons on regular surfaces.

We now analyze the behavior of the isosteric heat of adsorption. q_{st} versus coverage is plotted in Figs. 21–23, for honeycomb, square and triangular lattices, respectively. The curves are denoted as in Figs. 12–14.

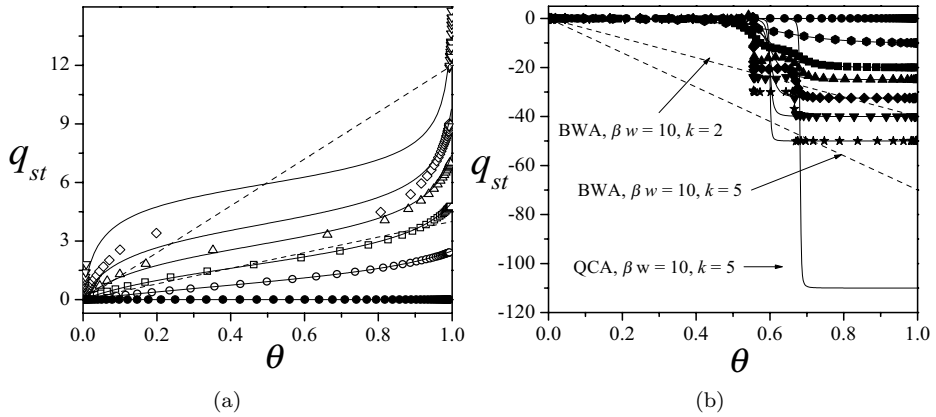

Fig. 21. Isosteric heat of adsorption q_{st}, versus surface coverage for attractive [part (a)] as well repulsive [part (b)] interacting dimers and 5-mers adsorbed on a honeycomb lattice. The curves are labeled as in Fig. 12. In two limit cases ($\beta w = 10$, $k = 2$ and $\beta w = 10$, $k = 5$), the data are compared with *BWA*.

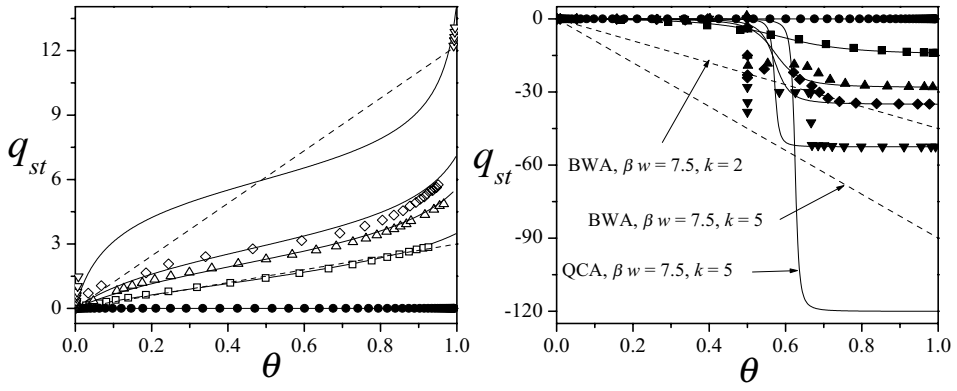

Fig. 22. Isosteric heat of adsorption q_{st}, versus surface coverage for attractive [part (a)] as well repulsive [part (b)] interacting dimers and 5-mers adsorbed on a square lattice. The curves are labeled as in Fig. 13. In two limit cases ($\beta w = 7.5$, $k = 2$ and $\beta w = 7.5$, $k = 5$), the data are compared with *BWA*.

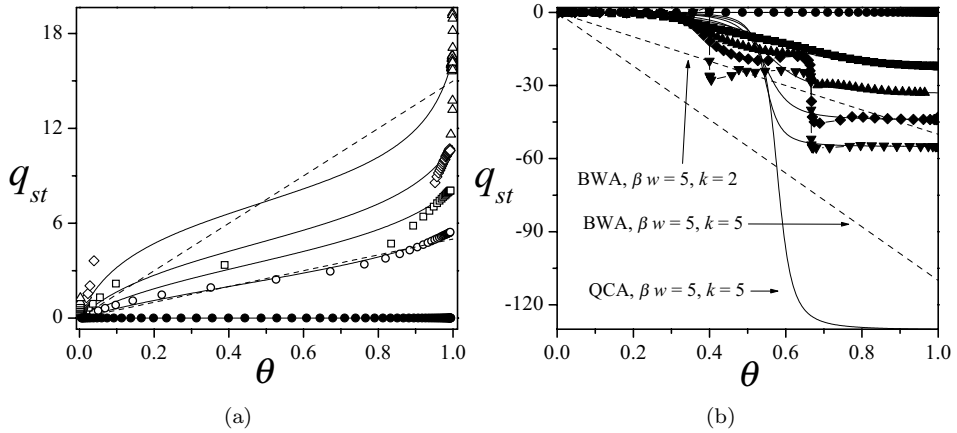

Fig. 23. Isosteric heat of adsorption q_{st}, versus surface coverage for attractive [part (a)] as well repulsive [part (b)] interacting dimers and 5-mers adsorbed on a triangular lattice. The curves are labeled as in Fig. 14. In two limit cases ($\beta w = 5$, $k = 2$ and $\beta w = 5$, $k = 5$), the data are compared with *BWA*.

The general features of the coverage dependence of the isosteric heat of adsorption for attractive k-mers are the following [see part (a) in Figs. 21–23]: q_{st} is monotonically increasing on coverage. As the ratio βw is increased, two main effects occur. (i) A plateau appears being $q_{st} = (\gamma - 1)w$. This behavior demonstrates that the island of adsorbed dimers grows through the perimeter, being $(\gamma - 1)w$, the involved energy in one adsorption-desorption of a dimer in the perimeter of the adsorbate island. (ii) The plateau flattens over a wide range of coverage since adsorbate islands are more compact for larger βw.

As it can be noticed, the differences between the theoretical approximations are notable. While *QCA* agrees very well with the curves of q_{st}, *BWA* presents a linear behavior and does not reproduce the main characteristics of q_{st}.

For the repulsive case [part (b) in Figs. 21–23], q_{st} varies from a smoothly decreasing (at high temperatures) to a double stepped function of θ (at low temperatures). The abrupt steps are traced to the presence of the ordered phases shown in Figs. 15–17. As in the attractive case, *BWA* varies linearly with the coverage and appears as a poor sensitive theory for studying q_{st}. On the other hand, even though *QCA* does not reproduce the two steps in the curves at very low temperatures, the approach agrees very well with the simulation data in a wide range of βw's and predicts the value of q_{st} at high coverage, $q_{st}(\theta \to 1)$. As it has been widely discussed in Refs. 87 and 112, the value of $q_{st}(\theta \to 1)$ can be only understood from reordering processes occurring in the adsorbate at high coverage, which do not appear in the case of monomers and, consequently, are a clear signal of the presence of multisite occupancy adsorption. These findings reinforce the validity of the proposed *QCA* to describe k-mers adsorption thermodynamics.

Finally, the behavior of the configurational entropy per site as a function of coverage is shown in Figs. 24–26. For attractive interactions [part (a) in Figs. 24–26], the overall behavior can be summarized as follows: for $\theta \to 0$ the entropy tends to zero. For low coverage, $s(\theta)$ is an increasing function of θ, reaches a maximum, then decreases monotonically. In the limit $\theta \to 1$ the entropy tends to a finite value, which is associated to the different ways to arrange the dimers at full coverage. This value depends on the geometry, being $s(\theta = 1)/k_B \approx 0.19$, 0.29 and 0.44 for $\gamma = 3, 4$ and 6, respectively. The effect of the interactions is to decrease the entropy for intermediate coverage ($0 < \theta < 1$), remaining constant in the limits $\theta \to 0$ and

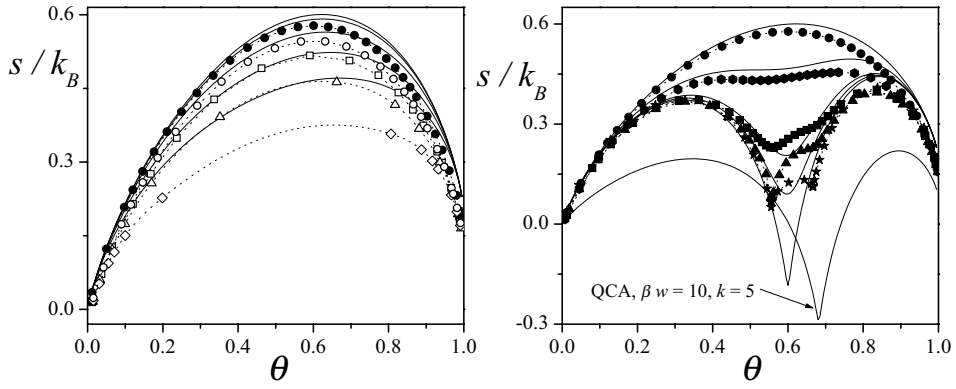

Fig. 24. Entropy per site as a function of coverage for homonuclear dimers and 5-mers adsorbed on a honeycomb lattice with nearest-neighbor interactions. The curves are labeled as in Fig. 12. (a) Attractive case and (b) repulsive case. Solid lines from top to bottom correspond one-to-one to the cases plotted with symbols. The dotted lines are included in the figure as a guide for the eyes.

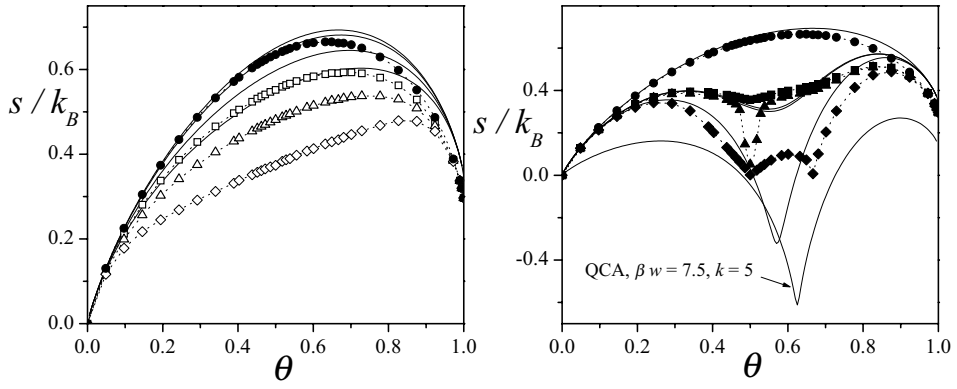

Fig. 25. Entropy per site as a function of coverage for homonuclear dimers and 5-mers adsorbed on a square lattice with nearest-neighbor interactions. (a) Attractive case: full circles, $\beta w = 0$; open squares, $\beta w = -0.5$; open up triangles, $\beta w = -1.0$ and open diamonds, $\beta w = -1.4$. (b) Repulsive case: full circles, $\beta w = 0$; full squares, $\beta w = 2.94$; full up triangles, $\beta w = 3.13$ and full diamonds, $\beta w = 7.5$. Solid lines from top to bottom correspond one-to-one to the cases plotted with symbols. The dotted lines are included in the figure as a guide for the eyes.

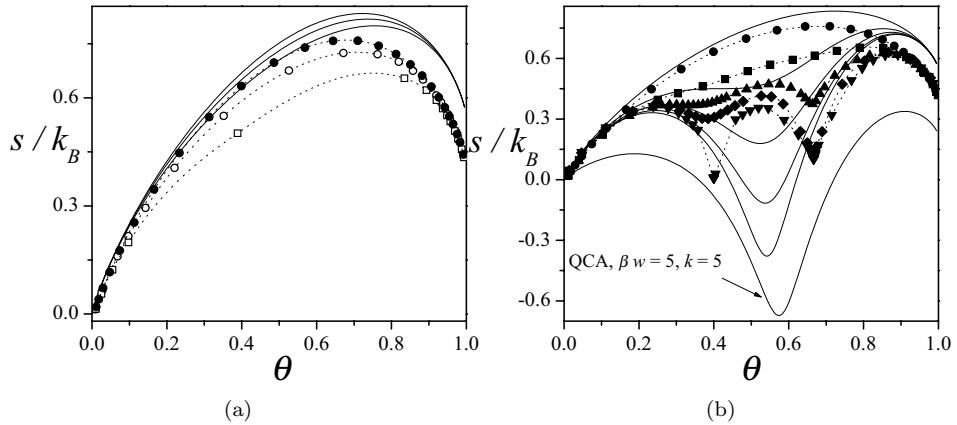

Fig. 26. Entropy per site as a function of coverage for homonuclear dimers and 5-mers adsorbed on a triangular lattice with nearest-neighbor interactions. The curves are labeled as in Fig. 14. (a) Attractive case and (b) repulsive case. Solid lines from top to bottom correspond one-to-one to the cases plotted with symbols. The dotted lines are included in the figure as a guide for the eyes.

$\theta \to 1$. The curves from QCA present a qualitative agreement with simulation data, but overestimate the value of the entropy in the whole range of θ.

In the case of repulsive interactions [part (b) in Figs. 24–26], s/k_B develops two minima as T decreases, corresponding to the presence of the LCOP and the HCOP. In the case of QCA, the curves present a minimum at θ_c^{QCA}. The value of $s(\theta = \theta_c^{QCA})/k_B$ decreases as βw is increased, reaching negative values for high

βw's. This spurious behavior also appears in the classical *QCA* for monomers.[73,110] On the other hand and as it was discussed above, the entropy per site from *BWA* does not depend on βw.

5. Applications

We consider here a few applications of the results presented in previous sections. Namely, analysis of complex adsorbates by using *FSTA*;[91,92] adsorption of non-interacting k-mers on heterogeneous surfaces;[2,96,97,114] and multilayer adsorption of polyatomics.[115,116]

5.1. *Analysis of complex adsorbates by using FSTA*

Analysis of simulation and experimental results have been carried out in order to illustrate the applicability and versatility of FSTA to describe complex adsorption systems. Thus, experimental adsorption isotherms of propane[117] and oxygen[3,4] in 5A and 13X zeolites, respectively, were examined in terms of the new isotherm function. In our analysis, Eq. (57) was used assuming that: (i) since $g =$ constant, if one molecule has m distinguishable ways of adsorbing per lattice site at zero density, then $g = mk'$ $[a = 1/(mk')]$ states are excluded when one k-mer is adsorbed occupying k' sites on the lattice; (ii) ad-ad interaction energy is introduced through a mean-field term as stated before. In addition, given that the analyzed experimental isotherms were reported in adsorbed amount v, against pressure p, we rewrite Eq. (57) in the more convenient form:

$$K(T)p/p_o = \frac{(v/v_m)[g-(g-1)v/v_m]^{g-1}}{[g-g(v/v_m)]^g}\exp\left[\beta w(v/v_m)\right] \tag{134}$$

where $\exp\left[\beta w(v/v_m)\right]$ is the mean-field term, $p = p_o\exp(\beta\mu)$ and $K(T) = K_\infty\exp\left(-\beta H_{st}\right)$ is the equilibrium constant, H_{st} being the isosteric heat of adsorption.

Figure 27 shows adsorption isotherms of C_3H_8 in a $13X$ zeolite. Lines correspond to FSTA and symbols represent experimental data from Ref. 117. As widely accepted, an alkane chain is considered a "bead segment", in which each methyl group is represented as a single site (bead). In this frame, we fix $k = 3$ for propane. In addition, the length of propane (6.7 Å) is relatively large with respect to the diameter of the cavity (11.6 Å). This fact suggests that the molecules should adsorb aligned along a preferential direction. Otherwise, five or six molecules would hardly fit in the cavity. Accordingly, we fix $g = 3$ ($k' = k = 3$ and $m = 1$ as in the one-dimensional case). Then, we determine, by multiple fitting, the set of parameters $[K(T), v_m, w]$ leading to the best fit to the experimental data of $C_3H_8/13X$ from Ref. 117 in the whole pressure and temperature range.

The fitting process is as follows. We considered the least-squares statistics.[118] Thus, suppose that we are fitting n_m data points (x_i, y_i, z_i), $i = 1, \ldots, n_m$, to

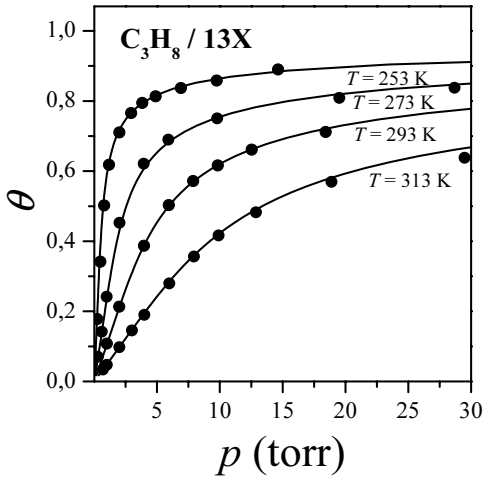

Fig. 27. Adsorption isotherms for C_3H_8 adsorbed in $13X$ zeolite fitted by FSTA. Symbols correspond to data from Ref. 117 and lines represent theoretical results from Eq. (134).

a model that has L adjustable parameters $a_j, j = 1, \ldots, L$. The model predicts a functional relationship between the measured independent and dependent variables,

$$z(x, y) \equiv z(x, y; a_1 \ldots a_L) \tag{135}$$

where the dependence on the parameters is indicated explicitly on the right-hand side. What, exactly, do we want to minimize to get fitted values for the a_js? The first thing that comes to mind is the familiar least-squares fit, minimize over $a_1 \ldots a_L$:

$$\sum_{i=1}^{n_m} [z_i - z(x_i, y_i; a_1 \ldots a_L)]^2 . \tag{136}$$

The parameters of the model are then adjusted to achieve a minimum in function (136), yielding best-fit parameters. The adjustment process is thus a problem in minimization in many dimensions.

In our particular case, the least-squares estimation of the isotherm parameters was performed for each adsorbate by minimizing the sum of the square difference between the experimental pressure and the predicted pressure, over all n_m data points corresponding to the complete set of isotherms. That is, the function $p(v, T) \equiv p(v, T; v_m, K(T), w)$ (from Eq. 134) corresponds to $z(x, y) \equiv z(x, y; a_1 \ldots a_L)$, being (v, T) and $(v_m, K(T), w)$ dependent variables and adjustable parameters, respectively. In the case of Fig. 27, the fitting parameters are indicated in Table 1.

As in the experiment, the resulting value of v_m is smaller than six molecules per cavity, and the fractional value of $v_m (= 5.75)$ is indicative that some molecules may stand across the cavity's windows. Concerning the lateral interaction at full coverage, the ratio between the value of w from fitting and the molecular interaction $C_3H_8 - C_3H_8$ in the liquid phase, ϵ, reported in Ref. 117 is $w/\epsilon \approx 2.5$. This value indicates that each propane molecule in the adsorbed phase at maximum loading

Table 1. Table of fitting parameters of data in Figs. 27 and 29. H_{st}^{FSTA}, $H_{st}^{\exp}$, w^{FSTA} and $w^{\exp}$ are expressed in kcal/mol (absolute values given). v_m is expressed in molecules/cavity [(a)] and cc_{STP}/g. of adsorbent [(b)] for data from Refs. 3 and 4, respectively. (c) and (d) represent experimental values from Refs. 4 and 117, respectively; (e), simulation data from Ref. 119 and (f), $C_3H_8 - C_3H_8$ interaction energy in the liquid phase (see Ref. 117).

System	k	m	g	v_m	H_{st}^{FSTA}	$H_{st}^{\exp}$	w^{FSTA}	$w^{\exp}$	D
$O_2/5A$	2	2	4	$12^{(a)} - 130.9^{(b)}$	3.10	$3.37^{(c)}$	0.72	$0.54^{(e)}$	5.60%
$C_3H_8/13X$	3	1	3	5.75	6.94	$6.81^{(d)}$	1.27	$0.50^{(f)}$	2.08%

interacts, in average, with 2.5 neighbors, and reinforces the argument that the system can be treated as a quasi-one-dimensional system.

An excellent agreement was also obtained in Fig. 28, by fitting non monotonically increasing data (in Fig. 28, we carried out the fitting of the derivative of the adsorbed amount versus pressure and obtained a good agreement).

The differences between experimental and theoretical data can be very easily rationalized with the help of the deviation D, which is defined as the ratio between the absolute value of the difference between the experimental and the corresponding theoretical value, averaged over the total set of data:

$$D = \sum_{i=1}^{n_m} \left\{ 100 \cdot \left| \frac{v_{\text{theo}}^i - v_{\text{sim}}^i}{v_{\text{sim}}^i} \right| \right\} . \tag{137}$$

The deviation between the set of experimental data and the fitting curves in Fig. 27 was 2.08% (see Table 1). This value is lower than the typical experimental errors in measurements of adsorption, which reinforces the robustness of the fits in the present contribution. In addition, it is worth emphasizing that a rather

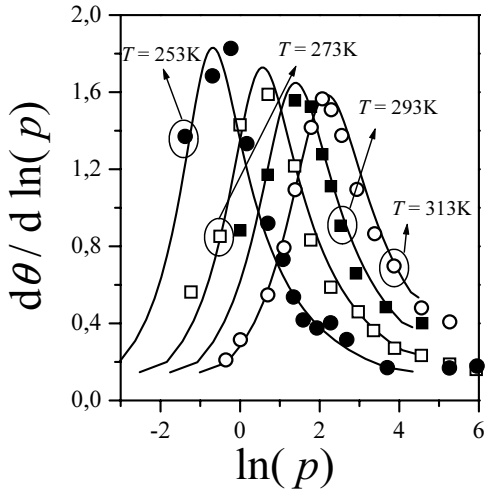

Fig. 28. Derivative of the adsorbed amount versus pressure ($\ln p$) for the same set of data plotted in Fig. 27.

artificial model with eight fitting parameters was necessary to interpret analogous data in Ref. 117. In the present description of adsorption, the complexity of the entropy of adsorbed polyatomics is characterized by the single parameter g carrying meaningful quantitative information about the spatial configuration of the admolecule.

Adsorption isotherms of $O_2/5A$ are shown in Fig. 29. Symbols are experimental data and lines represent theoretical results from Eq. (134). Experimental data were taken from two different sources in the literature, from Miller *et al.*[4] and Danner *et al.*[3] In the first set of data (empty symbols),[4] the amount adsorbed was measured in units of the number of molecules per cavity. In the other case (full symbols),[3] the amount adsorbed was reported in units of cc_{STP} per *gram* of adsorbent. In order to homogenize the plots, we have represented the amount adsorbed by using the adimensional surface coverage $\theta = v/v_m$.

The fit was carried out in two steps: (i) based on previous numerical simulations,[119] we fix $g = 4$ ($k' = k = 2$ and $m = 2$). Under these considerations, analytical isotherms in Fig. 27. The value obtained for w is in excellent agreement with the simulation calculation of w in Ref. 119. With respect to v_m, it was not possible from the work of Razmus *et al.*[120] to estimate v_m in order to compare with the one from Eq. (134). However, v_m was independently validated through a second stage of fitting; (ii) the values of g, $K(T)$ and w arising from (i) were fixed. Then, v_m, set as to fit the experimental isotherm measured by Danner *et al.*,[3] agrees with the monolayer volume reported in Ref. 3. The deviation between experimental and fitting curves was 5.60% (see Table 1). Based in the consistency of this analysis,

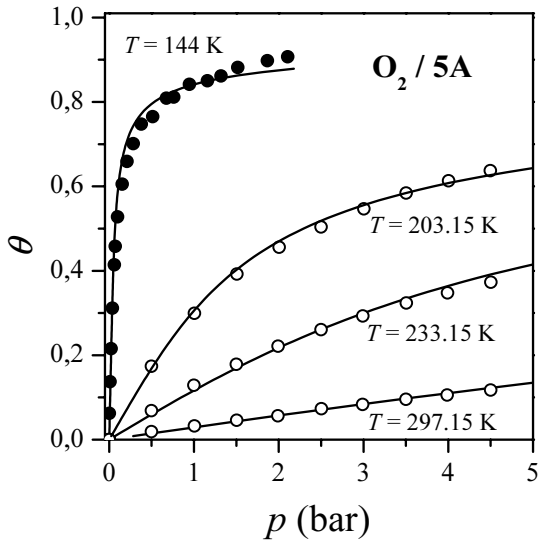

Fig. 29. Adsorption isotherms for O_2 adsorbed in $5A$ zeolite. Empty and full symbols correspond to data from Refs. 3 and 4, respectively. Lines correspond to the adsorption isotherm function of Eq. (134).

O_2 appears to adsorb flat with two possible orientations on a two-dimensional layer defined by the cavity's inner surface.

The values for H_{st} in Figs. 27 and 29 were obtained from the slope of $\ln K(T)$ vs. $1/T$. This procedure is shown in Fig. 30. The fitting results, which are presented

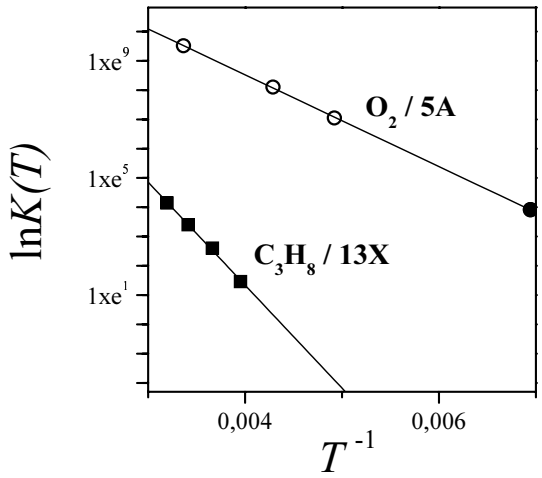

Fig. 30. Temperature dependence of equilibrium constant, $K(T)$, arising from fitting. Squares, empty circles and full circles correspond to fitting from Refs. MILLER, DANNER and TAREK, respectively. H_{st}^{FSTA} reported in Table 1 is the absolute value of the slope of the solid line.

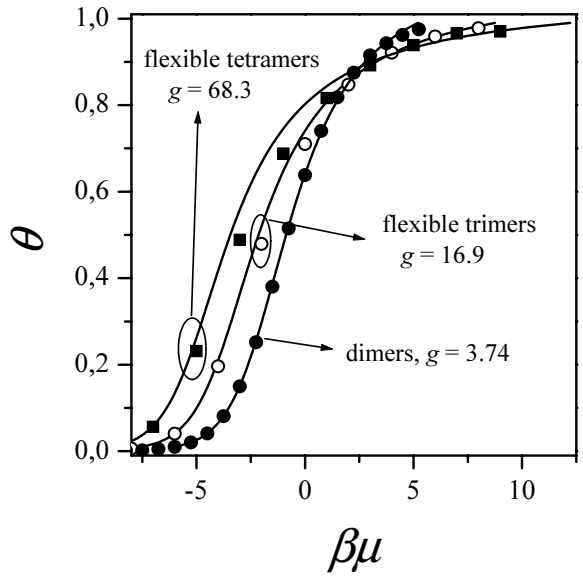

Fig. 31. Comparison between Monte-Carlo simulations of dimers, trimers and tetramers adsorbed on square lattices and theoretical isotherm from FSTA [Eq. (57)]. g values from best fitting are indicated in the figure for each case.

in Table 1, are in excellent agreement with the experimental value of H_{st} reported in Ref. 117 ($C_3H_8/13X$) and Ref. 120 ($O_2/5A$).

In order to describe systems more complex than the one in the experiments analyzed here, we show in Fig. 31 the fit (solid lines) to numerical isotherms (symbols) of dimers, flexible trimers and flexible tetramers adsorbed flat on a square lattice [a flexible k-mer is a chain of monomers occupying k adjacent sites of the lattice (without overlapping)]. Solid lines represent the best fitting to computer experiments in the crudest approximation [$g =$ constant, Eq. (57)] to the general isotherm of Eq. (56). The values obtained for g in all cases are very consistent to the ideal value $g = m\ k$. It is worth mentioning that, at this elementary degree of approximation FSTA is already more accurate than the classical Flory's theory[82,83] of adsorbed chains as well as the multisite-adsorption approaches of Refs. 71, 96 and 97.

For the case of dimers, Fig. 32 shows a comparison between the configurational entropy per site, s, versus coverage from simulation[80,81] and the corresponding ones obtained from FSTA [being $S = -(\frac{\partial F}{\partial T})_{N,M}$ and $s \equiv S/M$] for different values of g. As it was calculated for the isotherm, the best fit corresponds to $g = 3.74$ (solid line). The three curves in dashed (dotted) lines correspond to increments (decrements) of 2%, 4% and 6% with respect to $g = 3.74$. As it can be clearly visualized, small variations of g provide notable differences in the entropy curves. The more compact the configuration of the segments attached to the surface sites the smaller g. For instance, g may vary from $g = 6$ ($g = 8$) for straight trimers (tetramers), to $g = 18$ ($g = 72$) for flexible trimers (tetramers). From the previous considerations, it arises that the best fitting of adsorption data within the framework of the FSTA shows a

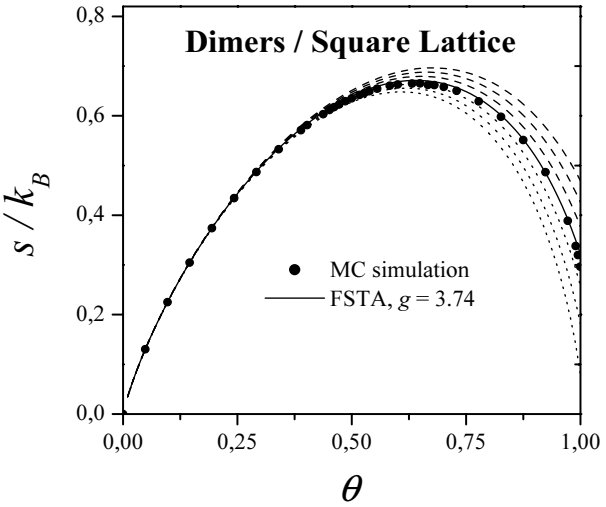

Fig. 32. Configurational entropy versus coverage for dimers adsorbed on square lattices. Symbols represent simulation data and lines provide theoretical results for different values of g as indicated in the text.

high sensitivity to the value of g for the cases studied. This represents an evidence of the physical and experimental significance of g.

5.2. *Non-interacting k-mers on heterogeneous surfaces*

We now turn to the description of multisite occupancy adsorption on heterogeneous surfaces in the lattice gas approximation. Hereafter, we present the main characteristics of Nitta's approach,[2,96,97] provided that we will further introduce the rigorous partition function for a homogeneous one-dimensional system into this approach to more accurately account for the entropic effects in the general case.

We assume a lattice with $M_1, M_2, \ldots, M_m$ sites of kind $1, 2, \ldots, m$, respectively. The total of adsorption sites amounts

$$M = \sum_{i=1}^{m} M_i \,. \tag{138}$$

The polyatomic adsorbate can be assumed as consisting of s type of units (groups) that adsorb individually on the lattice sites.

Provided the total number of units in a molecule is k, then

$$nk = \sum_{j=1}^{s} k_j \tag{139}$$

with k_j being the number of units of kind j in the molecule. The interaction energy of a group of j type on an adsorption site of the i kind is denoted ϵ_{ij}. The partition function in the canonical ensemble is given by

$$Q = \sum_{N_{ij}} \Omega_{\rm het}(M, N, N_{ij}) \exp \sum_i \sum_j \beta N_{ij} \epsilon_{ij} \tag{140}$$

where N_{ij} is the number of pairs group j-site i. The term $\Omega_{\rm het}$ can be approximated by following the configuration-counting procedure of the quasi-chemical approximation.

Thus,

$$\ln \Omega_{\rm het}(M, N, N_{ij}) = \ln \Omega(M, N) - \sum_i \sum_j \ln \frac{N_{ij}!}{N_{ij}^*!} \tag{141}$$

where Ω holds for k-mers on a homogeneous surface and the N^*'s does for the random distribution of N molecules on M sites. Accordingly the adsorption isotherm can be obtained by equalizing the chemical potentials of the adlayer, μ, and the gas phase, μ_g,

$$\begin{aligned} \beta\mu_g = \beta\mu &= \left(\frac{\partial \ln Q}{\partial N}\right)_{M,T} \\ &= -\left(\frac{\partial \ln \Omega}{\partial N}\right)_{M,T} + \sum_{j=1}^{s} k_j \ln\left[\frac{Y_j}{Y_j^*}\right] \end{aligned} \tag{142}$$

where

$$Y_{ij} = \frac{\theta_{ij}/\theta_{tj}}{1 - \sum_{j=1} \theta_{ij}} \tag{143}$$

and $Y_{1j} = Y_1$. θ_{ij} is the coverage of site of type i by units of type j, θ_{tj} the coverage of units type j on the whole surface, and $Y_j^* = (M_j/M)/(1 - kN/M)$.

The θ_{ij}'s and θ_{tj}'s come from constrain equations

$$\sum_{i=1}^{w} \frac{M_i}{M} \theta_{ij} = \theta_{tj}; \qquad j = 1, \ldots, s\,. \tag{144}$$

and

$$\frac{\theta_{ij}}{\left(1 - \sum_j \theta_{ij}\right)} = \frac{\theta_{1j} \exp \beta\,(\epsilon_{ij} - \epsilon_{1j})}{\left(1 - \sum_j \theta_{1j}\right)}; \qquad i = 1, \ldots, m; \quad j = 1, \ldots, s\,. \tag{145}$$

Using the Flory–Huggins's approximation for the first term on the right hand side of Eq. (142) one obtains[2,96,97]

$$\beta\mu = \ln \theta - k \ln(1 - \theta) + \sum_{i=1}^{s} k_j \ln \frac{Y_j}{Y_j^*}\,. \tag{146}$$

However, from the exact combinatorial factor of k-mers on a homogeneous one-dimensional lattice, Eq. (3),

$$\beta\mu = \ln \theta + (k-1) \ln \left[1 - \frac{(k-1)}{(k)} \theta\right] - k \ln(1 - \theta) + \sum_{i=1}^{s} k_j \ln \frac{Y_j}{Y_j^*} \tag{147}$$

where the term corresponding to the contribution of heterogeneity has been left identical in both equations.

As it will shown in the next, by comparison of Eqs. (146) and (147) with MC simulations for dimers and 4-mers, the modified isotherm [Eq. (147)] performs significantly better than Eq. (146) in fitting simulation results in one and two dimensions using the same set of parameters in all cases.

The results can be sorted in two sets. In Figs. 33–36 comparisons between MC simulation for dimers (Figs. 33 and 35) and 4-mers (Figs. 34 and 36) in one and two dimensions and analytical isotherms from Eqs. (146) and (147) are depicted.

In all cases simulation data are represented by solid circles, the results from the original (Eq. (146)) and modified isotherm [Eq. (147)] are plotted in dashed lines and solid lines, respectively. MC simulation were done by following the standard Metropolis algorithm in the grand canonical ensemble.

Three sets of curves are compared in each of these figures; one corresponds to the homogeneous surface, $\beta\Delta\epsilon = 0$, while the two remaining do for the simplest heterogeneous surfaces consisting of two types of sites whose relative adsorption energy difference is $\beta\Delta\epsilon = 2$ or 4 [since we are here dealing with homonuclear k-mers and only two type of sites $\beta\Delta\epsilon = \beta(\epsilon_{11} - \epsilon_{12})$]. This enable us to observe

the general effects of heterogeneity on the adsorption isotherm (which have been extensively discussed in Refs. 96, 97 and 2 as well as the accuracy of the model isotherms for fitting the simulation data.

For dimers (Figs. 33 and 35) both isotherms reproduce qualitatively well the trend of the data, even for fairly strong heterogeneous surfaces ($\beta\Delta\epsilon = 4$). The

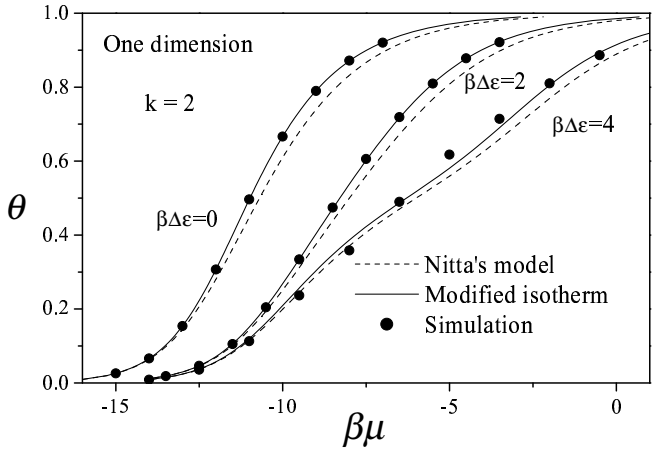

Fig. 33. Adsorption isotherm for multisite occupancy adsorption on homogeneous and heterogeneous surfaces. The surface is assumed to consist of two type of sites, with equal concentration distributed at random. The surface heterogeneity is related to the site energy difference $\beta\Delta\epsilon$. In this case MC simulation of dimer adsorption on a one-dimensional lattice are compared with analytical isotherms from Eqs. (146) and (147) for various values of surface heterogeneity; $\beta\Delta\epsilon = 2, 4$. The case of homogeneous surface, $\beta\Delta\epsilon = 0$, is also shown. Solid circles correspond to MC simulation in the grand canonical ensemble; dashed lines are isotherms from Nitta's equation (146); solid lines are results from modified equation (147).

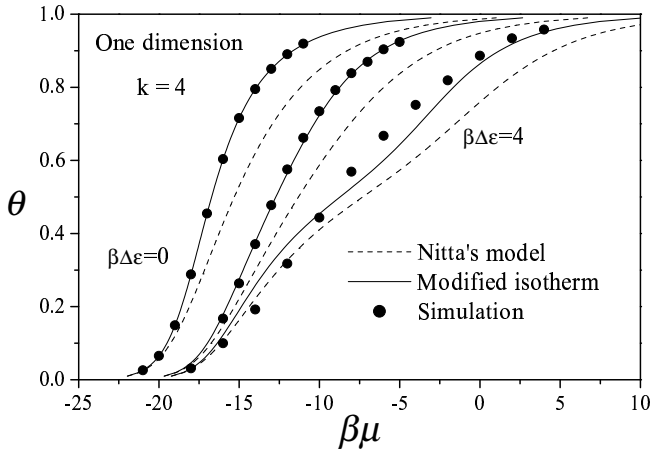

Fig. 34. Same as Fig. 33 for 4-mers in one dimension.

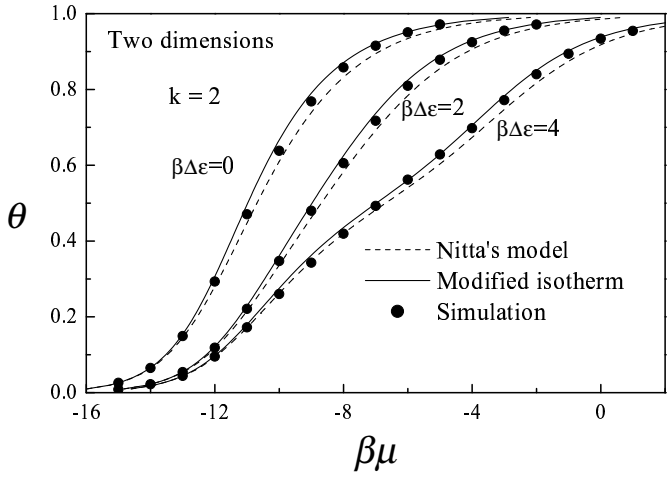

Fig. 35. Same as Fig. 33 for dimers in two dimensions.

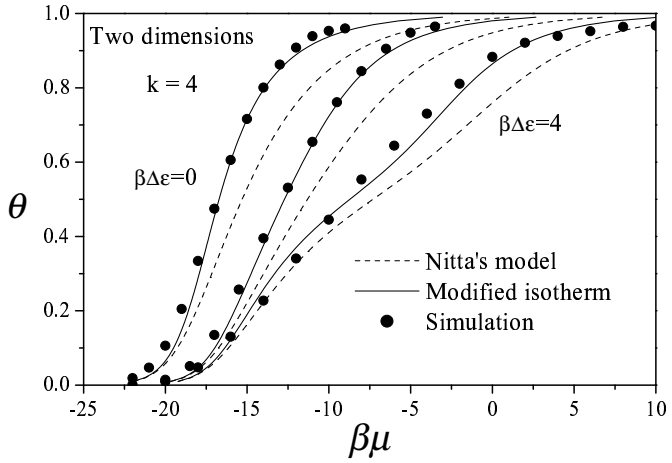

Fig. 36. Same as Fig. 33 for 4-mers in two dimensions.

modified isotherm [Eq. (147)] performs quantitatively better in all the cases studied. It is worth mentioning that (as a general characteristic) the accuracy is better for two dimensions compared to one dimension as the surface becomes more heterogeneous (see the case $\beta\Delta\epsilon = 4$ in Figs. 33 and 35). This is also valid for 4-mers (case $\beta\Delta\epsilon = 4$ in Figs. 34 and 36) and it is expected to be the general behavior for larger molecules.

It is also interesting to notice that for a given heterogeneity (a given value of $\beta\Delta\epsilon$), the larger the adsorbate molecule the better Eq. (147) reproduce the simulation. This is also observed for Eq. (146) although in a qualitatively sense. This behavior can be traced to the fact that as the size of the adsorbate increases

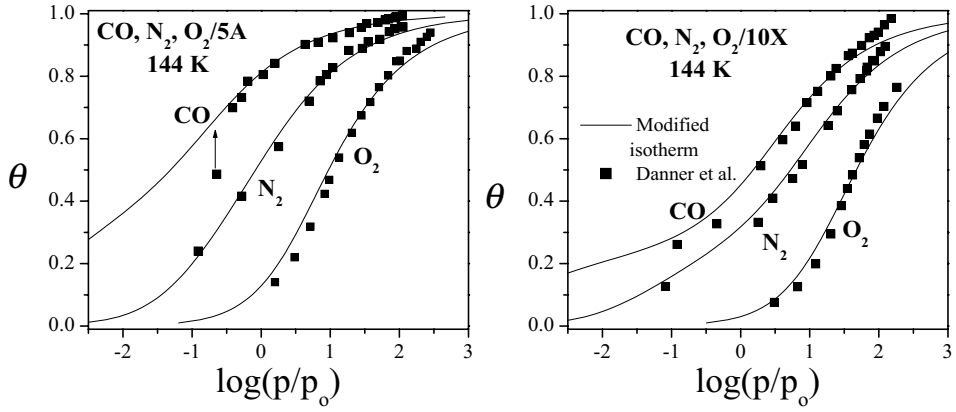

(a) (b)

Fig. 37. (a) Comparison between experimental adsorption isotherms from Ref. 3 for CO, N_2, O_2 on zeolite $5A$ and the theoretical isotherm from Eq. (147). Solid squares represent experimental data and solid lines correspond to the theoretical isotherm. The concentration of strongly and weakly adsorptive sites is $f_1 = 0.33$ and $f_2 = 0.67$ taken from Ref. 2. The site energy differences are $\Delta\epsilon/k_B = 0.00$ K; 242.42 K; 500.00 K for O_2, N_2, CO respectively. In order to compare with the experimental it has been assumed an ideal gas phase, thus $\beta\mu = \ln(p/p_o)$. In all the cases the adsorbed molecules are assumed to be dimers, thus the corresponding adsorbate size is $n = 2$. (b) Same as part (a) for CO, N_2, O_2 on zeolite $10X$. The concentration of strongly and weakly adsorptive sites is $f_1 = 0.22$ and $f_2 = 0.78$ taken from Ref. 2. The site energy differences are $\Delta\epsilon/k_B = 0.00$ K; 505.05 K; 757.57 K for O_2, N_2, CO respectively In all the cases the adsorbed molecules are assumed to be dimers, thus the corresponding adsorbate size is $n = 2$.

the adsorption energy distribution smoothes out owing to the appearance of a larger number of adsorption energy levels which decreases the effective heterogeneity seen by the adsorbate (a quantitative measure of this effective heterogeneity could be the ratio $\bar{\epsilon}_k/\Delta\epsilon$, where $\bar{\epsilon}_k$ is the mean adsorption energy of a k-mer and $\Delta\epsilon$ the site energy difference for individual units of the k-mer).

In Figs. 37(a) and 37(b) experimental adsorption isotherms of CO, N_2 and O_2 on zeolites $5A$ and $10X$ from Danner *et al.*[3] are fitted by the function Eq. (147). As discussed in Refs. 96, 97, 2 and 119 this systems can be characterized by an adsorption lattice with two type of sites. The agreement is good in all cases although no adsorbate-adsorbate interactions have been accounted for.

It should be mentioned that good quantitative agreement can also be obtained by fitting the data with Eq. (146) although values of $k \neq 2$ are sometimes necessary for a proper fitting.[2,96,97]

5.3. *Multilayer adsorption of polyatomics: An improved Isotherm for surface characterization*

Multilayer adsorption has been attracting a great deal of interest since long ago[110,113,121] and the progress in this field has gained a particular impetu due to its importance for the characterization of solid surfaces. Various theories have

been proposed to describe multilayer adsorption in equilibrium. Among them, the Brunauer-Emmet–Teller (BET) model[122] is one of the most widely used and practically applicable. The great popularity of the BET equation in experimental studies of adsorption has led some authors to extend the original theory of multilayer adsorption. Thus, numerous generalizations of the BET model have been reported in the literature, including surface heterogeneity, lateral interaction between the admolecules, differences between the adsorption energy and structure between the first and upper layers, etc.[113] These leading models, along with much recent contributions, have played a central role in the characterization of solid surfaces by means of gas adsorption.[2]

In practical situations, most adsorbates are polyatomic. Hence, a more accurate description of multilayer adsorption should account for the fact that it develops in general with multisite occupancy. Thus, the entropic contribution to the thermodynamic potentials will be appreciably different from the one expected for single-site occupancy.[71,80,81,87] Although many other factors have been considered in multilayer adsorption, multiple occupation of sites have been neglected at all. In this context, the aim of the present section is to extend the treatment of Ref. 122 to include adsorbates occupying more than one site. For this purpose, a new theoretical formalism[115] is presented based upon (i) the analytical expression of the adsorption isotherm at monolayer and (ii) a mapping from the grand partition function of the monolayer to the grand function of partition of the multilayer, where the fugacity of the monolayer transforms into the grand partition function of a single column of k-mers.

In order to maintain the simplest model that accounts for multisite-occupancy in multilayers we define it in the spirit of the BET's original formulation.[122] The adsorbent is a homogeneous lattice of sites. The adsorbate is assumed as linear molecules having k-identical units each of which occupies an adsorption site. Furthermore, (i) a k-mer can adsorb exactly onto an already adsorbed one; (ii) no lateral interactions are considered; (iii) the adsorption heat in all layers, except the first one, equals the molar heat of condensation of the adsorbate in bulk liquid phase. Thus, $c = q_1/q_i = q_1/q$ with $q_i = q(i = 2, \ldots, \infty)$ denotes the ratio between the single-molecule partition functions in the first and higher layers. The fact that k-mers can arrange in the first layer leaving sequences of l empty sites with $l < k$, where no further adsorption of a k-mer can occur in such a configuration, makes the calculation of entropy much elaborated than the one for monomer adsorption.

For a lattice having M adsorption sites, the maximum number of columns that can be grown up onto it is $n_{\max} = M/k$. Let us denote by $\Omega(n, M)$ the total number of distinguishable configurations of n columns on M sites. If an infinite number of layers is allowed to develop on the surface, the grand partition function, Ξ_{mul}, of the adlayer in equilibrium with a gas phase at chemical potential μ and temperature

T, is given by

$$\Xi_{\text{mul}} = \sum_{n=0}^{n_{\max}} \Omega(n, M)\xi^n \tag{148}$$

where ξ is the grand partition function of a single column of k-mers having at least one k-mer in the first layer. Then,

$$\xi = \sum_{i=1}^{\infty} q_1 q^{i-1} \lambda_{\text{mul}}^i = c \sum_{i=1}^{\infty} q^i \lambda_{\text{mul}}^i = \frac{c\lambda_{\text{mul}} q}{1 - \lambda_{\text{mul}} q} = \frac{cx}{1-x} \tag{149}$$

where $\lambda_{\text{mul}} = \exp(\mu/k_B T)$ is the fugacity. In addition, it is possible to demonstrate that $x = \lambda_{\text{mul}} q = p/p_o$ is the relative pressure.[2,115,116]

On the other hand, the grand partition function of the monolayer, Ξ_{mon}, can be written as

$$\Xi_{\text{mon}} = \sum_{n=0}^{n_{\max}} \Omega(n, M)\lambda_{\text{mon}}^n \tag{150}$$

in this case, n represents the number of adsorbed k-mers and λ_{mon} is the monolayer fugacity.

By comparing Eqs. (148) and (150) and from the condition,

$$\begin{aligned} \lambda_{\text{mon}} &= \xi \\ &= \frac{cp/p_o}{1 - p/p_o} \Rightarrow \frac{p}{p_o} = \frac{1}{1 + c\lambda_{\text{mon}}^{-1}}\,, \end{aligned} \tag{151}$$

we can write the monolayer coverage, θ_{mon}, as

$$\theta_{\text{mon}} = \frac{k}{M}\overline{n} = \frac{k}{M}\lambda_{\text{mon}} \left(\frac{d \ln \Xi_{\text{mon}}}{d\lambda} \right)_{M,T} = \frac{k}{M}\xi \left(\frac{d \ln \Xi_{\text{mul}}}{d\xi} \right)_{M,T} \tag{152}$$

where T and $\overline{n}$ are the temperature and the mean number of columns, respectively. In addition, the total coverage, θ, can be written as

$$\theta = \frac{k}{M}\overline{N} = \frac{k}{M}\lambda_{\text{mul}} \left(\frac{d \ln \Xi_{\text{mul}}}{d\lambda_{\text{mul}}} \right)_{M,T} \tag{153}$$

where $\overline{N}$ is the mean number of adsorbed k-mers. After some algebra the total coverage can be written in terms of the monolayer coverage,

$$\begin{aligned} \theta &= \frac{k}{M}\lambda_{\text{mul}} \left(\frac{d \ln \Xi_{\text{mul}}}{d\xi} \right)_{M,T} \frac{d\xi}{d\lambda_{\text{mul}}} \\ &= \frac{\theta_{\text{mon}}}{(1 - p/p_o)}\,. \end{aligned} \tag{154}$$

Finally, the theoretical procedure can be described as follows:

(1) By using θ_{mon} as a parameter ($0 \leq \theta_{\text{mon}} \leq 1$), the relative pressure is obtained by using Eq. (151). This calculation requires the knowledge of an analytical expression for the monolayer adsorption isotherm.

(2) The values of $\theta_{\rm mon}$ and p/p_o are introduced in Eq. (154) and the total coverage is obtained.

The items (1) and (2) are summarized in the following scheme:

$$\theta_{\rm mon} + \lambda(\theta_{\rm mon}) + \text{Eq. (151)} \rightarrow p/p_o \Rightarrow \theta_{\rm mon} + p/p_o + \text{Eq. (154)} \rightarrow \theta\,. \qquad (155)$$

By following the scheme presented in the last paragraph, we can obtain the exact solution for multilayer adsorption of k-mers on a one-dimensional lattice.

We start from the Eq. (13)

$$\lambda_{\rm mon} = \frac{\theta_{\rm mon}}{k} \frac{\left[1 - \dfrac{(k-1)}{k}\theta_{\rm mon}\right]^{k-1}}{(1-\theta_{\rm mon})^k} \qquad (156)$$

which represents the one-dimensional exact isotherm of k-mers adsorbed at monolayer.

Substituting Eq. (156) into Eq. (151), one obtains the following expression for the relative pressure,

$$\frac{p}{p_o} = \frac{\theta_{\rm mon}\left[1 - \dfrac{(k-1)}{k}\theta_{\rm mon}\right]^{k-1}}{kc\,(1-\theta_{\rm mon})^k + \theta_{\rm mon}\left[1 - \dfrac{(k-1)}{k}\theta_{\rm mon}\right]^{k-1}}\,. \qquad (157)$$

Equations (154) and (157) represent the exact solution describing the adsorption of k-mers at multilayer regime on a homogeneous surface in 1-D. In the case of monomer adsorption ($k = 1$), Eqs. (154) and (157) reduce to the well-known BET isotherm,[122] i.e.

$$\theta = \frac{cp/p_o}{(1-p/p_o)\,[1+(c-1)p/p_o]} \qquad k = 1\,. \qquad (158)$$

For $k = 2$, the dimer isotherm can be written in a simple form:

$$\theta = \frac{1}{(1-p/p_o)}\left\{1 - \left[\frac{1-p/p_o}{1+(4c-1)p/p_o}\right]^{1/2}\right\} \qquad k = 2\,. \qquad (159)$$

By using other methodology, Eq. (159) has been recently reported in the literature.[116]

In Fig. 38 we address the comparison between the analytical adsorption isotherm in 1-D and MC simulation. The simulations have been performed for monomers, dimers and 10-mers adsorbed on chains of $M/k = 1000$ sites with periodic boundary conditions. Different values of the parameter c have been considered. In all cases, the computational data fully agree with the theoretical predictions, which reinforces the robustness of the two methodologies employed here.

As it can be observed from Fig. 38, for certain values of the parameter c, the corresponding isotherm has a point of inflection. The point of inflection can be obtained in three steps: (1) differentiating twice the adsorption isotherm equation

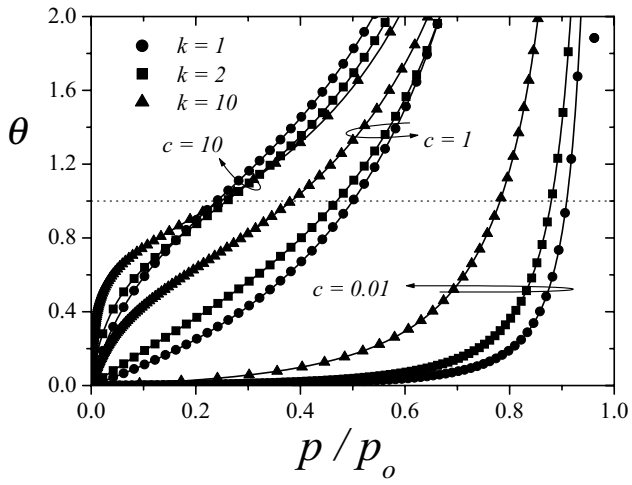

Fig. 38. Adsorption isotherms for k-mers on one-dimensional lattice and different values of the parameter c (as indicated). Solid lines and symbols represent theoretical and simulation results, respectively.

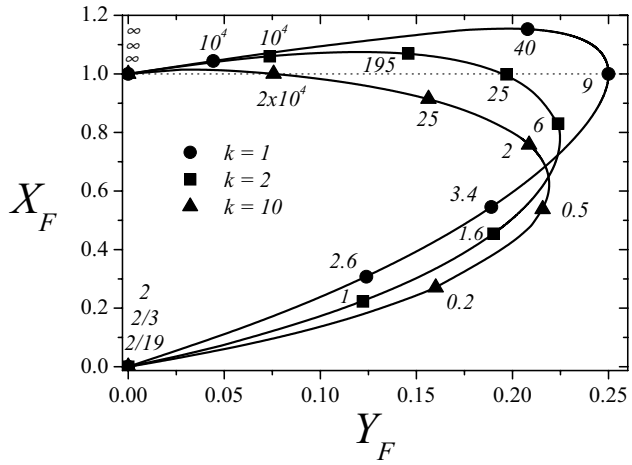

Fig. 39. Coordinates of the point of inflection (being X_F and Y_F coverage and relative pressure, respectively) for one-dimensional adsorption isotherms with different values of k ($k = 1, 2, 10$). Each point (solid circle) in a given curve corresponds to a determined value of c, as indicated.

to obtain $d^2\theta/dY^2$ (being $Y = p/p_o$ for the sake of simplicity); (2) equating the resulting expression to zero and solving for Y gives Y_F, the value of p/p_o at the point of inflection; and (3) inserting Y_F in the adsorption isotherm equation gives θ_F, the value of θ at the point of inflection.

The location of the point of inflection ($X_F \equiv \theta_F, Y_F$) is plotted in Fig. 39 for different values of c and k. Clearly, the value of θ at the point of inflection may deviate considerably from unity. However, there exist a certain value of $c =$

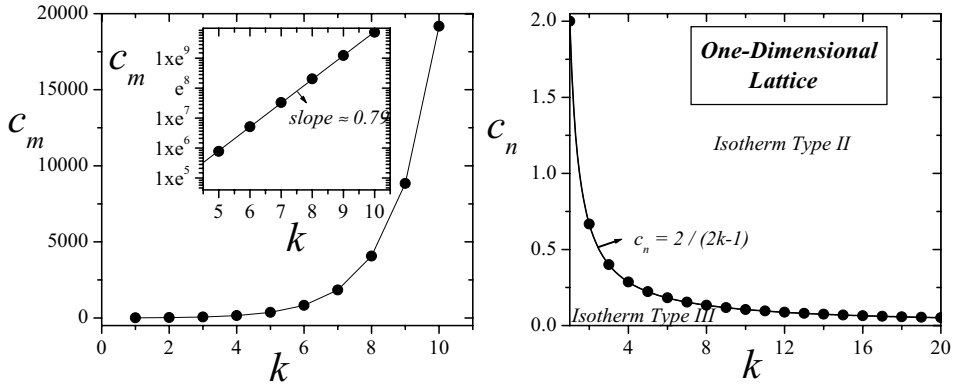

Fig. 40. (a) c_m (as it is indicated in the text) as a function of size of adsorbate, k, for adsorptionisotherms of k-mers on one-dimensional lattices. (b) c_n (as it is indicated in the text) as a function of size of adsorbate, k, for adsorption isotherms of k-mers on one-dimensional lattices.

c_m, where the point of inflection coincides with the point corresponding to the monolayer capacity. Figure 40(a) shows the behavior of c_m as a function of k. The values of c_m, which have been obtained numerically in the range $k = 1-10$, provide a exponential dependence $[\exp(bk)]$. As shown in the inset, $b \approx 0.79$, obtained from the slope of $\ln c_m$ vs. k. For values of c between c_m and infinity the adsorption at the point of inflection exceeds the monolayer capacity; for values of c below c_m the two quantities deviate more and more and for a limit value of $c = c_n$, the point of inflection disappears. c_n vs. k can be calculated analytically.[115] The result of this calculation is presented in Fig. 40(b). As it is can be visualized from the figure, the function $c_n(k) = 2/(2k-1)$ separates two well differentiate regions: (i) for $c > c_n$, the isotherm is of Type II and (ii) when c is less than c_n the isotherm is of Type III and discussion of the point of inflection is meaningless.

As it is well known, the main application of BET model consists in taking an experimental isotherm in the low-pressure region and fitting values of the monolayer volume, v_m, and the parameter c, from the slope and intercept of the linearized form of the BET equation,

$$\frac{p/p_o}{v(1-p/p_o)} = \frac{1}{c_{BET}\ v_{m,BET}} + \frac{(c_{BET}-1)}{c_{BET}\ v_{m,BET}} p/p_o\,. \tag{160}$$

The new adsorption isotherm can be presented similarly to the linearized form of the BET equation. If $\theta = v/v_m$, where v and v_m denote the adsorbed volume and the monolayer volume, respectively, it then follows from Eq. (159) that

$$\frac{p/p_o}{v(1-p/p_o)} = \frac{p/p_o}{v_m}\left\{1 - \left[\frac{(1-p/p_o)}{(4c-1)p/p_o + 1}\right]^{1/2}\right\}^{-1}. \tag{161}$$

Equation (161) is not a linear function of p/p_o as the one arising from the BET isotherm [Eq. (160)]. Then, it is of interest to study the behavior of k-mers multilayer isotherms (with $k \leq 2$) in the low-pressure region in comparison with BET

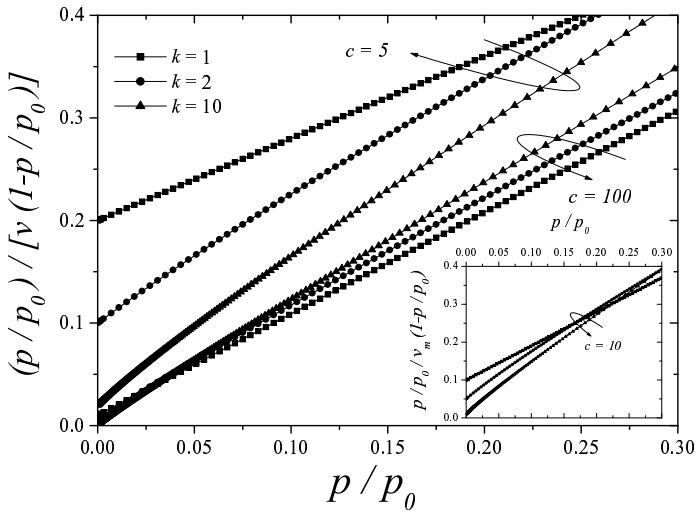

Fig. 41. $[p/p_o]/[v(1-p/p_o)]$ versus p/p_o for different values of c and k. All curves are plotted in the range $(0-0.3)$ of relative pressure and v_m is set equals to 1 (in arbitrary units).

isotherm ($k = 1$). This comparison is shown in Fig. 41 for $c = 5, 10, 100$; $k = 1, 2, 10$; and pressures ranging from $p/p_o = 0$ up to $p/p_o = 0.30$. A linear function is only obtained if $k = 1$. The nonlinear behavior of k-mers isotherms ($k > 1$) at low pressures, which is a distinctive characteristic of many experimental isotherms, is showing that the polyatomic character of the adsorbate must be taking into account.

The significant differences observed as k is varied indicate that the analysis of experimental isotherms of larger molecules by means of the k-mers isotherm [Eqs. (154) and (157)] would lead to values of the parameters c and v_m appreciably different from the BET ones. To analyze this effect, we expand the right hand of Eq. (161) in powers of p/p_o around $p/p_o = 0$, the first order approximation leads to

$$\frac{p/p_o}{v\,(1-p/p_o)} \approx \frac{1}{2cv_m} + \frac{(3c-1)}{2cv_m} p/p_o\,. \tag{162}$$

By matching the linear forms of Eqs. (160) and (162), it gives $c = c_{BET}/3$, and $v_m = (3/2)\ v_{m,BET}$. In fact, the value $v_m = 1.5\ v_{m,BET}$ is consistent with the fact that multiple site occupation of N_2 on graphite would lead to surface areas 1.22 times larger that the BET values, as discussed long ago in Ref. 123. Ultimately, the rigorous treatment of multilayer adsorption considering the polyatomic nature of the adsorbate, is indicating that the surfaces area that can be obtained by using the isotherm Eq. (159), results significantly larger than the BET area, consistently with much evidence about that the later generally underestimates the real surface area when nonspherical probe molecules are used. However, the influence of the nonlinear terms of Eq. (161) will ultimately lead to a different relationship between c, c_{BET}, v_m and $v_{m,BET}$, when fitting of experimental data is carried out.

The nonlinear behavior of isotherm Eq. (159) at low pressure matches also a distinctive characteristic of many experimental isotherm. Although there are many potential sources for such a nonlinearity (e.g. lateral interaction and surface heterogeneity), the present results are showing that the entropic contributions coming from the adsorbate structure are not non-negligible even though lateral interactions and surface heterogeneity are not accounted for in the model.

Nevertheless, the physical meaningfulness of the proposed adsorption isotherm for dimers has to be supported by an extensive analysis of experiments. Regarding this purpose, accurate isotherms of N_2, O_2, CO, and light alkanes on nonporous solids, with significant number of data in the low pressure regime, are necessary to ascertain the accuracy and applicability of adsorption isotherm of Eq. (159) as compared to the BET and other theories of multilayer adsorption.[124] In addition, calorimetric measurements would provide an independent test for the values obtained from adsorption data.

Although such a detailed analysis is out of the main goal and scope of the present work, fitting of standard data for the systems Ar, N_2/nonporous silica, and K_r, n-butane, $CHCl_2F$/ silver foil[121] is displayed in Figs. 42(a) and 42(b). The corresponding fitting parameters are shown in Tables 2 and 3. It is worth noticing that the values of v_m and c resulting of the fitting from the isotherm Eq. (159) differ from those corresponding with BET analysis, and in all cases $c < c_{BET}$ and $v_m > v_{m,BET}$.

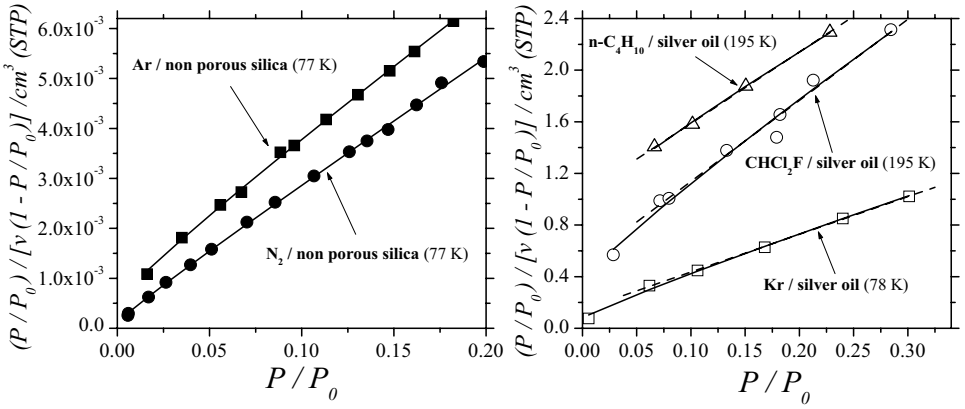

Fig. 42. (a) Fitting of experimental adsorption isotherms of the systems N_2, Ar/non porous silica, through the dimer isotherm Eq. (159). The resulting values of the parameters c and monolayer volume v_m are shown in the Table 2 along with the ones arising from fitting with the BET model. (b) Idem as in part (a) for Kr, n-butane, $CHCl_2F$/silver foil. The resulting values of c and v_m from fitting are shown in the Table 3. The solid line represents the isotherm for dimers obtained in the present work [Eq. (159)], and the dashed line represents the BET isotherm (monomers).

Table 2. Resulting values of the parameters c and monolayer volume v_m from fitting in Fig. 42 (a).

Adsorbate/ non porous silica	Dimer isotherm		BET			
	c	$v_m(cm^3g^{-1})$	c_{BET}	$v_{m,BET}(cm^3g^{-1})$	$v_m/v_{m,BET}$	c/c_{BET}
N_2	106.9 ± 17.8	40.8 ± 0.5	135.2 ± 20.6	37.7 ± 0.4	1.16	0.56
Ar	23.4 ± 1.6	37.6 ± 0.4	41.5 ± 3.2	32.5 ± 0.5	1.08	0.79

Table 3. Resulting values of the parameters c and monolayer volume v_m from fitting in Fig. 42(b).

Adsorbate/ silver foil	Dimer isotherm		BET			
	c	$v_m \cdot 10^1$ (cm^3g^{-1})	c_{BET}	$v_{m,BET} \cdot 10^1$ (cm^3g^{-1})	$v_m/v_{m,BET}$	c/c_{BET}
K_r	17.34 ± 3.78	3.57 ± 1.19	21.24 ± 1.30	3.26 ± 0.00	1.09	0.82
$CHCl_2F$	7.50 ± 1.63	1.71 ± 0.01	13.33 ± 2.72	1.47 ± 0.01	1.16	0.56
$n-C_4H_{10}$	2.58 ± 0.10	1.97 ± 0.00	6.35 ± 0.17	1.52 ± 0.00	1.30	0.41

6. Conclusions

The problem of equilibrium adsorption of polyatomics has been dealt from various perspectives. In one dimension, a comprehensive description of thermodynamic functions and their dependence on parameters as the type of interactions, adsorbate size, temperature, and surface coverage was given through their exact forms. The model also provides a background to approximate the thermodynamic functions of more complex quasi-one-dimensional adsorbents as carbon nanotube bundles, where molecules within a channel can interact with their neighbors along the same channel, as well as with others adsorbed in neighboring channels because of the bundle packing. Transversal interactions can be easily accounted for by incorporating them through a mean-field in the free energy expression.

On the other hand, the knowledge of thermodynamic properties of polyatomic gases in two dimensions is limited owing, basically, to the difficulties that accurate calculations of entropy and free energies pose. It is worth noticing that even for the simple problem of non-interacting dimers on regular lattices, which we are addressing here, there no exist a rigorous solution for the configurational entropy. However, new analytical contributions to this problem have been presented in our contribution and and contrasted with former development on k-mers themodynamics.

The behavior of the analytical adsorption isotherms can be explained as follows. *FHL* and *GD* predict a smaller θ than the simulation data over all range of coverage. In the case of *EA*, the disagreement turns out to be large for intermediate θ's and a good approximation is recovered for high coverage. With respect to the connectivity, *EA* and *FSTA* (*FHL* and *GD*) become more accurate as γ diminishes (increases). The behavior of *GD* and *EA* justifies the methodology used to build

the SE isotherm in Eq. (86), being SE approximation the most accurate for all cases.

Of special interest results fractional statistics thermodynamic theory of adsorption of polyatomics. In fact, even in its simplest degree of approximation, *FSTA* provides already a good approximation with very small differences between simulated and theoretical results. The superiority of this description relies in its scope (potentially applicable to a wide set of adsorption systems ranging from small polyatomics, hydrocarbons, and perhaps up to light polymers), its simplicity (closed forms of functions), the smallest number of parameters necessary to account for the surface-molecule/molecule-molecule interactions and the configuration state of the admolecule, and the proposition of a general relationship to address the configuration spectrum of the admolecules upon density from thermodynamic (adsorption) data.

With respect to interacting polyatomic adsorbates in two dimensions, a generalization of the Bragg–Williams and quasi-chemical approximations has been presented. The main thermodynamic functions of adsorption (adsorption isotherm, configurational energy, isosteric heat of adsorption, specific heat and configurational entropy of the adlayer) have been calculated. *QCA* leads to exact results in one dimension and provides a close approximation to study adsorption of polyatomics on two-dimensional surfaces with different geometries (square, honeycomb and triangular).

From the comparison with MC simulations, appreciable differences can be seen for the different approximations, *QCA* being the most accurate for all cases. In addition, the artificial effects that the *BWA* induces on the main thermodynamic functions can now be rationalized and compared with other analytical approaches.

In summary, the proposed theoretical scheme represents a qualitative advance with respect to the existing development on k-mers thermodynamics and seems to be a promising way toward a more accurate description of the adsorption thermodynamics of polyatomic molecules. In this sense, future efforts will be directed to (1) study the critical behavior of the system for attractive and repulsive interactions, (2) extend the calculations to kinetic properties as diffusion coefficient, thermal desorption, etc and (3) consider different forms for $\Omega(N, M, \gamma)$ in Eqs. (105) and (120), analyzing its influence on the thermodynamic functions.

Finally, three applications of the theoretical results presented in this review have been discussed. In the first case, the applicability and versatility of *FSTA* to describe complex adsorption systems have been analyzed. For this purpose, simulation data of flexible k-mers and experimental data of $C_3H_8/13X$ and $O_2/5A$ have been studied by using *FSTA* model. The results show that the concept of statistical exclusion ($g > 1$) allows to handle the complexity of the entropy of adsorbed polyatomics traced to the adsorbate's configuration and interactions, and thus, the spatial mode of adsorption can be quantitatively assessed from experiments through the parameter g. Additionally, *FSTA* provides the basis to investigate the changes of

adsorbate's configuration upon density [configurational spectroscopy, $\tilde{G_0}'(N)$] from thermodynamic data. The theory gives a framework and compact equations to consistently interpret thermodynamic adsorption experiments ranging from simple species to elaborated polyatomics such as alkanes, alkenes, and other hydrocarbons on regular surfaces.

In the second case, the modification of the Nitta's original isotherm for multisite occupancy adsorption on heterogeneous surfaces, by incorporating the exact form for the homogeneous part of the Helmholtz free energy (instead of the approximate form of it resulting from the Flory–Huggins's approach) has been proposed. The formalism leads to an improved modified adsorption isotherm equation enable to accurately reproduce MC simulations of dimers and 4-mers adsorption on one and two dimensional heterogeneous surfaces. In addition, experimental isotherms of dimers adsorbed in zeolites cages with two type of sites can be reproduced by the modified isotherm with a set of parameters that are thermodynamically reasonable and in agreement with previous studies.[2,96,97,119]

The knowledge of the exact coverage and temperature dependence of the free energy of linear adsorbates in a homogeneous one-dimensional space allows the development of a more accurate description of the adsorption isotherm for heterogeneous surfaces. In this case, the observed differences with respect to former approaches can be attributed to the configurational entropy that is more properly taken into account in the present case.

In the last case, an analytical approach to the multilayer adsorption isotherm of polyatomic adsorbates has been proposed. The approximation provides the isotherm in the multilayer regime from the isotherm at monolayer. In this framework, exact solution in one dimension was obtained and calculations can be extended to k-mers in two-dimensional surfaces.

Preliminary analysis of polyatomic adsorption data indicates that the values of monolayer volume, v_m, and c, arising from using the dimers isotherm equation are more realistic than the ones from BET characterization. The monolayer volume (or equivalently, surface area) and the parameter c resulting from experiments by using the linearized form of the new isotherm could be up to 1.5 and 1/3 times the corresponding ones from BET.

The proposed model is simple, easy to apply in practice, and leads to new values of surface area and adsorption heats. Physically, these advantages are a consequence of properly considering the configurational entropy of the adsorbate. This treatment, in which the entropic effects of the adsorbate size are accounted for, bears theoretical interest because it represents a qualitative advance with respect to the existing models of multilayer adsorption.

Acknowledgments

This work was supported in part by CONICET (Argentina) under the project PIP 6294 and the Universidad Nacional de San Luis (Argentina) under the projects 328501 and 322000.

References

1. L. W. Bruch, M. W. Cole and E. Zaremba, *Physical Adsorption: Forces and Phenomena* (Oxford University Press, Oxford, 1997).
2. W. Rudziński and D. H. Everett, *Adsorption of Gases on Heterogeneous Surfaces* (Academic Press, London, 1992).
3. R. P. Danner and L. A. Wenzel, *AIChE J.* **15**, 515 (1969).
4. G. W. Miller, K. S. Knaebel and K. G. Ikels, *AIChE J.* **33**, 2 (1987).
5. R. A. Koble and T. E. Corrigan, *Ind. Eng. Chem.* **44**, 383 (1952).
6. A. C. Balazs, M. C. Gempe and Z. Zhou, *Macromolecules* **24**, 4918 (1991).
7. G. D. Parfitt, in Adsorption from Solution at the Solid-Liquid Interface (Academic Press, London, 1983), Vol. 3, pp. 167.
8. S. Iijima, *Nature* **345**, 56 (1991).
9. S. Iijima and T. Ichihaschi, *Nature* **363**, 603 (1993).
10. D. S. Bethune, C. H. Kianig, M. S. de Vries, G. Gorman, R. Savoy, J. Vasques and R. Beyers, *Nature* **363**, 605 (1993).
11. P. M. Ajayan and S. Iijima, *Nature* **361**, 333 (1993).
12. T. W. Ebbensen, *Science* **265**, 1850 (1994).
13. S. T. Wilson, B. M. Lok, C. A. Messia, T. R. Cannan and E. M. Flanigen, *J. Am. Chem. Soc.* **104**, 1146 (1982).
14. T. Wilson, A. Tyburski, M. R. DePies, O. E. Vilches, D. Becquet and M. Bienfait, *J. Low Temp. Phys.* **126**, 403 (2002).
15. M. Bienfait, P. Zeppenfeld, N. Dupont-Pavlovsky, M. Muris, M. R. Johnson, T. Wilson, M. DePies and O. E. Vilches, *Phys. Rev. B* **70**, 035410 (2004).
16. W.-F. Du, L. Wilson, J. Ripmeester, R. Dutrisac, B. Simard and S. Denommee, *Nano Lett.* **2**, 343 (2002).
17. M. Cinke, J. Li, B. Chen, A. Cassell, L. Delzeit, J. Han and M. Meyyappan, *Chem. Phys. Lett.* **365**, 69 (2002).
18. C.-M. Yang, K. Kaneko, M. Yudasaka and S. Iijima, *Nano Lett.* **2**, 385 (2002).
19. A. Fujiwara, K. Ishii, H. Suematsu, H. Kataura, Y. Minawa, S. Suzuki and Y. Achiba, *Chem. Phys. Lett.* **336**, 205 (2001).
20. S. Ramachandran, T. A. Wilson, D. Vandervelde, D. K. Holmes and O. E. Vilches, *J. Low Temp. Phys.* **134**, 115 (2004).
21. H. Ulbricht, G. Moos and T. Hertel, *Phys. Rev. B* **66**, 075404 (2002).
22. M. Muris, M. Bienfait, P. Zeppenfeld, N. Dupont-Pavlovsky, M. R. Johnson, O. E. Vilches and T. Wilson, *Appl. Phys. A* **74**, S1293 (2002).
23. Q. Wang, S. R. Challa, D. S. Sholl and J. K. Johnson, *Phys. Rev. Lett.* **82**, 956 (1999).
24. S. R. Challa, D. S. Sholl and J. K. Johnson, *Phys. Rev. B* **63**, 245419 (2001).
25. S. R. Challa, D. S. Sholl and J. K. Johnson, *J. Chem. Phys.* **116**, 814 (2002).
26. K. Bradley, S.-H. Jhi, P. G. Collins, J. Hone, M. L. Cohen, S. G. Louie and A. Zettl, *Phys. Rev. Lett.* **85**, 4361 (2000).
27. G. U. Sumanasekera, C. K. W. Adu, S. Fang and P. C. Eklund, *Phys. Rev. Lett.* **85**, 1096 (2000).
28. C. M. Brown, T. Yildrim, D. D. Neumann, M. J. Heben, T. Gennett, A. C. Dillon, J. L. Alleman and J. E. Fischer, *Chem. Phys. Lett.* **329**, 311 (2000).
29. D. G. Narehood, J. V. Pearce, P. C. Eklund, P. E. Sokol, R. E. Lechner, J. Pieper, J. R. D. Copley and J. C. Cook, *Phys. Rev. B* **67**, 205409 (2003).
30. C. Matranga and B. Bockrath, *J. Phys. Chem. B* **109**, 4853 (2005).
31. S. Santucci, S. Picozzi, F. Di Gregorio, L. Lozzi, C. Cantalini, L. Valentini, J. M. Kenny and B. Delley, *J. Chem. Phys.* **119**, 10904 (2003).

32. S. Chopra, K. McGuire, N. Gothard and A. M. Rao, *Appl. Phys. Lett.* **83**, 2280 (2003).
33. A. D. Migone and S. Talapatra, *Gas Adsorption on Carbon Nanotubes, Encyclopedia of Nanoscience and Nanotechnology*, ed. H. S. Nalwa (American Scientific Publishers, Los Angeles 2004), Vol. 4, pp. 749–767.
34. S. Talapatra, A. J. Zambano, S. E. Weber and A. D. Migone, *Phys. Rev. Lett.* **85**, 138 (2000).
35. A. J. Zambano, S. Talapatra and A. D. Migone, *Phys. Rev. B* **64**, 075415 (2001).
36. S. Talapatra and A. D. Migone, *Phys. Rev. Lett.* **87**, 206106 (2001).
37. S. Talapatra and A. D. Migone, *Phys. Rev. B* **65**, 045416 (2002).
38. A. J. Zambano, S. Talapatra, K. Lafdi, M. T. Aziz, W. Mc Millin, G. Shaughnessy, A. D. Migone, M. Yudasaka, S. Iijima, F. Kokai and K. Takahashi, *Nanotechnology* **13**, 201 (2002).
39. S. Talapatra, D. S. Rawat and A. D. Migone, *J. Nanosci. Nanotech.* **2**, 467 (2002).
40. S. Talapatra, V. Krungleviciute and A. D. Migone, *Phys. Rev. Lett.* **89**, 246106 (2002).
41. V. Krungleviciute, L. Heroux, S. Talapatra and A. D. Migone, *Nano Lett.* **4**, 1133 (2004).
42. M. Muris, N. Dupont-Pavlovsky, M. Bienfait and P. Zeppenfeld, *Surf. Sci.* **492**, 67 (2001).
43. M. Muris, N. Dufau, M. Bienfait, N. Dupont-Pavlovsky, Y. Grillet and J. P. Palmari, *Langmuir* **16**, 7019 (2000).
44. M. R. Johnson, S. Rols, P. Wass, M. Muris, M. Bienfait, P. Zeppenfeld and N. Dupont-Pavlovsky, *Chem. Phys.* **293**, 217 (2003).
45. M. Cinke, J. Li, C. W. Bauschlicher, A. Ricca and M. Meyyappan, *Chem. Phys. Lett.* **376**, 761 (2003).
46. C. Matranga, L. Cheng, M. Smith, E. Bittner, J. K. Johnson and B. Bockrath, *J. Phys. Chem. B* **107**, 12930 (2003).
47. W. L. Yim, O. Byl, J. T. Yates Jr. and J. Karl Johnson, *J. Chem. Phys.* **120**, 5377 (2004).
48. C. Matranga and B. Bockrath, *J. Phys. Chem. B* **108**, 6170 (2004).
49. C. Matranga, L. Cheng, B. Bockrath and J. K. Johnson, *Phys. Rev. B* **70**, 165416 (2004).
50. L. Cheng and J. K. Johnson, *Phys. Rev. Lett.* **94**, 125701 (2005).
51. K. W. Herwig, J. C. Newton and H. Taub, *Phys. Rev. B* **50**, 15287 (1994).
52. G. J. Trott, H. Taub, F. Y. Hansen and H. R. Danner, *Chem. Phys. Lett.* **78**, 504 (1981).
53. J. Z. Larese, L. Passelll and B. Ravel, *Can. J. Chem.* **66**, 633 (1988).
54. J. C. Newton and H. Taub, *Surf. Sci.* **364**, 273 (1996).
55. V. L. Eden and S. C. Fain Jr., *Phys. Rev. B* **43**, 10697 (1990).
56. S. K. Satija, L. Passell, J. Eckart and W. Ellenson, *Phys. Rev. Lett.* **51**, 411 (1983).
57. S. C. Fain Jr. and B. Bunsenges, *Phys. Chem.* **90**, 211 (1986).
58. A. Inaba, T. Shirakami and H. Chihara, *Chem. Phys. Lett.* **146**, 63 (1988).
59. W. A. Steele, *Langmuir* **12**, 145 (1996).
60. S. Zhang and A. D. Migone, *Surf. Sci.* **222**, 31 (1989).
61. F. Y. Hansen and H. Taub, *Phys. Rev. Lett.* **69**, 652 (1992).
62. F. Y. Hansen, J. C. Newton and H. Taub, *J. Chem. Phys.* **98**, 4128 (1993).
63. F. Y. Hansen, K. W. Herwig, B. Matthies and H. Taub, *Phys. Rev. Lett.* **83**, 2362 (1999).
64. S. Zhang and A. D. Migone, *Phys. Rev. B* **42**, 8674 (1990).

65. M. T. Alkhafaji and A. D. Migone, *Phys. Rev. B* **45**, 5729 (1992).
66. M. T. Alkhafaji and A. D. Migone, *Phys. Rev. B* **48**, 1761 (1993).
67. M. T. Alkhafaji and A. D. Migone, *Phys. Rev. B* **53**, 11152 (1996).
68. M.-A. Lee, M. T. Alkhafaji and A. D. Migone, *Langmuir* **13**, 2791 (1997).
69. H. K. Kim, Q. M. Zhang and M. H. W. Chan, *Phys. Rev. Lett.* **56**, 1579 (1986).
70. F. Rittner, B. Boddenberg, M. J. Bojan and W. A. Steele, *Langmuir* **15**, 1456 (1999).
71. A. J. Ramirez-Pastor, T. P. Eggarter, V. D. Pereyra and J. L. Riccardo, *Phys. Rev. B* **59**, 11027 (1999).
72. A. Maltz and E. E. Mola, *J. Math. Phys.* **22**, 1746 (1981).
73. T. L. Hill, *An Introduction to Statistical Thermodynamics* (Addison-Wesley Publishing Company, Reading, MA, 1960).
74. A. J. Ramirez-Pastor, A. Aligia, F. Romá and J. L. Riccardo, *Langmuir* **16**, 5100 (2000).
75. A. Aligia, *Phys. Rev. B* **47**, 15308 (1993).
76. Kikuchi, *Phys. Rev.* **81**, 988 (1951).
77. J. C. Martin, N. Tosi-Pellenq, J. Patarin and J. P. Coulomb, *Langmuir* **14**, 1774 (1998).
78. V. Lachet, A. Boutin, R. M. Pellenq, D. Nicholson and A. Fuchs, *J. Phys. Chem.* **100**, 9006 (1996).
79. T. Maris, T. J. H. Vlugt and B. Smit, *J. Phys. Chem.* **B102**, 7183 (1998).
80. F. Romá, A. J. Ramirez-Pastor and J. L. Riccardo, *Langmuir* **16**, 9406 (2000).
81. F. Romá, A. J. Ramirez-Pastor and J. L. Riccardo, *J. Chem. Phys.* **114**, 10932 (2001).
82. P. Flory, *J. Chem. Phys.* **10**, 51 (1942).
83. P. Flory, *Principles of Polymer Chemistry* (Ithaca, N. Y., Cornell, 1953).
84. M. L. Huggins, *J. Phys. Chem.* **46**, 151 (1942).
85. M. L. Huggins, *Ann. N. Y. Acad. Sci.* **41**, 151 (1942).
86. M. L. Huggins, *J. Am. Chem. Soc.* **64**, 1712 (1942).
87. A. J. Ramirez-Pastor, J. L. Riccardo and V. D. Pereyra, *Langmuir* **16**, 10167 (2000).
88. F. Romá, A. J. Ramirez-Pastor and J. L. Riccardo, *Langmuir* **19**, 6770 (2003).
89. E. A. Guggenheim, *Proc. R. Soc. London A* **183**, 203 (1944).
90. E. A. DiMarzio, *J. Chem. Phys.* **35**, 658 (1961).
91. J. L. Riccardo, F. Romá and A. J. Ramirez-Pastor, *Phys. Rev. Lett.* **93**, 186101 (2004).
92. J. L. Riccardo, F. Romá and A. J. Ramirez-Pastor, *Applied Surf. Sci.* **252**, 505 (2005).
93. F. Romá, J. L. Riccardo and A. J. Ramirez-Pastor, *Langmuir* **22**, 3192 (2006).
94. J. Des Cloizeaux and G. Jannink, *Polymers in Solution. Their Modelling and Structure* (Clarendon, Oxford, 1990).
95. P. D. Gujrati and M. Chhajar, *J. Chem. Phys.* **106**, 5599 (1997).
96. T. Nitta, M. Kuro-oka and T. Katayama, *J. Chem. Eng. Jpn.* **17**, 45 (1984).
97. T. Nitta and A. J. Yamaguchi, *J. Chem. Eng. Jpn.* **25**, 420 (1992).
98. F. D. M. Haldane, *Phys. Rev. Lett.* **67**, 937 (1991).
99. Y. S. Wu, *Phys. Rev. Lett.* **73**, 922 (1994).
100. F. Romá, Ph.D. Thesis, Univ. Nacional de San Luis, Argentina, 2005.
101. A. Patrykiejew, S. Sokolowski and K. Binder, *Surf. Sci. Rep.* **37**, 207 (2000).
102. M. Plischke and B. Bergersen, *Equilibrium Statistical Physics* (Prentice Hall, New Jersey, 1989).
103. N. Goldenfeld, *Lectures on Phase Transitions and the Renormalization Group* (Addison-Wesley Publishing Company, Reading, MA, 1992).

104. J. M. Yeomans, *Statistical Mechanics of Phase Transitions* (Clarendon Press, Oxford, 1992).
105. E. Ising, *Z. Physik* **31**, 253 (1925).
106. C. Domb, in *Phase Transitions and Critical Phenomena*, eds. C. Domb and M. S. Green (Academic Press, London-New York, 1974), Vol. 3, pp. 1–95.
107. M. E. Fisher, *Rep. Prog. Phys.* **30**, 731 (1967).
108. L. Onsager, *Phys. Rev.* **65**, 117 (1944).
109. H. Bethe, *Proc. R. Soc. London A* **150**, 552 (1935).
110. A. Clark, *The Theory of Adsorption and Catalysis* (Academic Press, New York-London, 197).
111. A. J. Ramirez-Pastor, J. L. Riccardo and V. Pereyra, *Surf. Sci.* **411**, 294 (1998).
112. J. E. González, A. J. Ramirez-Pastor and V. D. Pereyra, *Langmuir* **17**, 6974 (2001).
113. W. A. Steele, *The Interaction of Gases with Solid Surfaces* (Pergamon Press, New York, 1974).
114. A. J. Ramirez-Pastor, V. D. Pereyra and J. L. Riccardo, *Langmuir* **15**, 5707 (1999).
115. F. Romá, A. J. Ramirez-Pastor and J. L. Riccardo, *Surf. Sci.* **583**, 213 (2005).
116. J. L. Riccardo, A. J. Ramirez-Pastor and F. Romá, *Langmuir* **18**, 2130 (2002).
117. M. Tarek, R. Kahn and E. Cohen de Lara, *Zeolites* **15**, 67 (1995), and references therein.
118. W. H. Press, S. A. Teukolsky, W. T. Vetterling and B. P. Flannery, *Numerical Recipes in C: the Art of Scientific Computing* (Cambridge University Press, New York, 1992).
119. A. J. Ramirez-Pastor, M. S. Nazzarro, J. L. Riccardo and G. Zgrablich, *Surf. Sci.* **341**, 249 (1995).
120. D. Razmus and C. Hall, *AIChE J.* **37**, 769 (1991).
121. S. J. Gregg and K. S. W. Sing, *Adsorption, Surface Area, and Porosity* (Academic Press, New York, 1991).
122. S. Brunauer, P. H. Emmet and E. Teller, *J. Am. Chem. Soc.* **60**, 309 (1938).
123. C. Pierce and B. S. Ewing, *J. Phys. Chem.* **68**, 2562 (1964).
124. A. W. Adamson, *Physical Chemistry of Surfaces* (John Wiley, New York, 1990).